International Ocean Discovery Program Expedition 374 Scientific Prospectus

Ross Sea West Antarctic Ice Sheet History

Ocean–ice sheet interactions and West Antarctic Ice Sheet vulnerability: clues from the Neogene and Quaternary record of the outer Ross Sea continental margin

Robert M. McKay
Co-Chief Scientist
Antarctic Research Centre
Victoria University of Wellington
New Zealand

Laura De Santis
Co-Chief Scientist
Istituto Nazionale di Oceanografia e di Geofisica Sperimentale (OGS)
Italy

Denise K. Kulhanek
Expedition Project Manager/Staff Scientist
International Ocean Discovery Program
Texas A&M University
USA

IODP
INTERNATIONAL OCEAN DISCOVERY PROGRAM

Publisher's notes

This publication was prepared by the *JOIDES Resolution* Science Operator (JRSO) at Texas A&M University (TAMU) as an account of work performed under the International Ocean Discovery Program (IODP). Funding for IODP is provided by the following international partners:

National Science Foundation (NSF), United States
Ministry of Education, Culture, Sports, Science and Technology (MEXT), Japan
European Consortium for Ocean Research Drilling (ECORD)
Ministry of Science and Technology (MOST), People's Republic of China
Korea Institute of Geoscience and Mineral Resources (KIGAM)
Australia-New Zealand IODP Consortium (ANZIC)
Ministry of Earth Sciences (MoES), India
Coordination for Improvement of Higher Education Personnel (CAPES), Brazil

Portions of this work may have been published in whole or in part in other IODP documents or publications.

This IODP *Scientific Prospectus* is based on precruise *JOIDES Resolution* Facility advisory panel discussions and scientific input from the designated Co-Chief Scientists on behalf of the drilling proponents. During the course of the cruise, actual site operations may indicate to the Co-Chief Scientists, the Staff Scientist/Expedition Project Manager, and the Operations Superintendent that it would be scientifically or operationally advantageous to amend the plan detailed in this prospectus. It should be understood that any proposed changes to the science deliverables outlined in the plan presented here are contingent upon the approval of the IODP JRSO Director.

Disclaimer

Copyright

Citation

McKay, R.M., De Santis, L., and Kulhanek, D.K., 2017. *Expedition 374 Scientific Prospectus: Ross Sea West Antarctic Ice Sheet History.* International Ocean Discovery Program. https://doi.org/10.14379/iodp.sp.374.2017

ISSN
World Wide Web: 2332-1385

Abstract

Observations from the past several decades indicate that the Southern Ocean is warming significantly and that Southern Hemisphere westerly winds have migrated southward and strengthened due to increasing atmospheric CO_2 concentrations and/or ozone depletion. These changes have been linked to thinning of Antarctic ice shelves and marine terminating glaciers. Results from geologic drilling on Antarctica's continental margins show late Neogene marine-based ice sheet variability, and numerical models indicate a fundamental role for oceanic heat in controlling this variability over at least the past 20 My. Although evidence for past ice sheet variability has been observed in marginal settings, sedimentological sequences from the outer continental shelf are required to evaluate the extent of past ice sheet variability and the role of oceanic heat flux in controlling ice sheet mass balance.

International Ocean Discovery Program (IODP) Expedition 374 proposes a latitudinal and depth transect of six drill sites from the outer continental shelf and rise in the eastern Ross Sea to resolve the relationship between climatic/oceanic change and West Antarctic Ice Sheet (WAIS) evolution through the Neogene and Quaternary. This location was selected because numerical ice sheet models indicate that it is highly sensitive to changes in ocean heat flux and sea level. The proposed drilling is designed for optimal data-model integration, which will enable an improved understanding of the sensitivity of Antarctic Ice Sheet mass balance during warmer-than-present climates (e.g., the early Pliocene and middle Miocene). Additionally, the proposed transect links ice-proximal records from the inner Ross Sea continental shelf (e.g., ANDRILL sites) to deep-water Southwest Pacific drilling sites/targets to obtain an ice-proximal to far-field view of Neogene climate and Antarctic cryosphere evolution. The proposed scientific objectives directly address Ocean and Climate Challenges 1 and 2 of the 2013–2023 IODP Science Plan.

Drilling Neogene and Quaternary strata from the Ross Sea continental shelf-to-rise sedimentary sequence is designed to achieve five scientific objectives:

1. Evaluate the contribution of West Antarctica to far-field ice volume and sea level estimates.
2. Reconstruct ice-proximal atmospheric and oceanic temperatures to identify past polar amplification and assess its forcings/feedbacks.
3. Assess the role of oceanic forcing (e.g., sea level and temperature) on Antarctic Ice Sheet stability/instability.
4. Identify the sensitivity of the AIS to Earth's orbital configuration under a variety of climate boundary conditions.
5. Reconstruct eastern Ross Sea bathymetry to examine relationships between seafloor geometry, ice sheet stability/instability, and global climate.

To achieve these objectives, we will (1) use data and models to reconcile intervals of maximum Neogene and Quaternary Antarctic ice advance with far-field records of eustatic sea level change; (2) reconstruct past changes in oceanic and atmospheric temperatures using a multiproxy approach; (3) reconstruct Neogene and Quaternary ice margin fluctuations in datable marine continental slope and rise records and correlate these records to existing inner continental shelf records; (4) examine relationships among WAIS stability/instability, Earth's orbital configuration, oceanic temperature and circulation, and atmospheric pCO_2; and (5) constrain the timing of Ross Sea continental shelf overdeepening and assess its impact on Neogene and Quaternary ice dynamics.

Schedule for Expedition 374

International Ocean Discovery Program (IODP) Expedition 374 is based on IODP drilling Proposals 751-Full2, 751-Add, and 751-Add2 (available at **http://iodp.tamu.edu/scienceops/expeditions/ross_sea_ice_sheet_history.html**). Following evaluation by the IODP Scientific Advisory Structure, the expedition was scheduled for the research vessel (R/V) *JOIDES Resolution*, operating under contract with the *JOIDES Resolution* Science Operator (JRSO). At the time of publication of this *Scientific Prospectus*, the expedition is scheduled to start in Wellington, New Zealand, on 4 January 2018 and to end in Wellington, New Zealand, on 8 March. A total of 63 days will be available for the transit, drilling, coring, and downhole measurements described in this report (for the current detailed schedule, see **http://iodp.tamu.edu/scienceops**). Further details about the facilities aboard the *JOIDES Resolution* can be found at **http://iodp.tamu.edu/publicinfo/drillship.html**.

Introduction

Drilling eastern Ross Sea outer continental shelf-to-rise sedimentary sequences will provide a direct record of Neogene to Quaternary West Antarctic Ice Sheet (WAIS) evolution and improve understanding of associated climate forcings/feedbacks. In combination with model sensitivity tests, tectonic considerations, and the well-developed seismic stratigraphic framework of the Ross Sea, proposed drilling will enable researchers to determine if the large far-field Neogene sea level estimates (20–60 m) (cf. Miller et al., 2005, 2012; Naish and Wilson, 2009) reflect changes in Antarctic ice volume (Figure **F1**). The proposed continental shelf-to-rise transect in an area of demonstrated climate sensitivity (Figures **F2**, **F3**, **F4**) allows for improved understanding of ocean–ice sheet interactions on orbital to million year timescales.

The onset of the Neogene (23 Ma; Oligocene/Miocene [O/M] boundary) is characterized by an abrupt increase in Antarctic ice volume attributed to changes in Earth's orbital parameters (Naish et al., 2001; Zachos et al., 1997) and declining atmospheric CO_2 (Figure **F1**) (Pagani et al., 2005). Following the O/M glaciation, both near- and far-field proxy records indicate a period of sustained (~3°C warmer than present) (You et al., 2009) warmth and carbon cycle reorganization (e.g., Foster et al., 2012; Vincent and Berger, 1985), referred to as the Middle Miocene Climatic Optimum (MMCO; ~17–15 Ma) (Flower and Kennett, 1994; Shevenell et al., 2004). During the MMCO, polar amplification of temperature is suggested (Feakins et al., 2012; Lewis et al., 2008; Shevenell et al., 2004; Warny et al., 2009) but not yet successfully modeled (e.g., You et al., 2009). The MMCO was immediately followed by an interval of Antarctic ice growth and cooling, termed the Middle Miocene Climate Transition (MMCT; 14.2–13.8 Ma), as observed in both far-field benthic foraminifer $\delta^{18}O$ records and ice-proximal data (Figure **F1**) (Cramer et al., 2009; Flower and Kennett, 1994; Holbourn et al., 2007; Kennett, 1977; Shevenell et al., 2008, 2004; Zachos et al., 2001) and is believed to have resulted in the extinction of the Antarctic tundra vegetation (Lewis et al., 2008). Although ice expansion has traditionally been inferred in East Antarctica, Ross Sea seismic evidence also suggests WAIS expansion (Bart, 2003). However, the timing of the Ross Sea event, WAIS development, and

forcings and feedbacks involved in the MMCT remain enigmatic (De Santis et al., 1995). During the mid-Pliocene, global sea levels were ~20 ± 10 m above present-day levels, indicating a reduction/collapse of both the Greenland Ice Sheet and the WAIS (Miller et al., 2012). Ice-proximal sedimentary facies indicate orbitally paced advances and retreats of the WAIS from the early Pliocene (Figures **F4**, **F5**, **F6**) until at least 1.0 Ma, although equivocal evidence exists for collapse as recently as the last interglacial (Kopp et al., 2009; McKay et al., 2012b; Naish et al., 2009; Dahl-Jensen et al., 2013; Scherer et al., 1998).

Background

Oceanographic setting

Most of the abyssal ocean is presently filled with cold dense waters produced within the large polynyas of the Weddell and Ross Seas and mixed with ambient waters. Thus, changes in temperature and/or meltwater input to the Ross Sea could disrupt global meridional overturning circulation (MOC) (Jacobs et al., 2002; Orsi and Wiederwohl, 2009; Purkey and Johnson, 2010). Over the past 40 y, Ross Sea–derived Antarctic Bottom Water (AABW) has freshened as a result of increased meltwater input to the Amundsen and Bellingshausen Seas from melting ice shelves/glacial systems (Jacobs et al., 2002, 2011).

Unlike in the Amundsen and Bellingshausen Seas, where the Antarctic Circumpolar Current (ACC) impinges the continental shelf and cross-shelf bathymetry encourages the presence of relatively warm Circumpolar Deep Water (CDW) on the inner shelf, the eastern limb of the Ross Gyre brings cooler Modified CDW (MCDW) to the Ross Sea along the lower continental slope (Orsi and Wiederwohl, 2009; Whitworth et al., 1995). The strong westward-flowing Antarctic Slope Current (ASC), with a sharp subsurface front (Antarctic Slope Front [ASF]), separates Antarctic Surface Water (AASW) on the shelf from CDW on the lower continental slope (Figure **F7**). This front serves as a dynamical barrier that limits the transfer of CDW and MCDW onto the Ross Sea continental shelf (Ainley and Jacobs, 1981). Thus, ASC vigor and the formation of fresh AASWs regulate the volume of MCDW on the Ross Sea continental shelf.

Geological setting and previous drilling

The break-up of Gondwana during the Middle Jurassic began with the initiation of the West Antarctic Rift, which led to the opening of the Ross Sea (Behrendt et al., 1991) and the development of three sedimentary basins (Figures **F2**, **F3**; Cooper et al., 1991). The westernmost Victoria Land Basin (VLB) has been the focus of previous regional geological drilling (e.g., Dry Valley Drilling Project [DVDP], MSSTS-1, CIROS-1 and CIROS-2, Cape Roberts Project [CRP], and ANDRILL). This proposal focuses on the Eastern Basin, which contains up to 6 km of Cenozoic sediment infill.

The basement geology of the Central High adjacent to the Eastern Basin was penetrated at Deep Sea Drilling Project (DSDP) Site 270 and consists of high-grade Paleozoic calcareous metamorphics (Ford and Barrett, 1975) that were mylonitized during Late Cretaceous uplift (Siddoway et al., 2004). Upper Cretaceous mylonites were also recovered from the eastern part of the Eastern Basin (Luyendyk et al., 2001). The lack of basement younger than Devonian at CRP-3 and Site 270 suggests that younger Permian–Triassic Beacon Supergroup strata are likely absent in the western (and eastern) Ross Sea. This suggestion is supported by paleogeographic maps from Barrett (1981), which suggest that the western (and eastern) Ross Sea was likely an area of uplift and erosion through much of the Permian–Triassic, although these maps are poorly constrained. The Devonian lower part of the Beacon Supergroup is dominated by coarse clastics (Barrett, 1981). The tectonic models for the formation of the Ross Sea, through the thinning of thickened (~40 km) crust that covered the entire Transantarctic Mountain (TAM)–Ross Sea–Marie Byrd Land region (Decesari et al., 2007; Karner et al., 2005), would also tend to argue against the preservation of younger Beacon strata because uplift and erosion of large amounts of strata would be predicted during early rifting, and this rifting would likely include the removal of any upper Beacon Supergroup strata even if they had been present.

The ANTOSTRAT seismic stratigraphic scheme defines eight seismic units (RSS-1 to RSS-8) within the sediment infill lying above the basement, bounded by six major shelf-wide unconformities (RSU1 to RSU6) (Table **T1**; Figure **F6**) (Brancolini et al., 1995; De Santis et al., 1995), but their ages are only partially constrained by drilling (see synthesis by Bart and De Santis, 2012). In the western Ross Sea, CIROS-1 and CRP-3 indicate marine-terminating glaciation in the TAM by the earliest Oligocene (Barrett, 2007, 1989). In the central Ross Sea, seismic-based reconstructions suggest ice caps nucleated on the subaerially elevated basement highs in the central Ross Sea during the Oligocene. The adjacent deep-water basins in the outer Ross Sea appear to have remained free of grounded ice to the late Oligocene, although they were probably influenced by voluminous sediment-laden meltwater discharge under a more temperate style of glacial sedimentation, resulting in progressive shoaling of the Eastern Basin as accommodation space was filled (Hayes et al., 1975). Expedition 374 seeks to constrain the ages of Unconformities RSU4 to RSU1 to understand how these unconformities relate to the evolution of the marine-based WAIS.

Seismic Unit RSS-1 (underlying seismic Unconformity RSU6) is the oldest and deepest basin infill sedimentary package in the central Ross Sea. It is divided into a lower and upper package. The lower part of Unit RSS-1 has not been drilled in any holes, whereas the upper part has been drilled in the western Ross Sea (CRP and CIROS-1) and consists of upper Eocene to Oligocene high-energy fluvial and deltatic/shelfal rift-fill strata, with a glacial influence in its upper parts (Fielding et al., 2000; Galeotti et al., 2016). The lithology and age of lowermost Unit RSS-1 is uncertain because it has not been sampled, but it likely consists of high-energy, coarse-grained fluvial facies deposited in the initial phases of Late Cretaecous to Paleocene rifting in the central Ross Sea (Wilson and Luyendyk, 2009).

Units overlying Unconformity RSU6 (Units RSS-2 to RSS-8) have all been partially sampled by drilling, and the stratigraphic architecture in the Ross Sea is relatively well constrained, although most drill holes are located in isolated basins in the western Ross Sea (Figure **F2**) and basin-to-basin correlations remain uncertain. It is difficult to make a direct correlation of Unconformity RSU6 from across the various Ross Sea basins because it onlaps the basement flanks (Figures **F3**, **F6**). However, an inferred correlation can be made due to the distinctive acoustic character of the underlying seismic facies.

Upper Oligocene (28 Ma) to lower Miocene (23 Ma) strata within Unit RSS-2 at Site 270 consist of a 365 m sequence of lithified glaciomarine mudstones with ice-rafted debris (IRD) and common macro- and microfossils, suggesting a shallow continental shelf environment with abundant terrestrial runoff. Above 100 meters be-

low seafloor (mbsf) (Unit RSS-3), many of the units (originally classified as mudstones) are diamictites (i.e., >20% sand) that were eroded and transported by glacial ice (Barrett, 1975).

Two ANDRILL sites drilled on the inner continental shelf of the western Ross Sea (98% recovery) contain an unprecedented record of marine-based ice sheet variability in the Ross Sea (Levy et al., 2016; Naish et al., 2009; Wilson et al., 2012) over the past 20 My, although both of these sites are heavily influenced by the East Antarctic Ice Sheet (EAIS). Site AND-2A recovered a ~20 to 14 Ma sequence interpreted to reflect TAM tidewater outlet glaciers overriding and/or calving near the site (Fielding et al., 2011; Levy et al., 2016; Passchier et al., 2011). At 15.7 Ma, a diatomite with abundant pollen, algae, and other biomarkers suggests a warmer than present (mean surface temperature of ~10°C) climate during the MMCO (Feakins et al., 2012; Warny et al., 2009). At 300 mbsf, a 300 ky disconformity is thought to be equivalent to Unconformity RSU4, suggesting a shelf-wide advance of the marine-based ice sheet during the MMCT (Figures **F6**, **F8**) (De Santis et al., 1999; Passchier et al., 2011).

The first unequivocal seismic evidence of a glacially carved trough in the central Ross Sea (key target of proposed Eastern Basin Outer Continental Shelf [EBOCS] Sites EBOCS-01D and EBOCS-02B) occurs at Unconformity RSU4 (mid-Miocene) and is interpreted as an expansion of a grounded marine-based ice stream originating from the west (Figures **F8**, **F9**) (Anderson, 1999; De Santis et al., 1995; Ten Brink et al., 1995). At DSDP Site 272, a ~400 m thick middle–upper Miocene sequence of glaciomarine mudstones was recovered (Figure **F6**). Combined with the presence of numerous outwash channels above Unconformity RSU4, up to 250 m of till delta foreset and aggrading bottomset strata suggest that glaciomarine sedimentation was dominated by the release of abundant erosive sediment-laden meltwater during the middle Miocene (~14 Ma; Figure **F9**) (Anderson and Bartek, 1992; Chow and Bart, 2003). This meltwater release was likely associated with extensive channel-levee systems above Unconformity RSU4 on the continental slope and rise (De Santis et al., 1995, 1999). A downlapping till delta thickening toward the Central High (dated at Site 272 at 14.2–13.8 Ma) suggests that middle Miocene glaciation was characterized by local ice caps on the Central High and that the continental shelf was shallow and seaward dipping (cf. Figures **F8**, **F9**). Another possibility is that this feature was a grounding zone wedge forming on the flank of the Central High, where ice remained pinned during retreat after the ice expansion that carved Unconformity RSU4 over the central Ross Sea.

Unconformity RSU3 (key target of proposed Site EBOCS-03C) provides the first evidence for a major cross-shelf paleotrough eroded by an expanded WAIS, although the age of this event(s) is poorly constrained (~14–4 Ma; Figures **F6**, **F8**) (Bart, 2003; De Santis et al., 1995, 1999). Large meltwater and outwash features are absent and laminated seismic facies are progressively thinner/less common in strata younger than Unconformity RSU3, suggesting sediment starvation and a transition to a colder glacial regime. Site AND-1B sediments indicate that this transition may not have occurred until the Pliocene (McKay et al., 2009), although evidence for meltwater outburst features is lacking in the TAM after 12.4 Ma (Lewis et al., 2006). High-velocity seismic units above Unconformities RSU3 and RSU2 suggest overcompaction by ice loading during WAIS expansion (Böhm et al., 2009). Bathymetric reconstructions suggest overdeepening and a transition to a landward-deepening continental shelf occurred by the Unconformity RSU2 event during the early Pliocene to early Pleistocene(?) (Figures **F8**, **F10**) (De Santis et al., 1995, 1999). A trough-mouth fan on the upper slope and a sediment-starved continental rise (typical of the Pliocene–Pleistocene Antarctic margin) coincided with overdeepening (Bart et al., 1999; Bart and Iwai, 2012; Cooper and O'Brien, 2004; Rebesco et al., 2006).

At Site AND-1B, ~58 sedimentary cycles of ice sheet advance and retreat can be observed within the Ross Embayment over the past 13 My (McKay et al., 2009). Diatomites indicate frequent collapses of the WAIS in the Pliocene (5.3–2.6 Ma), during which diatom assemblages and geochemical paleothermometry indicate ocean temperatures up to 4°C warmer than present (McKay et al., 2012a; Naish et al., 2009). However, sedimentary lithofacies indicate that meltwater discharge was reduced during Pliocene interglacials compared with the latest Miocene (11–5.3 Ma; Figure **F5**). By the mid-Pleistocene (1.0 Ma), the Ross Ice Shelf persisted through most interglacials (McKay et al., 2009).

Seismic facies above Unconformity RSU2 consist of till sheets bound by erosional unconformities in an aggrading shelf margin that is indicative of shelf-wide advances of the WAIS (Figures **F8**, **F10**) (Alonso et al., 1992; Bart et al., 2011; Brancolini et al., 1995). Unlike other sectors of the Antarctic, the eastern Ross Sea trough mouth contains thick (~2000 m) sedimentary sequences on the shelf and upper continental slope (Figure **F10**) that may contain a detailed WAIS history. Above Unconformity RSU1 (0.7? Ma; key target of proposed Site EBOCS-04B), shelf-edge sediments are aggrading or backstepping (rather than prograding), indicating that most sediment delivered from land was sequestered on the outer shelf.

Site survey data

Multichannel and single-channel seismic profiles have been collected in the Ross Sea by several nations since 1980. The multichannel seismic data are available through the Antarctic Seismic Data Library System, which works under the auspices of the Scientific Committee on Antarctic Research and the Antarctic Treaty (ATCM XVI-12). Prestack data are available only from the Italian cruises (1988, 1989, 1991, 1994, and 2006) and recently also from the BGR80 cruise.

We located the sites for scientific reasons such as maximum thickness of target sequence, better potential for dating sediments, and acoustic facies and geometry, which usually can be seen much better on high-resolution profiles. In most cases, high-resolution profiles are single channel or, in the case of the TAN lines, they have a very short streamer (200 m) compared with the water depth (>1000 m). In some cases, crossing lines are not available and the remoteness of Antarctic waters prevents the easy collection of new site survey data. New multichannel seismic (MCS) Profiles KSL14-02 and KSL14-04 (unpublished) were collected in February 2013 and in 2015 by the Korea Polar Research Institute (KOPRI) with the aim to provide the cross-lines for proposed Ross Sea Continental Shelf (RSCR) Sites RSCR-08C and RSCR-12B, respectively. Another SCS survey cruise was conducted in 2017 in the frame of the EU/FP7 EUROFLEETS2, Programma Nazionale di Ricerche in Antartide (PNRA) WHISPERS, and PNRA ODYSSEA projects, with the aim to collect more cross-lines of the proposed sites and identify future alternate sites that will be detailed in an addendum to this *Scientific Prospectus*.

Single-channel seismic data, collected by National Science Foundation (NSF) Cruises 1990 and 1994-95, were made available by John Anderson (Rice University, TX, USA) in the format of digital Society of Exploration Geophysicists (SEGY) data (PD90 cruise)

and paper copies (NBP 94-95 cruise). We made the conversion of the TIFF or JPG image to SEGY format to depth convert the sections and load the data in the HIS Kingdon interpretation software with the other available data sets. The supporting site survey data for Expedition 374 are archived at the IODP Site Survey Data Bank (**https://ssdb.iodp.org/SSDBquery/SSDBquery.php**; select P751 for proposal number).

Scientific objectives

1. *Evaluate the contribution of West Antarctica to far-field ice volume and sea level estimates*

Far-field benthic foraminifer $\delta^{18}O$ and sequence stratigraphic records suggest that large global ice volume and sea level (20–60 m) variations occurred during the Miocene and Pliocene (Figures **F1**, **F6**) (Cramer et al., 2009; Miller et al., 2005, 2012; Raymo et al., 2011; Zachos et al., 2001). Miocene to Pliocene sea level reconstructions could potentially be reconciled without invoking Northern Hemisphere contributions if Antarctica's ice sheets expanded to the continental shelf edge (~14 m sea level equivalent [SLE]) (Figure **F4**). The modeled difference between the glacial maxima states and loss of the marine-based WAIS (assuming present bathymetry) represent ~21 m SLE (with some minor loss of the EAIS), although changes in Ross Sea bathymetry could increase this value (Figure **F4**) (see Objective 5). Expedition 374 records will constrain the timing of the first WAIS advances to the shelf edge, and integration with the ANDRILL records allows assessment of the WAIS contribution to Neogene sea level estimates.

Sedimentologic analyses at the proposed continental shelf sites (primary Sites EBOCS-01D, EBOCS-02B, EBOCS-03C, and EBOCS-04B), combined with seismic stratigraphic correlations, will identify deposition under grounded ice, glacial marine, and open-marine conditions, following ANDRILL/CRP methodology (Fielding et al., 2000, 2011; McKay et al., 2009; Passchier et al., 2011; Powell and Cooper, 2002). Magneto-, bio-, and tephrochronology will enable identification of orbital-scale ice sheet variations and have been employed in discontinuous Antarctic margin sequences (Florindo et al., 2003, 2005; Tauxe et al., 2012; Wilson et al., 2012) (Figure **F4**). Furthermore, new quantitative techniques have greatly enhanced the biostratigraphic framework of the Southern Ocean (Cody et al., 2012, 2008; Crampton et al., 2016). Glacially reworked volcanic clasts (Wilson et al., 2012) and radiometrically datable felsic ashes from Marie Byrd Land may be used to provide maximum ages (Wilch et al., 1999). Climate snapshots near magnetic reversals will be targeted (cf. the M2 glacial in Figure **F4**) because these events can be traced to more continuous records from the continental rise (proposed primary Sites RSCR-11A and RSCR-02B) and global sea level records (Figure **F10**). Sediment provenance studies (clast/sand petrology and Nd-, Sr-, and Pb-isotopic analysis) at proposed Sites EBOCS-01D through EBOCS-04B will enable understanding of the changes in the origin of sediments (e.g., local ice caps vs. ice sheet expansion) (Figure **F8**) (Cook et al., 2013; Licht et al., 2005). As with all objectives, data integration with modeling studies will be undertaken (cf. Figure **F4**) (DeConto and Pollard, 2016; Gasson et al., 2016; Golledge et al., 2012; Wilson et al., 2013).

2. *Reconstruct ice-proximal atmospheric and oceanic temperatures to identify past polar amplification and assess its forcings/feedbacks*

Obtaining atmospheric and ocean temperatures from the proposed Expedition 374 drill sites will enable the paleoclimate community to address the following key scientific questions:

- Were polar temperatures sensitive to the low-amplitude variations in Neogene atmospheric pCO_2?
- Were Neogene ocean and atmospheric temperatures at Antarctica's margin amplified relative to the global mean, and if so, what were the forcings?
- How did ocean temperatures evolve as Antarctica's ice sheets expanded and contracted during major Neogene climate transitions and on orbital timescales?

Although ANDRILL's records provide important archives of high-latitude oceanic conditions, they only provide snapshots of temperature and sea ice conditions through interglacials, when these sites were not covered by ice (McKay et al., 2012a; Warny et al., 2009). In contrast, proposed primary Sites EBOCS-01D to EBOCS-04B will likely provide intervals of more continuous sedimentation (albeit with some periods of erosion during large glaciations) because they are farther out on the margin and overridden by ice less frequently (Bart et al., 2011; Pollard and DeConto, 2009). Near-continuous records of oceanographic change are anticipated at the proposed continental rise sites (RSCR sites), providing high-latitude (~60°S) information on Neogene ocean and atmospheric temperatures, meltwater input, and bottom water production.

Facies analysis will be used to reconstruct glacial thermal regimes and glacial cyclicity (cf. Naish et al., 2009; McKay et al., 2009), whereas diatom census counts, palynology, organic biomarkers (e.g., TEX86 and BIT index; cf. McKay et al., 2012a), and redox-sensitive metals (e.g., Mn, U, Re, and Mo for paleoproductivity, along with monitoring alteration of the biomarkers by methanogenesis and shifting redox boundaries) provide insights into high-latitude climate. Carbonate (e.g., calcareous nannofossils/foraminifers) may also be present in late Pleistocene interglacial sequences (e.g., Escutia, Brinkhuis, Klaus, and the Expedition 318 Scientists, 2011; Scherer et al., 2008; Theissen et al., 2003; Villa et al., 2008). In the lower to middle Miocene, biogenic carbonate is more common in the Southern Ocean and Antarctica's margins (Figure **F5**) (Escutia, Brinkhuis, Klaus, and the Expedition 318 Scientists, 2011; Exon, Kennett, Malone, et al., 2001; Fielding et al., 2011; Hayes et al., 1975; Kennett and Barker, 1990; Shevenell et al., 2004), making stable isotope ($\delta^{18}O$ and $\delta^{13}C$), trace element (e.g., Mg/Ca, Li/Ca, U/Ca, Ba/Ca, and B/Ca), and clumped isotope analyses possible, with careful consideration of proxy strengths/weaknesses in a marginal marine setting.

3. *Assess the role of oceanic forcing (e.g., sea level and temperature) on WAIS stability/instability*

WAIS collapse events during past warmer-than-present climates may be the consequence of intensified ocean-cryosphere interactions (Naish et al., 2009; Pollard and DeConto, 2009). Interactions between the wind-driven upwelling of warm CDW and

the ice shelves that buttress the WAIS appear to play a significant role in modern ice mass loss in West Antarctica (Joughin et al., 2012; Mercer, 1978; Pritchard et al., 2012; Shepherd et al., 2012). Observations and numerical ice sheet models suggest that changes in ocean heat flux are the key factor influencing the stability/instability of the WAIS (DeConto and Pollard, 2016; Golledge et al., 2012; Pritchard et al., 2012). We postulate that changes in either the formation of Antarctic Surface and Deep Waters or the vigor of the wind-driven ASC control incursions of CDW and thus WAIS retreats (Figure **F7**). This expedition aims to test this hypothesis by assessing changes in these two variables (from grain size and facies analysis of sediment drifts on the continental rise, e.g., proposed primary Sites RSCR-02B and RSCR-11A) and ice sheet extent in the Ross Embayment (proposed primary Sites EBOCS-01D to EBOCS-04B and ANDRILL).

The Ross Sea is also one of the three main sources of AABW that feeds the abyssal ocean (to become Southern Component Water [SCW]). In the middle Miocene, benthic foraminifer $\delta^{13}C$ indicates changes in the relative input of SCW and Northern Component Water into the global ocean (Cramer et al., 2009; Shevenell et al., 2004; Woodruff and Savin, 1985; Wright et al., 1991). Newer proxies, such as Nd isotopes, are now used to further refine the geographic source (e.g., Newkirk and Martin, 2009; Scher and Martin, 2006). Thus, it is anticipated that the records obtained during this drilling program and comparison to far-field records will provide insight into temporal changes in SCW production through the Neogene (Flower and Kennett, 1994; Hodell and Venz-Curtis, 2006; Vincent and Berger, 1985).

Paleocurrent strength associated with past ASC changes will be reconstructed by examining the sedimentologic (e.g., facies analysis and grain size) and magnetic characteristics of continental rise sites (e.g., Bianchi et al., 1999; Hall et al., 2001; Joseph et al., 2004; Prins et al., 2002). Micropaleontological, geochemical, and sedimentological records from drill cores from all Expedition 374 sites will provide reconstructions of changing regional surface conditions (e.g., sea ice, surface stratification, sea-surface temperatures [SSTs], polynya mixing, glacial meltwater discharge, nutrient uptake, and supercooling of dense waters by ice shelves) proximal to Antarctica's ice sheets (e.g., Houben et al., 2013; Levy et al., 2016; McKay et al., 2012a; Shevenell et al., 2011) and thus AASW (and SCW) formation. Additionally, downslope currents resulting from the transfer of High-Salinity Shelf Water into the abyssal ocean can also be assessed (and distinguished from ASC flow) by integrated facies analysis, geochemistry, micropaleontology, and seismic profiles (e.g., Caburlotto et al., 2010; Hepp et al., 2006; Lucchi and Rebesco, 2007) at primary Sites RSCR-11A and RSCR-02B. Carbonate-based paleotemperature and carbonate ion proxies (e.g., foraminiferal Mg/Ca, Li/Ca, U/Ca, and clumped isotopes) will also be applied if appropriate species are preserved (see Objective 2).

4. *Identify the sensitivity of WAIS to Earth's orbital configuration under a variety of climate boundary conditions*

Fundamental questions remain about the orbital pacing of Antarctic ice sheet development and variability. The Ross Sea Expedition 374 sequences may shed light on (1) the absence of the 20 ky precession cycle in benthic $\delta^{18}O$ records (Figure **F4**) (Huybers, 2006; Lisiecki and Raymo, 2005; Raymo et al., 2006) and (2) the origin of transient shifts in the sensitivity of Earth's climate system to orbital forcing (e.g., 40–100 ky dominated frequencies) in the middle Miocene (Shevenell et al., 2004) and Pliocene–Pleistocene (Tzedakis et al., 2017).

A recent hypothesis suggests that the last such shift in Earth's history (the mid-Pleistocene transition) was initiated by an abrupt increase in Antarctic ice volume (Elderfield et al., 2012). This hypothesis may be tested by identifying and dating grounding events on the outer Ross Sea continental shelf (proposed primary Site EBOCS-04B). If the dominant frequency of Antarctic ice sheet advance and retreat shifted from 40 to 100 ky at 0.8 Ma, records from this sensitive region will likely record this transition.

Recent evidence from ice-proximal drill sites indicates that Antarctic ice sheets did advance and retreat with 40 and 100 ky cyclicity in the Neogene (Grützner et al., 2003; Naish et al., 2009; Patterson et al., 2014; Williams and Handwerger, 2005). However, these records are from single locations. We envision a more complete picture of the forcings and feedbacks involved with ice advance and retreat from our outer shelf to slope/rise transect. Sedimentologic analyses (complimented by downhole logs) will enable development of an orbital-scale continental shelf-to-rise sequence stratigraphy of glacial advance and retreat (all Expedition 374 sites; see Objective 1). Additional micropaleontologic, inorganic and organic geochemistry (e.g., $\delta^{18}O$, $\delta^{13}C$, $\delta^{30}Si$, and Nd), minor and trace elements (X-ray fluorescence and discrete samples), and organic biomarkers may be used to assess associated frequencies of change in the continental rise sites (RSCR-01B and RSCR-02B).

5. *Reconstruct eastern Ross Sea bathymetry to examine relationships between seafloor geometry, ice sheet stability/instability, and global climate*

The transition from a terrestrial (or shallow marine)-based West Antarctica with a seaward-dipping shallow continental shelf to that of the modern overdeepened (i.e., landward-dipping) continental shelf would have a first order control on Antarctic ice sheet volume and mass balance (Gasson et al., 2016; Wilson et al., 2013). First, the cooling threshold for the development of a terrestrial-based ice sheet is lower than that of a marine-based ice sheet, which is highly sensitive to changes in oceanic heat flux (Figure **F4**) (Golledge et al., 2012; Pollard and DeConto, 2009). A terrestrial (or shallow marine) West Antarctica may have supported a larger ice sheet in warmer-than-present climates, whereas overdeepening of the continental shelves may have resulted in a smaller ice sheet with less frequent ice sheet advances, as hypothesized for the Antarctic Peninsula (e.g., Bart and Iwai, 2012). Ice sheet models indicate that a largely terrestrial West Antarctica could accommodate an extra ~13 million km^2 of grounded ice in the warmer-than-present climates of the Eocene (~30 m SLE; Figure **F4**) (Wilson et al., 2013). Therefore, constraining the timing of overdeepening in the Ross Sea is critical to reconcile far-field records of eustatic sea level variance into the late Neogene (see Objective 1).

The timing of Ross Sea shelf overdeepening is currently unconstrained. However, the Ross Sea has the most developed seismic framework in Antarctica and the highest resolution history of WAIS variability currently available (ANDRILL), making this location ideal for achieving this objective. Dating of Unconformities RSU3 and RSU2 (Figure **F6**) at proposed primary Sites EBOCS-02B and EBOCS-03C in the eastern Ross Sea (via methodologies in Objective 1) will constrain the timing of this overdeepening (Figure **F8**).

Drilling and coring strategy

Proposed drill sites

We plan to drill a total of six primary sites, four on the continental shelf and two on the continental slope or rise (Table **T2**). These

sites comprise both a depth (present water depths of 490 to 2400 m) and latitudinal transect, with links to ANDRILL and DSDP drilling (78° to 74°S). We expect to recover lower Miocene to present sequences (Tables **T1**, **T2**) of subglacial, glaciomarine, and open-marine/pelagic sediments with macrofossils, microfossils, and organic material that will enable the development of sedimentological and geochemical proxy records. Our operations plan is prioritized to maximize objectives in case we do not have time to core at all primary sites (Table **T3**). We also have eight alternate sites (Table **T4**) that can be occupied if any of the primary sites are ice covered. We will be adding additional alternate sites in an addendum to this *Scientific Prospectus*.

Continental shelf (EBOCS) sites

We propose four primary continental shelf sites: EBOCS-01D, EBOCS-02B, EBOCS-03C, and EBOCS-04B. High-quality ANDRILL core material covering WAIS minima from the inner continental shelf will be integrated with our sites to provide a stratigraphic framework unmatched elsewhere in Antarctica. This integrated framework will enable us to constrain the spatial extent of Neogene glacial advance events across the Ross Sea and determine if these events are isochronous. Major hiatuses are likely to occur in continental shelf sequences, but the existing sediments provide critical snapshots into past interglacial intervals. The timing of major hiatuses will allow us to determine if widespread WAIS advances coincided with major global cooling steps (e.g., Anderson, 1999; Zachos et al., 2001; Bart, 2003; Naish et al., 2009; Passchier et al., 2011; Fielding et al., 2011; Bart et al., 2011).

Proposed primary Site EBOCS-01D is located on the mid- to outer shelf near a northeast–southwest oriented paleotrough (Figure **F8**) and will penetrate the oldest strata overlying Unconformity RSU4 (middle Miocene) to establish the timing of the first expansion of marine-based ice streams into the Ross Sea (Figure **F9**). The paleotrough orientation suggests that these streams may be of EAIS origin (De Santis et al., 1995) and the provenance of till associated with this unconformity will establish the geographic origin of these ice streams. Above Unconformity RSU4, the acoustic facies at Site EBOCS-01D indicates the presence of layered units (similar to those cored at Sites 270 and 272) that are likely glaciomarine and contain abundant terrestrial and marine biogenic material useful for dating and environmental reconstructions. These units lie between acoustically opaque (till) tongues that may provide direct evidence of ice sheet grounding onto the outer Ross Sea continental shelf during the middle to late Miocene (Objectives 1 and 4) (Figure **F9**). Site EBOCS-01D will also recover a climatic/ice sheet record of the MMCO (17–15 Ma) below Unconformity RSU4. The layered strata below Unconformity RSU4 are likely glaciomarine ice-proximal to ice-distal MMCO-aged deposits (Objective 2). Proposed alternate Site EBOCS-05A would recover a younger glaciomarine section below Unconformity RSU4, although Site EBOCS-01D is prioritized because it enables recovery of the section immediately overlying Unconformity RSU4. Proposed primary Site EBOCS-02B (~70 km east of Site EBOCS-01D) has similar objectives but targets a thicker and younger (late Miocene?) interval of layered glaciomarine strata above Unconformity RSU4.

Proposed primary Site EBOCS-03C is located at the shelf break during the middle Miocene (Figure **F8**) and is designed to recover a post-Unconformity RSU4 sedimentary sequence that spans the MMCT to the Pleistocene (Unconformities RSU3 to RSU1) (Figure **F6**). It targets laminated and massive acoustic facies interpreted as interlayered glaciomarine/open-marine mudstones and massive diamictites (tills) (Figure **F10**). The massive facies display wedgelike or channel structures consistent with deposition and erosion by streaming ice (Objectives 1 and 4) (Figure **F10**). The primary objectives at this site are to date WAIS advances associated with Unconformities RSU3 and RSU2 (Objective 1) and to constrain the timing of the Ross Sea overdeepening (Objective 5). The glaciomarine mudstones are anticipated to be biogenic rich, enabling paleoenvironmental reconstructions for late Miocene to Pleistocene interglacials (Objective 2). Proposed alternate Site EBOCS-06A would achieve the same objectives.

Proposed primary Site EBOCS-04B will recover a Pliocene–Pleistocene sequence to date Unconformities RSU2 and RSU1. The upper ~140 m of sediment consists of tabular units interpreted as aggradational subglacial till sheets deposited by a grounded ice sheet during the late Pleistocene (Figure **F10**) (De Santis et al., 1995). Underlying the till sheets is ~40 m of acoustically laminated facies interpreted as glaciomarine or hemipelagic sediments and ~40 m of massive facies directly overlying Unconformity RSU1 (<0.7 Ma?). The sedimentary succession underlying the Pleistocene till sheets is progradational and hypothesized to represent interlayered subglacial till and glaciomarine/hemipelagic sediments of early to late Pliocene age. This site will enable us to determine if ice sheet overriding events observed at Site AND-1B advanced to the shelf edge, allowing determination of Antarctic ice sheet contribution to Pliocene sea level lowstands (Objective 1) (Naish et al., 2009; Miller et al., 2012). Glaciomarine deposits at this site will allow reconstruction of paleoceanographic and paleoecological conditions at the outermost Ross Sea continental shelf (Objective 2). We anticipate that these sequences will provide insights to the orbital controls on marine-based ice sheet extent (Objective 4). Proposed alternate Site EBOCS-07C would achieve the same objectives.

Continental slope/rise (RSCR) sites

We propose two primary continental slope/rise sites: RSCR-02B and RSCR-11A (Figure **F11**). Sediment deposition on Antarctica's continental rises results from the interplay among (1) downslope marine sediment gravity flows (turbidity currents) triggered by glacial meltwater discharge and/or subglacial transport (Lucchi et al., 2007), (2) along-slope transport (contour currents), (3) biogenic sedimentation (Escutia, Brinkhuis, Klaus, and the Expedition 318 Scientists, 2011), and (4) iceberg rafting (Anderson 1999; Williams et al., 2012; Passchier et al., 2011). Suborbital resolution Neogene and Quaternary sequences with high recovery (87% in the advanced piston corer [APC] interval of Integrated Ocean Drilling Program Site U1361) and excellent chronostratigraphies have previously been recovered from the Wilkes Land (Integrated Ocean Drilling Program Expedition 318) and Prydz Bay (Ocean Drilling Program [ODP] Leg 188) continental rise (Florindo et al., 2003; Escutia, Brinkhuis, Klaus, and the Expedition 318 Scientists, 2011; Tauxe et al., 2012) and provide records of EAIS retreat events (Passchier et al., 2011; Cook et al., 2013). However, these locations do not offer paired high-resolution Neogene continental shelf records suitable for reconstructing the oceanographic response/drivers for changes in ice sheet extent.

Proposed primary Site RSCR-02B is located in 2550 m of water on the upper continental rise near the western levee of a channel system at the head of the Hillary Canyon (Figure **F11**), which is one of the main AAWB outflows in the central Ross Sea (Figure **F7**) (Orsi and Wiederwohl, 2009). This site is designed to penetrate sediments above and below Unconformity RSU3 but with no major hiatus between Unconformities RSU2 and RSU3. The fine-grained

component of overbank deposits is expected to be interstratified with bioturbated hemipelagic sediments during periods of reduced turbidity current activity. This site will provide a mostly continuous record of overbank turbidite (i.e., nonerosive) deposition that should reflect late Neogene changes in SCW formation, ASC flow, and ice sheet advance to the shelf edge (Figures **F7**, **F10**). Three proposed alternate sites (RSCR-01B, RSCR-03A, and RSCR-10A) would achieve the same objectives.

Proposed primary Site RSCR-11A is located on Iselin Bank outside of the Eastern Basin (Figure **F11**) but will provide an important regional constraint for ASC and help distinguish local from regional processes (Objectives 2 and 3). It is also a drift deposit on the upper slope (in 1534 m of water) and will thus complement the deeper water Site RSCR-02B with a broader geographic context. Site RSCR-11A targets Pliocene–Pleistocene deposits and will recover a high-resolution record of oceanographic change at the shelf edge. The oceanographic connection at this site with the shelf (EBOCS) sites is very strong, despite the geographic disconnect. The more westerly location of this site will also link directly with the benchmark Site AND-1B core in the western Ross Sea. Proposed alternate Sites RSCR-08C and RSCR-12B would achieve similar objectives.

Operations plan

The overall operations plan and time estimates for Expedition 374 are summarized in Table **T3**. After departing Wellington, New Zealand, we will transit for ~6 days to the rendezvous point with the R/V *Nathaniel B. Palmer*. This ship will escort us for ~2 days through the sea ice to the Ross Sea polynya, where we will prepare for coring operations on the continental shelf. Our operations plan is designed to maximize achievement of scientific objectives rather than minimize transit, so we plan to conduct coring operations at three shelf sites, followed by coring at two slope/rise sites. We will then return to the shelf to core the final shelf site. However, the actual order of operations will be dictated by ice and weather conditions, and alternate sites (Table **T4**) may be occupied if primary sites are covered by ice (see **Risks and contingency**). The operations plan and time estimates are based on prior DSDP drilling in the region, together with formations and depths inferred from regional seismic stratigraphy.

Shelf (EBOCS) sites

The operations plan includes a single rotary core barrel (RCB) hole to total depth (500–950 mbsf) at each of the primary shelf sites due to the overconsolidated nature of anticipated glaciomarine and subglacial diamictites and presence of boulders in surficial sediments. Ross Sea continental shelf sediments, including Quaternary sediments, are typically lithified muddy diamictites/mudstones (e.g., Site 270 and both ANDRILL holes) (Barrett, 1975; McKay et al., 2009; Passchier et al., 2011). Although drilling unconsolidated diamict is difficult and may result in poor recovery, drilling lithified glacial sediment with an indurated mud matrix is easier because it is homogeneous and cohesive. If rotary coring indicates the lithologies in the upper sections of any the shelf sites (in particular the Pliocene–Pleistocene in Sites EBOCS-03C and EBOCS-04B) are suitable for piston coring, we may core a second hole using the APC and/or half-length APC (HLAPC) systems together with the extended core barrel (XCB) system through more indurated intervals to recover a more complete section. Note that the use of the APC/HLAPC system at any of the shelf sites would be at the expense of other planned operations and would require either coring fewer sites (e.g., not coring at Site EBOCS-02B) or decreasing total penetration depth at one or more sites. Following completion of coring, we will condition the hole for downhole logging.

Slope/rise (RSCR) sites

The operations plan for the slope/rise sites includes two APC holes to refusal (estimated at 250 mbsf). At Site RSCR-11A, we will then use the XCB coring system to extend the second hole to total depth (500 mbsf). Because penetration to 1000 mbsf is proposed for Site RSCR-02B, a third hole will consist of an RCB hole to total depth. Following completion of coring, we will condition the final hole at each site for downhole logging measurements.

Upon completion of coring/logging operations at the last site, we will transit ~7 days back to Wellington, New Zealand.

Downhole measurements strategy

Wireline logging

The downhole measurements plan for Expedition 374 aims to provide continuous stratigraphic coverage of in situ formation properties at all primary drilling sites. Downhole logging data will provide the only stratigraphic data where core recovery is incomplete, which is likely when sites are single-cored with XCB and RCB coring and in the challenging coring conditions of the continental shelf. As demonstrated by Williams et al. (2012) for ANDRILL, downhole logging allows a complete lithostratigraphy to be developed, and holes are generally stable for logging on the shelf and rise (e.g., Escutia, Brinkhuis, Klaus, and the Expedition 318 Scientists, 2011; Williams et al., 2012). This approach was also used in Prydz Bay (ODP Site 1166), where recovery was only 18% due to mostly sandy lithologies in the Oligocene sequences (Cooper and O'Brien, 2004).

The three standard IODP tool strings will be deployed at each logged site if conditions and time permit (Table **T2**). The first run will be the triple combo tool string, which logs formation resistivity, density, porosity, natural gamma radiation (NGR), and borehole diameter. The General Purpose Inclinometry Tool (GPIT) will be added to the triple combo because it includes a fluxgate magnetometer. We will also likely deploy the Lamont-Doherty magnetic susceptibility sonde (MSS) with the triple combo to provide magnetic field and susceptibility information. The borehole diameter log provided by the caliper on the density tool will allow assessment of hole conditions (e.g., washouts of sandy beds), log quality, and the potential for success of the following runs.

The second logging run will be the Formation MicroScanner (FMS)-sonic tool string, which provides an oriented resistivity image of the borehole wall and logs formation acoustic velocity, NGR, GPIT magnetometry, and borehole diameter. To provide a link between borehole stratigraphy and the seismic section, sonic velocity and density data can be combined to generate synthetic seismograms for detailed well-seismic correlations. If time and hole conditions allow, the third run will consist of a check shot survey using the Versatile Seismic Imager (VSI) with a station spacing of ~50–100 m where the borehole diameter is narrow enough to give good coupling of the tool's geophone with the borehole wall. The objective is to directly establish the link between lithostratigraphic depths in the borehole and reflectors in the seismic profiles. The seismic source for the check shots will be either a generator-injector (GI) air gun (most suitable for the shelf sites) or two 250 inch^3 Sercel G guns in parallel clusters 1 m apart (most suitable for slope/rise sites). Deployment of the seismic source is subject to the IODP marine mammal policy; the check shot survey would have to

be postponed or canceled if policy conditions are not met. Details of the logging tools are available at **http://iodp.ldeo.columbia.edu/TOOLS_LABS/tools.html**.

Downhole temperature measurements

Temperature measurements are planned for all sites with APC coring to reconstruct the thermal gradient at each location. Typically, ~3–5 measurements are made in one hole per site using the advanced piston corer temperature tool (APCT-3), potentially supplemented by the Sediment Temperature Tool (SET) if necessary where sediments are more consolidated.

Risks and contingency

There have been extensive shallow coring and seismic survey expeditions in the Ross Sea over the last few decades, and weather and sea ice conditions in those waters are well understood. There have also been significant improvements in coring technology since DSDP Leg 28, which cored in the Ross Sea in 1973. Specifically, the *JOIDES Resolution* has improved dynamic positioning and heave compensation. New drill bit technology and advances in bottomhole assembly technology also give drillers more options to improve core recovery and core quality in glacial diamicts. Continuous recovery is not required to achieve our paleoceanographic scientific objectives at the proposed continental shelf (EBOCS) sites. Core recovery for sites on the continental slope and rise (RSCR) should be comparable with that of lower latitude paleoceanographic conditions and will hopefully allow for recovery of complete or nearly complete stratigraphic sections in the upper part of the stratigraphy.

Ice conditions

Extensive sea ice–free conditions occur in the vicinity of the continental shelf sites from January to mid-February within the Ross Sea polynya. To gain entrance to the polynya, we have arranged to meet the *Nathaniel B. Palmer* near the ice edge on 15 January 2018. The icebreaker will escort us through the sea ice to the open waters of the polynya. In addition, the *Nathaniel B. Palmer* will be operating within 2 days of our position throughout our operations in the Ross Sea should we require assistance. The *Nathaniel B. Palmer* must depart the Ross Sea no later than 24 February if we require an escort out of the polynya. The *JOIDES Resolution* captain will assess the sea ice conditions by 19 February to determine if we must exit with *Nathaniel B. Palmer* support or if we can continue operations in the polynya after the *Nathaniel B. Palmer*'s departure.

To maximize achievement of the expedition scientific objectives regardless of sea ice conditions in the Ross Sea, we have included a number of alternate sites that can be occupied should the primary sites be ice covered. We will also include additional alternate sites in an addendum to this *Scientific Prospectus* once the sites have been approved at all levels of the IODP Science Advisory Structure. We note that the sea ice–free season is shorter and less predictable near continental slope/rise Sites RSCR-11B and RSCR-02B. If we can access these sites, the rim of sea ice will act to dampen local wave heights, which will reduce ship heave and enhance core recovery. We include western Ross Sea continental rise alternate sites in a more ice-free setting that should achieve similar scientific objectives should the primary sites be ice covered.

Icebergs pose an additional threat to drilling operations and will require the *JOIDES Resolution* to move off station if an iceberg approaches a site location. In these instances, we will deploy a free-fall funnel (FFF) to allow for hole reentry after the iceberg passes.

Coring in glacial sediment

Core recovery from ship-based drilling on Antarctica's continental shelves has been variable and is primarily affected by the nature of the sediment and adverse weather and ice conditions. Previous drilling during Leg 28 demonstrated that reasonably good core recovery is possible (up to 67% for that expedition) for the proposed Ross Sea sites. On the continental shelf, recovery is likely to be lowest in the upper ~50 mbsf. Below that depth, the driller can use weight on bit to help stabilize drilling and improve core recovery. Less consolidated sediment will be more difficult to recover, which may particularly impact the Pliocene–Pleistocene sequences at Site EBOCS-04B. Heave in the Ross Sea should be lower than other Antarctic regions (e.g., Prydz Bay, Wilkes Land, and the Antarctic Peninsula) due to reduced storm frequency in the Ross Sea sector and the dampening influence of sea ice north of the Ross Sea polynya.

Other operational risks

The proposed penetration at some sites (up to 1000 mbsf) presents several challenges for successful drilling. Hole stability is always a risk during coring operations, and the risk increases with longer open hole sections. Casing long open-hole sections (especially over intervals of unconsolidated sediment) is the best way to mitigate this risk, but we do not plan to case any holes during this expedition. Casing adds a significant amount of operational time and would also be compromised if ice approached the site. Instead, we will use drilling mud to help stabilize the open hole, although lower annular velocities will make hole cleaning more challenging in the deeper sections of these holes. Increasing flow rates to clean the hole could result in washing out unconsolidated sections in the upper part of the hole. This could lead to hole stability problems toward the end of drilling and during logging operations.

We will likely need to deploy a FFF for some holes in order to allow reentry capability if we have to move off site during coring operations. There are several risks associated with FFF deployment. The FFF can be dislodged while pulling out of the hole or can become buried or impossible to use for reentry. The use of a FFF also leaves the open-hole section open for a longer duration, which can contribute to hole stability problems.

A stuck drill string is always a risk during coring operations and can consume expedition time with attempts to free the stuck drill string. If the drill string cannot be extracted, then additional time is spent to sever the stuck pipe. This process can result in the complete loss of the hole, lost equipment, and lost time while starting a new hole. The *JOIDES Resolution* carries sufficient spare drilling equipment to enable the continuation of coring, but the time lost to the expedition can be significant.

Downhole logging risks

There are a few risks involved in any downhole logging operations. First, the upper parts of the holes have been open longer before logging, and high levels of fluid circulation might have been used to raise the cuttings and clear the hole. Therefore, the hole could be washed out (wide) over intervals through unconsolidated sediment, and log quality will be reduced for those tools that need good contact with the borehole wall (density, porosity, FMS resistivity images, and VSI check shots). Second, there is a risk of bridging where the hole closes up. This bridging would mean either not reaching the total depth of the hole or, in the worst case scenario, getting a tool string stuck in the hole. A good guide to this will be

the conditions encountered during drilling and a wiper trip before logging. If the risk is considered to be significant, the radioactive source will be left out of the density tool.

Sampling and data sharing strategy

Shipboard and shore-based researchers should refer to the IODP Sample, Data, and Obligations policy (**http://www.iodp.org/top-resources/program-documents/policies-and-guidelines**). This document outlines the policy for distributing IODP samples and data to research scientists, curators, and educators. The document also defines the obligations that sample and data recipients incur.

The Sample Allocation Committee (SAC) must approve all requests for core samples and data. The SAC is composed of the Co-Chief Scientists, Expedition Project Manager, and IODP Curator on shore or curatorial representative on board the ship. The SAC will work with the entire scientific party to formulate a formal expedition-specific sampling plan for shipboard and postexpedition sampling.

Scientists are expected to submit sample and data requests using the Sample and Data Request Database (**http://iodp.tamu.edu/sdrm**) several months before the beginning of the expedition. Based on shipboard and shore-based research plans submitted by this deadline, the SAC will prepare a tentative sampling plan that will be revised on the ship as dictated by recovery and expedition objectives. The sampling plan will be subject to modification depending upon the actual material recovered and collaborations that may evolve between scientists during the expedition. Modification of the strategy during the expedition must be approved by the SAC.

The minimum permanent archive will be the standard archive half of each core. All sample frequencies and sizes must be justified on a scientific basis and will depend on core recovery, the full spectrum of other requests, and the expedition objectives. Some redundancy of measurement is unavoidable, but minimizing the duplication of measurements among the shipboard party and identified shore-based collaborators will be a factor in evaluating sample requests.

If some critical intervals are recovered, there may be considerable demand for samples from a limited amount of cored material. These intervals may require special handling, a higher sampling density, reduced sample size, or continuous core sampling for the highest priority research objectives.

Following Expedition 374, cores will be delivered to the IODP Gulf Coast Repository in College Station, Texas (USA). All collected data and samples will be protected by a 1 y moratorium period following the completion of the postexpedition sampling meeting, during which time data and samples will be available only to the Expedition 374 science party and approved shore-based participants.

Expedition scientists and scientific participants

The current list of participants for Expedition 374 can be found at **http://iodp.tamu.edu/scienceops/expeditions/ross_sea_ice_sheet_history.html**.

References

Ainley, D.G., and Jacobs, S.S., 1981. Sea-bird affinities for ocean and ice boundaries in the Antarctic. *Deep Sea Research, Part A: Oceanographic Research Papers,* 28(10):1173–1185. **https://doi.org/10.1016/0198-0149(81)90054-6**

Alonso, B., Anderson, J.B., Diaz, J.I., and Bartek, L.R., 1992. Pliocene–Pleistocene seismic stratigraphy of the Ross Sea: evidence for multiple ice sheet grounding episodes. *In* Elliot, D.H. (Ed.), *Antarctic Research Series* (Volume 57): *Contributions to Antarctic Research III:* Washington DC (American Geophysical Union), 93–103. **https://doi.org/10.1029/AR057p0093**

Anderson, J.B., 1999. *Antarctic Marine Geology:* Cambridge, United Kingdom (Cambridge University Press). **https://doi.org/10.1017/CBO9780511759376**

Anderson, J.B., and Bartek, L.R., 1992. Cenozoic glacial history of the Ross Sea revealed by intermediate resolution seismic reflection data combined with drill site information. *In* Kennett J.P., and Warnke D. (Eds.), *Antarctic Research Series* (Volume 56): *The Antarctic Paleoenvironment: A Perspective on Global Change: Part One:* Washington DC (American Geophysical Union), 231–263. **https://doi.org/10.1029/AR056p0231**

Barrett, P.J., 1975. Textural characteristics of Cenozoic preglacial and glacial sediments at site 270, Ross Sea, Antarctica. *In* Hayes, D.E., Frakes, L.A., et al., *Initial Reports of the Deep Sea Drilling Project,* 28. Washington, DC (U.S Government Printing Office), 757–767. **https://doi.org/10.2973/dsdp.proc.28.122.1975**

Barrett, P.J., 1981. History of the Ross Sea region during the deposition of the Beacon Supergroup 400–180 million years ago. *Journal of the Royal Society of New Zealand,* 11(4):447–458. **https://doi.org/10.1080/03036758.1981.10423334**

Barrett, P.J., 1989. Antarctic Cenozoic history from the CIROS-1 drillhole, McMurdo Sound. *DRIS Bulletin,* 245.

Barrett, P.J., 2007. Cenozoic climate and sea level history from glaciomarine strata off the Victoria Land coast, Cape Roberts Project, Antarctica. *In* Hambrey, M.J., Christoffersen, P., Glasser, N.F., and Hubbard, B. (Eds.), *Glacial Sedimentary Processes and Products.* Special Publication of the International Association of Sedimentologists, 39:259–288.

Bart, P.J., 2003. Were West Antarctic Ice Sheet grounding events in the Ross Sea a consequence of East Antarctic Ice Sheet expansion during the middle Miocene? *Earth and Planetary Science Letters,* 216(1–2):93–107. **https://doi.org/10.1016/S0012-821X(03)00509-0**

Bart, P.J., De Batist, M., and Jokat, W., 1999. Interglacial collapse of Crary Trough-mouth fan, Weddell Sea, Antarctica: implications for Antarctic glacial history. *Journal of Sedimentary Research,* 69(6):1276–1289. **https://doi.org/10.2110/jsr.69.1276**

Bart, P.J., and De Santis, L., 2012. Glacial intensification during the Neogene: a review of seismic stratigraphic evidence from the Ross Sea, Antarctica, continental shelf. *Oceanography,* 25(3):166–183. **http://dx.doi.org/10.5670/oceanog.2012.92**

Bart, P.J., and Iwai, M., 2012. The overdeepening hyphothesis: how erosional modification of the marine-scape during the early Pliocene altered glacial dynamics on the Antarctic Peninsula's Pacific margin. *Palaeogeography, Palaeoclimatology, Palaeoecology,* 335–336:42–51. **https://doi.org/10.1016/j.palaeo.2011.06.010**

Bart, P.J., Sjunneskog, C., and Chow, J.M., 2011. Piston-core based biostratigraphic constraints on Pleistocene oscillations of the West Antarctic Ice Sheet in western Ross Sea between North Basin and AND-1B drill site. *Marine Geology,* 289(1–4):86–99. **https://doi.org/10.1016/j.margeo.2011.09.005**

Behrendt, J.C., LeMasurier, W.E., Cooper, A.K., Tessensohn, F., Tréhu, A., and Damaske, D., 1991. Geophysical studies of the West Antarctic rift system. *Tectonics,* 10(6):1257–1273. **https://doi.org/10.1029/91TC00868**

Bianchi, G.G., Hall, I.R., McCave, I.N., and Joseph, L., 1999. Measurement of the sortable silt current speed proxy using the Sedigraph 5100 and Coulter Multisizer IIe: precision and accuracy. *Sedimentology,* 46(6):1001–1014. **https://doi.org/10.1046/j.1365-3091.1999.00256.x**

Böhm, G., Ocakoğlu, N., Picotti, S., and De Santis, L., 2009. West Antarctic Ice Sheet evolution: new insights from a seismic tomographic 3D depth model in the Eastern Ross Sea (Antarctica). *Marine Geology,* 266(1–4):109–128. **https://doi.org/10.1016/j.margeo.2009.07.016**

Brancolini, G., Busetti, M., Marchetti, M., De Santis, L., Zanolla, C., Cooper, A.K., Cochrane, G.R., Zayatz, I., Belyaev, V., Knyazev, M., Vinnikovskaya, O., Davey, F.J., and Hinz, K., 1995. Seismic stratigraphic atlas of the Ross Sea, Antarctica. *In* Cooper, A.K., Barker, P.F., and Brancolini, G. (Eds.), *Antarctic Research Series* (Volume 68): *Geology and Seismic Stratigraphy of the Antarctic Margin:* Washington, DC (American Geophysical Union).

Caburlotto, A., Lucchi, R.G., De Santis, L., Macrì, P., and Tolotti, R., 2010. Sedimentary processes on the Wilkes Land continental rise reflect changes in glacial dynamic and bottom water flow. *International Journal of Earth Sciences,* 99(4):909–926. **https://doi.org/10.1007/s00531-009-0422-8**

Chow, J.M., and Bart, P.J., 2003. West Antarctic Ice Sheet grounding events on the Ross Sea outer continental shelf during the middle Miocene. *Palaeogeography, Palaeoclimatology, Palaeoecology,* 198(1–2):169–186. **https://doi.org/10.1016/S0031-0182(03)00400-0**

Cody, R., Levy, R., Crampton, J., Naish, T., Wilson, G., and Harwood, D., 2012. Selection and stability of quantitative stratigraphic age models: Plio–Pleistocene glaciomarine sediments in the ANDRILL 1B drillcore, McMurdo Ice Shelf. *Global and Planetary Change,* 96–97:143–156. **https://doi.org/10.1016/j.gloplacha.2012.05.017**

Cody, R.D., Levy, R.H., Harwood, D.M., and Sadler, P.M., 2008. Thinking outside the zone: high-resolution quantitative diatom biochronology for the Antarctic Neogene. *Palaeogeography, Palaeoclimatology, Palaeoecology,* 260(1–2):92–121. **http://dx.doi.org/10.1016/j.palaeo.2007.08.020**

Cook, C.P., van de Flierdt, T., Williams, T., Hemming, S.R., Iwai, M., Kobayashi, M., Jimenez-Espejo, F.J., Escutia, C., González, J.J., Khim, B.-K., McKay, R.M., Passchier, S., Bohaty, S.M., Riesselman, C.R., Tauxe, L., Sugisaki, S., Lopez Galindo, A., Patterson, M.O., Sangiorgi, F., Pierce, E.L., Brinkhuis, H., Klaus, A., Fehr, A., Bendle, J.A.P., Bijl, P.K., Carr, S.A., Dunbar, R.B., Flores, J.A., Hayden, T.G., Katsuki, K., Kong, G.S., Nakai, M., Olney, M.P., Pekar, S.F., Pross, J., Röhl, U., Sakai, T., Shrivastava, P.K., Stickley, C.E., Tuo, S., Welsh, K., and Yamane, M., 2013. Dynamic behaviour of the East Antarctic ice sheet during Pliocene warmth. *Nature Geoscience,* 6:765–769. **https://doi.org/10.1038/ngeo1889**

Cooper, A.K., Barrett, P.J., Hinz, K., Traube, V., Leitchenkov, G., and Stagg, H.M.J., 1991. Cenozoic prograding sequences of the Antarctic continental margin: a record of glacio-eustatic and tectonic events. *Marine Geology,* 102(1–4):175–213. **https://doi.org/10.1016/0025-3227(91)90008-R**

Cooper, A.K., and O'Brien, P.E., 2004. Leg 188 synthesis: transitions in the glacial history of the Prydz Bay region, East Antarctica, from ODP drilling. *In* Cooper, A.K., O'Brien, P.E., and Richter, C. (Eds.), *Proceedings of the Ocean Drilling Program, Scientific Results,* 188: College Station, TX (Ocean Drilling Program), 1–42. **https://doi.org/10.2973/odp.proc.sr.188.001.2004**

Cramer, B.S., Toggweiler, J.R., Wright, J.D., Katz, M.E., and Miller, K.G., 2009. Ocean overturning since the Late Cretaceous: inferences from a new benthic foraminiferal isotope compilation. *Paleoceanography,* 24(4). **https://doi.org/10.1029/2008PA001683**

Crampton, J.S., Cody, R.D., Levy, R., Harwood, D., McKay, R., and Naish, T.R., 2016. Southern Ocean phytoplankton turnover in response to stepwise Antarctic cooling over the past 15 million years. *Proceedings of the National Academy of Sciences,* 113(25):6868–6873. **https://doi.org/10.1073/pnas.1600318113**

Dahl-Jensen, D., Albert, M.R., Aldahan, A., et al., 2013. Eemian interglacial reconstructed from a Greenland folded ice core. *Nature,* 493(7433):489–494. **https://doi.org/10.1038/nature11789**

Davey, F.J., 2004. Ross Sea bathymetry, 1:200,000. *Institute of Geological & Nuclear Sciences Geophysical Map,* 16.

De Santis, L., Anderson, J.B., Brancolini, G., and Zayatz, I., 1995. Seismic record of late Oligocene through Miocene glaciation on the Central and Eastern Continental Shelf of the Ross Sea. *In* Cooper, A.K., Barker, P.F., and Brancolini, G. (Eds.), *Antarctic Research Series* (Volume 68): *Geology and Seismic Stratigraphy of the Antarctic Margin:* Washington, DC (American Geophysical Union), 235–260. **https://doi.org/10.1029/AR068p0235**

De Santis, L., Prato, S., Brancolini, G., Lovo, M., and Torelli, L., 1999. The eastern Ross Sea continental shelf during the Cenozoic: implications for the West Antarctic ice sheet development. *Global and Planetary Change,* 23(1–4):173–196. **https://doi.org/10.1016/S0921-8181(99)00056-9**

Decesari, R.C., Sorlien, C.C., Luyendyk, B.P., Wilson, D.S., Bartek, L., Diebold, J., and Hopkins, S.E., 2007. Regional seismic stratigraphic correlations of the Ross Sea: implications for the tectonic history of the West Antarctic rift system. *In* Cooper, A.K., Raymond, C.R., et al. (Eds.), *Antarctica: A Keystone in a Changing World–Online Proceedings of the 10th ISAES.* USGS Open File Report 2007-1047, Short Research Paper 052. **https://doi.org/10.3133/of2007-1047.srp052**

DeConto, R.M., and Pollard, D., 2016. Contribution of Antarctica to past and future sea-level rise. *Nature,* 531(7596):591–597. **https://doi.org/10.1038/nature17145**

Elderfield, H., Ferretti, P., Greaves, M., Crowhurst, S., McCave, I.N., Hodell, D., and Piotrowski, A.M., 2012. Evolution of ocean temperature and ice volume through the mid-Pleistocene Climate Transition. *Science,* 337(6095):704–709. **https://doi.org/10.1126/science.1221294**

Escutia, C., Brinkhuis, H., Klaus, A., and the Expedition 318 Scientists, 2011. *Proceedings of the Integrated Ocean Drilling Program,* 318: Tokyo (Integrated Ocean Drilling Program Management International, Inc.). **https://doi.org/10.2204/iodp.proc.318.2011**

Exon, N.F., Kennett, J.P., Malone, M., et al., 2001. *Proceedings of the Ocean Drilling Program, Initial Reports,* 189: College Station, TX (Ocean Drilling Program). **https://doi.org/10.2973/odp.proc.ir.189.2001**

Feakins, S.J., Warny, S., and Lee, J.-E., 2012. Hydrologic cycling over Antarctica during the middle Miocene warming. *Nature Geoscience,* 5(8):557–560. **https://doi.org/10.1038/ngeo1498**

Fielding, C.R., Browne, G.H., Field, B., Florindo, F., Harwood, D.M., Krissek, L.A., Levy, R.H., Panter, K.S., Passchier, S., and Pekar, S.F., 2011. Sequence stratigraphy of the ANDRILL AND-2A drillcore, Antarctica: a long-term, ice-proximal record of early to mid-Miocene climate, sea-level and glacial dynamism. *Palaeogeography, Palaeoclimatology, Palaeoecology,* 305(1–4):337–351. **https://doi.org/10.1016/j.palaeo.2011.03.026**

Fielding, C.R., Naish, T.R., Woolfe, K.J., and Lavelle, M.A., 2000. Facies analysis and sequence stratigraphy of CRP-2/2A, Victoria Land Basin, Antarctica. *Terra Antartica* ,7(3):323–338. **https://epic.awi.de/27384/1/Fie2000b.pdf**

Florindo, F., Bohaty, S.M., Erwin, P.S., Richter, C., Roberts, A.P., Whalen, P.A., and Whitehead, J.M., 2003. Magnetobiostratigraphic chronology and palaeoenvironmental history of Cenozoic sequences from ODP sites 1165 and 1166, Prydz Bay, Antarctica. *In* Florindo, F., Cooper, A.K., and O'Brien, P.E. (Eds.), *Antarctic Cenozoic Palaeoenvironments: Geologic Record and Models.* Palaeogeography, Palaeoclimatology, Palaeoecology, 198(1–2):69–100. **https://doi.org/10.1016/S0031-0182(03)00395-X**

Florindo, F., Wilson, G.S., Roberts, A.P., Sagnotti, L., and Verosub, K.L., 2005. Magnetostratigraphic chronology of a late Eocene to early Miocene glaciomarine succession from Victoria Land Basin, Ross Sea, Antarctica. *Global and Planetary Change,* 45(1–3):207–236. **http://dx.doi.org/10.1016/j.gloplacha.2004.09.009**

Flower, B.P., and Kennett, J.P., 1994. The middle Miocene climatic transition: East Antarctic ice sheet development, deep ocean circulation and global carbon cycling. *Palaeogeography, Palaeoclimatology, Palaeoecology,* 108(3–4):537–555. **http://dx.doi.org/10.1016/0031-0182(94)90251-8**

Ford, A.B., and Barrett, P.J., 1975. Basement rocks of the south-central Ross Sea, Site 270, DSDP Leg 28. *In* Hayes, D.E., Frakes, L.A., et al., *Initial Reports of the Deep Sea Drilling Project,* 28. Washington DC (U.S. Government Printing Office), 861–868. **https://doi.org/10.2973/dsdp.proc.28.131.1975**

Foster, G.L., Lear, C.H., and Rae, J.W.B., 2012. The evolution of pCO_2, ice volume and climate during the middle Miocene. *Earth and Planetary Science Letters,* 341–344:243–254. **https://doi.org/http://dx.doi.org/10.1016/j.epsl.2012.06.007**

Galeotti, S., DeConto, R., Naish, T., Stocchi, P., Florindo, F., Pagani, M., Barrett, P., Bohaty, S.M., Lanci, L., Pollard, D., Sandroni, S., Talarico, F.M., and Zachos, J.C., 2016. Antarctic Ice Sheet variability across the Eocene–Oligocene boundary climate transition. *Science,* 352(6281):76–80. **https://doi.org/10.1126/science.aab0669**

Gasson, E., DeConto, R.M., Pollard, D., and Levy, R.H., 2016. Dynamic Antarctic Ice Sheet during the early to mid-Miocene. *Proceedings of the National Academy of Sciences of the United States of America,* 113(13):3459–3464. **https://doi.org/10.1073/pnas.1516130113**

Golledge, N.R., Fogwill, C.J., Mackintosh, A.N., and Buckley, K.M., 2012. Dynamics of the Last Glacial Maximum Antarctic Ice Sheet and its response to ocean forcing. *Proceedings of the National Academy of Sciences of the United States of America,* 109(40):16052–16056. **https://doi.org/10.1073/pnas.1205385109**

Grützner, J., Rebesco, M.A., Cooper, A.K., Forsberg, C.F., Kryc, K.A., and Wefer, G., 2003. Evidence for orbitally controlled size variations of the East Antarctic Ice Sheet during the late Miocene. *Geology,* 31(9):777–780. **https://doi.org/10.1130/G19574.1**

Hall, I.R., McCave, I.N., Shackleton, N.J., Weedon, G.P., and Harris, S.E., 2001. Intensified deep Pacific inflow and ventilation in Pleistocene glacial times. *Nature,* 412(6849):809–812. **https://doi.org/10.1038/35090552**

Hayes, D.E., Frakes, L.A., et al., 1975. *Initial Reports of the Deep Sea Drilling Project,* 28: Washington, DC (U.S. Govt. Printing Office). **https://doi.org/10.2973/dsdp.proc.28.1975**

Hepp, D.A., Mörz, T., and Grützner, J., 2006. Pliocene glacial cyclicity in a deep-sea sediment drift (Antarctic Peninsula Pacific Margin). *Palaeogeography, Palaeoclimatology, Palaeoecology,* 231(1–2):181–198. **https://doi.org/10.1016/j.palaeo.2005.07.030**

Hodell, D.A., and Venz-Curtis, K.A., 2006. Late Neogene history of deepwater ventilation in the Southern Ocean. *Geochem., Geophys. Geosyst.,* 7(9). **https://doi.org/10.1029/2005GC001211**

Holbourn, A., Kuhnt, W., Schulz, M., Flores, J.-A., and Andersen, N., 2007. Orbitally-paced climate evolution during the middle Miocene "Monterey" carbon-isotope excursion. *Earth and Planetary Science Letters,* 261(3–4):534–550. **http://dx.doi.org/10.1016/j.epsl.2007.07.026**

Houben, A.J.P., Bijl, P.K., Pross, J., Bohaty, S.M., Passchier, S., Stickley, C.E., Röhl, U., Sugisaki, S., Tauxe, L., van de Flierdt, T., Olney, M., Sangiorgi, F., Sluijs, A., Escutia, C., Brinkhuis, H., and the Expedition 318 Scientists, 2013. Reorganization of Southern Ocean plankton ecosystem at the onset of Antarctic glaciation. *Science,* 340(6130):341–344. **https://doi.org/10.1126/science.1223646**

Huybers, P., 2006. Early Pleistocene glacial cycles and the integrated summer insolation forcing. *Science,* 313(5786):508–511. **https://doi.org/10.1126/science.1125249**

Jacobs, S.S., Giulivi, C.F., and Mele, P.A., 2002. Freshening of the Ross Sea during the late 20th Century. *Science,* 297(5580):386–389. **https://doi.org/10.1126/science.1069574**

Jacobs, S.S., Jenkins, A., Giulivi, C.F., and Dutrieux, P., 2011. Stronger ocean circulation and increased melting under Pine Island Glacier ice shelf. *Nature Geoscience,* 4(8):519–523. **https://doi.org/10.1038/ngeo1188**

Joseph, L.H., Rea, D.K., and van der Pluijm, B.A., 2004. Neogene history of the Deep Western Boundary Current at Rekohu sediment drift, Southwest Pacific (ODP Site 1124). *In* McCave, I.N., Carter, L., Carter, R.M., and Hayward, B.W. (Eds.), *Cenozoic Oceanographic Evolution of the Southwest Pacific Gateway, ODP Leg 181.* Marine Geology, 205(1–4):185–206. **https://doi.org/10.1016/S0025-3227(04)00023-4**

Joughin, I., Alley, R.B., and Holland, D.M., 2012. Ice-sheet response to oceanic forcing. *Science,* 338(6111):1172–1176. **https://doi.org/10.1126/science.1226481**

Karner, G.D., Studinger, M., and Bell, R.E., 2005. Gravity anomalies of sedimentary basins and their mechanical implications: application to the Ross Sea basins, West Antarctica. *Earth and Planetary Science Letters,* 235(3–4):577–596. **https://doi.org/10.1016/j.epsl.2005.04.016**

Kennett, J.P., 1977. Cenozoic evolution of Antarctic glaciation, the circum-Antarctic Ocean, and their impact on global paleoceanography. *Journal of Geophysical Research,* 82(27):3843–3860. **https://doi.org/10.1029/JC082i027p03843**

Kennett, J.P., and Barker, P.F., 1990. Latest Cretaceous to Cenozoic climate and oceanographic developments in the Weddell Sea, Antarctica: an ocean-drilling perspective. *In* Barker, P.F., Kennett, J.P., et al., *Proceedings of the Ocean Drilling Program, Scientific Results,* 113: College Station, TX (Ocean Drilling Program), 937–960. **https://doi.org/10.2973/odp.proc.sr.113.195.1990**

Kominz, M.A., Browning, J.V., Miller, K.G., Sugarman, P.J., Misintseva, S., and Scotese, C.R., 2008. Late Cretaceous to Miocene sea-level estimates from the New Jersey and Delaware coastal plain coreholes: an error analysis. *Basin Research,* 20(2):211–226. **http://dx.doi.org/10.1111/j.1365-2117.2008.00354.x**

Kopp, R.E., Simons, F.J., Mitrovica, J.X., Maloof, A.C., and Oppenheimer, M., 2009. Probabilistic assessment of sea level during the last interglacial stage. *Nature,* 462(7275):863–867. **https://doi.org/10.1038/nature08686**

Levy, R., Harwood, D., Florindo, F., Sangiorgi, F., Tripati, R., von Eynatten, H., Gasson, E., Kuhn, G., Tripati, A., DeConto, R., Fielding, C., Field, B., Golledge, N., McKay, R., Naish, T., Olney, M., Pollard, D., Schouten, S., Talarico, F., Warny, S., Willmott, V., Acton, G., Panter, K., Paulsen, T., Taviani, M., and the SMS Science Team, 2016. Antarctic Ice Sheet sensitivity to atmospheric CO_2 variations in the early to mid-Miocene. *Proceedings of the National Academy of Sciences of the United States of America,* 113(13):3453–3458. **https://doi.org/10.1073/pnas.1516030113**

Lewis, A.R., Marchant, D.R., Ashworth, A.C., Hedenäs, L., Hemming, S.R., Johnson, J.V., Leng, M.J., Machlus, M.L., Newton, A.E., Raine, J.I., Willenbring, J.K., Williams, M., and Wolfe, A.P., 2008. Mid-Miocene cooling and the extinction of tundra in continental Antarctica. *Proceedings of the National Academy of Sciences of the United States of America,* 105(31):10676–. **https://doi.org/10.1073/pnas.0802501105**

Lewis, A.R., Marchant, D.R., Kowalewski, D.E., Baldwin, S.L., and Webb, L.E., 2006. The age and origin of the Labyrinth, western Dry Valleys, Antarctica: evidence for extensive middle Miocene subglacial floods and freshwater discharge to the Southern Ocean. *Geology,* 34(7):513–516. **https://doi.org/10.1130/G22145.1**

Licht, K.J., Lederer, J.R., and Swope, R.J., 2005. Provenance of LGM glacial till (sand fraction) across the Ross Embayment, Antarctica. *Quaternary Science Reviews,* 24(12–13):1499–1520. **https://doi.org/10.1016/j.quascirev.2004.10.017**

Lisiecki, L.E., and Raymo, M.E., 2005. A Pliocene–Pleistocene stack of 57 globally distributed benthic $\delta^{18}O$ records. *Paleoceanography,* 20(1):PA1003. **http://dx.doi.org/10.1029/2004PA001071**

Lucchi, R.G., and Rebesco, M., 2007. Glacial contourites on the Antarctic Peninsula margin: insight for palaeoenvironmental and palaeoclimatic conditions. *Geological Society Special Publication,* 276(1):111–127. **https://doi.org/10.1144/GSL.SP.2007.276.01.06**

Luyendyk, B.P., Sorlien, C.C., Wilson, D.S., Bartek, L.R., and Siddoway, C.S., 2001. Structural and tectonic evolution of the Ross Sea rift in the Cape Colbeck region, Eastern Ross Sea, Antarctica. *Tectonics,* 20(6):933–958. **https://doi.org/10.1029/2000TC001260**

Masson-Delmotte, V., Schulz, M., Abe-Ouchi, A., Beer, J., Ganopolski, A., González Rouco, J.F., Jansen, E., Lambeck, K., Luterbacher, J., Naish, T., Osborn, T., Otto-Bliesner, B., Quinn, T., Ramesh, R., Rojas, M., Shao, X., and Timmerman, A., 2013. Information from paleoclimate archives. *In* Stocker, T.F., Qin, D., Plattner, G.-K., Tignor, M., Allen, S.K., Boschung, J., Nauels, A., Xia, Y., Bex, V., and Midgley, P.M. (Eds.), *Climate Change 2013: The Physical Science Basis. Contribution of Working Group I to the Fifth Assessment Report of the Intergovernmental Panel on Climate Change:* Cambridge, United Kingdom (Cambridge University Press), 383–464. **http://www.climatechange2013.org/images/report/WG1AR5_Chapter05_FINAL.pdf**

McKay, R., Browne, G., Carter, L., Cowan, E., Dunbar, G., Krissek, L., Naish, T., Powell, R., Reed, J., Talarico, F., and Wilch, T., 2009. The stratigraphic signature of the late Cenozoic Antarctic Ice Sheets in the Ross Embayment. *Geological Society of America Bulletin,* 121(11–12):1537–1561. **https://doi.org/10.1130/B26540.1**

McKay, R., Naish, T., Carter, L., Riesselman, C., Dunbar, R., Sjunneskog, C., Winter, D., Sangiorgi, F., Warren, C., Pagani, M., Schouten, S., Willmott, V., Levy, R., DeConto, R., and Powell, R.D., 2012a. Antarctic and Southern Ocean influences on late Pliocene global cooling. *Proceedings of the National Academy of Sciences of the United States of America,* 109(17):6423–6428. **https://doi.org/10.1073/pnas.1112248109**

McKay, R., Naish, T., Powell, R., Barrett, P., Scherer, R., Talarico, F., Kyle, P., Monien, D., Kuhn, G., Jackolski, C., and Williams, T., 2012b. Pleistocene variability of Antarctic ice sheet extent in the Ross Embayment. *Quaternary Science Reviews,* 34:93–112. **https://doi.org/10.1016/j.quascirev.2011.12.012**

Meinshausen, M., Smith, S.J., Calvin, K., Daniel, J.S., Kainuma, M.L.T., Lamarque, J.-F., Matsumoto, K., Montzka, S.A., Raper, S.C.B., Riahi, K., Thomson, A., Velders, G.J.M., and van Vuuren, D.P.P., 2011. The RCP greenhouse gas concentrations and their extensions from 1765 to 2300. *Climatic Change,* 109:213–241. **https://doi.org/10.1007/s10584-011-0156-z**

Mercer, J.H., 1978. West Antarctic Ice Sheet and CO_2 greenhouse effect: a threat of disaster. *Nature,* 271(5643):321–325. **https://doi.org/10.1038/271321a0**

Miller, K.G., Kominz, M.A., Browning, J.V., Wright, J.D., Mountain, G.S., Katz, M.E., Sugarman, P.J., Cramer, B.S., Christie-Blick, N., and Pekar, S.F., 2005. The Phanerozoic record of global sea-level change. *Science,* 310(5752):1293–1298. **https://doi.org/10.1126/science.1116412**

Miller, K.G., Mountain, G.S., Wright, J.D., and Browning, J.V., 2011. A 180-million-year record of sea level and ice volume variations from continental margin and deep-sea isotopic records. *Oceanography,* 24(2):40–53. **https://doi.org/10.5670/oceanog.2011.26**

Miller, K.G., Wright, J.D., Browning, J.V., Kulpecz, A., Kominz, M., Naish, T.R., Cramer, B.S., Rosenthal, Y., Peltier, W.R., and Sosdian, S., 2012. High tide of the warm Pliocene: implications of global sea level for Antarctic deglaciation. *Geology,* 40(5):407–410. **https://doi.org/10.1130/G32869.1**

Naish, T., Powell, R., Levy, R., Wilson, G., Scherer, R., Talarico, F., Krissek, L., Niessen, F., Pompilio, M., Wilson, T., Carter, L., DeConto, R., Huybers, P., McKay, R., Pollard, D., Ross, J., Winder, D., Barrett, P., Browne, G., Cody, R., Cowan, E., Crampton, J., Dunbar, G., Dunbar, N., Florindo, F., Gebhardt, C., Graham, I., Hannah, M., Hansaraj, D., Harwood, D., Helling, D., Henrys, S., Hinnov, L., Kuhn, G., Kyle, P., Läufer, A., Maffioli, P., Magens, D., Mandernack, K., McIntosh, W., Millan, C., Morin, R., Ohneiser, C., Paulsen, T., Persico, D., Raine, I., Reed, J., Riesselman, C., Sagnotti, L., Schmitt, D., Sjunneskog, C., Strong, P., Taviani, M., Vogel, S., Wilch, T., and Williams, T., 2009. Obliquity-paced Pliocene West Antarctic ice sheet oscillations. *Nature,* 458(7236):322–328. **https://doi.org/10.1038/nature07867**

Naish, T.R., and Wilson, G.S., 2009. Constraints on the amplitude of mid-Pliocene (3.6–2.4 Ma) eustatic sea-level fluctuations from the New Zealand shallow-marine sediment record. *Philosophical Transactions of the Royal Society, A: Mathematical, Physical & Engineering Sciences,* 367(1886):169–187. **https://doi.org/10.1098/rsta.2008.0223**

Naish, T.R., Woolfe, K.J., Barrett, P.J., Wilson, G.S., Atkins, C., Bohaty, S.M., Bücker, C.J., Claps, M., Davey, F.J., Dunbar, G.B., Dunn, A.G., Fielding, C.R., Florindo, F., Hannah, M.J., Harwood, D.M., Henrys, S.A., Krissek, L.A., Lavelle, M., van der Meer, J., McIntosh, W.C., Niessen, F., Passchier, S., Powell, R.D., Roberts, A.P., Sagnotti, L., Scherer, R.P., Strong, C.P., Talarico, F., Verosub, K.L., Villa, G., Watkins, D.K., Webb, P.-N., and Wonik, T., 2001. Orbitally induced oscillations in the East Antarctic Ice Sheet at the Oligocene/Miocene boundary. *Nature,* 413(6857):719–723. **https://doi.org/10.1038/35099534**

Newkirk, D., and Martin, E.E., 2009. Circulation through the Central American Seaway during the Miocene carbonate crash. *Geology,* 37(1):87–90. **https://doi.org/10.1130/G25193A.1**

Orsi, A.H., and Wiederwohl, C.L., 2009. A recount of Ross Sea waters. *Deep Sea Research, Part II: Topical Studies in Oceanography,* 56(13–14):778–795. **https://doi.org/10.1016/j.dsr2.2008.10.033**

Pagani, M., Zachos, J.C., Freeman, K.H., Tipple, B., and Bohaty, S., 2005. Marked decline in atmospheric carbon dioxide concentrations during the Paleogene. *Science,* 309(5734):600–603. **http://dx.doi.org/10.1126/science.1110063**

Passchier, S., Browne, G., Field, B., Fielding, C.R., Krissek, L.A., Panter, K., Pekar, S.F., and ANDRILL-SMS Science Team, 2011. Early and middle Miocene Antarctic glacial history from the sedimentary facies distribution in the AND-2A drill hole, Ross Sea, Antarctica. *Geological Society of America Bulletin,* 123(11–12):2352–2365. **https://doi.org/10.1130/B30334.1**

Patterson, M.O., McKay, R., Naish, T., Escutia, C., Jimenez-Espejo, F.J., Raymo, M.E., Meyers, S.R., Tauxe, L., Brinkhuis, H., and IODP Expedition 318 Scientists, 2014. Orbital forcing of the East Antarctic ice sheet during the Pliocene and early Pleistocene. *Nature Geoscience,* 7:841–847. **https://doi.org/10.1038/ngeo2273**

Pollard, D., and DeConto, R.M, 2009. Modelling West Antarctic ice sheet growth and collapse through the past five million years. *Nature,* 458(7236):329–332. **https://doi.org/10.1038/nature07809**

Powell, R.D., and Cooper, J.M., 2002. A glacial sequence stratigraphic model for temperate, glaciated continental shelves. *In* Dowdeswell, J.A., and Ó'Cofaigh, C. (Eds.), *Glacier-Influenced Sedimentation on High-Latitude Continental Margins.* Geological Society Special Publication, 203:215–244. **https://doi.org/10.1144/GSL.SP.2002.203.01.12**

Prins, M.A., Bouwer, L.M., Beets, C.J., Troelstra, S.R., Weltje, G.J., Kruk, R.W., Kuijpers, A., and Vroon, P.Z., 2002. Ocean circulation and iceberg discharge in the glacial North Atlantic: inferences from unmixing of sediment size distributions. *Geology,* 30(6):555–558. **https://doi.org/10.1130/0091-7613(2002)030<0555:OCAIDI>2.0.CO;2**

Pritchard, H.D., Ligtenberg, S.R.M., Fricker, H.A., Vaughan, D.G., van den Broeke, M.R., and Padman, L., 2012. Antarctic ice-sheet loss driven by basal melting of ice shelves. *Nature,* 484(7395):502–505. **https://doi.org/10.1038/nature10968**

Purkey, S.G., and Johnson, G.C., 2010. Warming of global abyssal and deep Southern Ocean waters between the 1990s and 2000s: contributions to global heat and sea level rise budgets. *Journal of Climate,* 23(23):6336–6351. **https://doi.org/10.1175/2010JCLI3682.1**

Raymo, M.E., Lisiecki, L.E., and Nisancioglu, K.H., 2006. Plio–Pleistocene ice volume, Antarctic climate, and the global $\delta^{18}O$ record. *Science,* 313(5786):492–495. **https://doi.org/10.1126/science.1123296**

Raymo, M.E., Mitrovica, J.X., O'Leary, M.J., DeConto, R.M., and Hearty, P.J., 2011. Departures from eustasy in Pliocene sea-level records. *Nature Geoscience,* 4(5):328–332. **https://doi.org/10.1038/ngeo1118**

Rebesco, M., Camerlenghi, A., Geletti, R., and Canals, M., 2006. Margin architecture reveals the transition to the modern Antarctic Ice Sheet (AIS) ca. 3 Ma. *Geology,* 34(4):301–304. **https://doi.org/10.1130/G22000.1**

Scher, H.D., and Martin, E.E., 2006. Timing and climatic consequences of the opening of Drake Passage. *Science,* 312(5772):428–430. **https://doi.org/10.1126/science.1120044**

Scherer, R.P., Aldahan, A., Tulaczyk, S., Possnert, G., Engelhardt, H., and Kamb, B., 1998. Pleistocene collapse of the West Antarctic Ice Sheet. *Science,* 281(5373):82–85. **https://doi.org/10.1126/science.281.5373.82**

Scherer, R.P., Bohaty, S.M., Dunbar, R.B., Esper, O., Flores, J.-A., Gersonde, R., Harwood, D.M., Roberts, A.P., and Taviani, M., 2008. Antarctic records of precession-paced insolation-driven warming during early Pleistocene marine isotope Stage 31. *Geophysical Research Letters,* 35(3):L03505. **https://doi.org/10.1029/2007GL032254**

Shepherd, A., Ivins, E.R., Geruo, A., Barletta, V.R., Bentley, M.J., Bettadpur, S., Briggs, K.H., Bromwich, D.H., Forsberg, R., Galin, N., Horwath, M., Jacobs, S., Joughin, I., King, M.A., Lenaerts, J.T.M., Li, J., Ligtenberg, S.R.M., Luckman, A., Luthcke, S.B., McMillan, M., Meister, R., Milne, G., Mouginot, J., Muir, A., Nicolas, J.P., Paden, J., Payne, A.J., Pritchard, H., Rignot, E., Rott, H., Sandberg Sørensen, L., Scambos, T.A., Scheuchl, B., Schrama, E.J.O., Smith, B., Sundal, A.V., van Angelen, J.H., van de Berg, W.J., van den Broeke, M.R., Vaughan, D.G., Velicogna, I., Wahr, J., Whitehouse, P.L., Wingham, D.J., Yi, D., Young, D., and Zwally, H.J., 2012. A reconciled estimate of ice-sheet mass balance. *Science,* 338(6111):1183–1189. **https://doi.org/10.1126/science.1228102**

Shevenell, A.E., Ingalls, A.E., Domack, E.W., and Kelly, C., 2011. Holocene Southern Ocean surface temperature variability west of the Antarctic Peninsula. *Nature,* 470(7333):250–254. **https://doi.org/10.1038/nature09751**

Shevenell, A.E., Kennett, J.P., and Lea, D.W., 2004. Middle Miocene Southern Ocean cooling and Antarctic cryosphere expansion. *Science,* 305(5691):1766–1770. **http://dx.doi.org/10.1126/science.1100061**

Shevenell, A.E., Kennett, J.P., and Lea, D.W., 2008. Middle Miocene ice sheet dynamics, deep-sea temperatures, and carbon cycling: a Southern Ocean perspective. *Geochemistry, Geophysics, Geosystems,* 9(2):Q02006. **https://doi.org/10.1029/2007GC001736**

Siddoway, C.S., Baldwin, S.L., Fitzgerald, P.G., Fanning, C.M., and Luyendyk, B.P., 2004. Ross Sea mylonites and the timing of intracontinental extension within the West Antarctic rift system. *Geology,* 32(1):57–60. **https://doi.org/10.1130/G20005.1**

Smith, W.O., Jr., Sedwick, P.N., Arrigo, K.R., Ainley, D.G., and Orsi, A.H., 2012. The Ross Sea in a sea of change. *Oceanography,* 25(3):90–103. **https://doi.org/10.5670/oceanog.2012.80**

Tauxe, L., Stickley, C.E., Sugisaki, S., Bijl, P.K., Bohaty, S.M., Brinkhuis, H., Escutia, C., Flores, J.A., Houben, A.J.P., Iwai, M., Jiménez-Espejo, F., McKay, R., Passchier, S., Pross, J., Riesselman, C.R., Röhl, U., Sangiorgi, F., Welsh, K., Klaus, A., Fehr, A., Bendle, J.A.P., Dunbar, R., Gonzàlez, J., Hayden, T., Katsuki, K., Olney, M.P., Pekar, S.F., Shrivastava, P.K., van de Flierdt, T., Williams, T., and Yamane, M., 2012. Chronostratigraphic framework for the IODP Expedition 318 cores from the Wilkes Land Margin: constraints for paleoceanographic reconstruction. *Paleoceanography,* 27(2):PA2214. **https://doi.org/10.1029/2012PA002308**

Ten Brink, U.S., Schneider, C., and Johnson, A.H., 1995. Morphology and stratal geometry of the Antarctic continental shelf: insights from models. *In* Cooper, A.K., Barker, P.F., and Brancolini, G. (Eds.), *Antarctic Research Series* (Volume 68): *Geology and Seismic Stratigraphy of the Antarctic Margin:* Washington, DC (American Geophysical Union), 1–24. **https://doi.org/10.1029/AR068p0001**

Theissen, K.M., Dunbar, R.B., Cooper, A.K, Mucciarone, D.A., and Hoffmann, D., 2003. The Pleistocene evolution of the East Antarctic Ice Sheet in the Prydz bay region: stable isotopic evidence from ODP Site 1167. *Global and Planetary Change,* 39(3–4):227–256. **https://doi.org/10.1016/S0921-8181(03)00118-8**

Tzedakis, P.C., Crucifix, M., Mitsui, T., and Wolff, E.W., 2017. A simple rule to determine which insolation cycles lead to interglacials. *Nature,* 542(7642):427–432. **https://doi.org/10.1038/nature21364**

Villa, G., Lupi, C., Cobianchi, M., Florindo, F., and Pekar, S.F., 2008. A Pleistocene warming event at 1 Ma in Prydz Bay, East Antarctica: evidence from ODP Site 1165. *Palaeogeography, Palaeoclimatology, Palaeoecology,* 260(1–2):230–244. **https://doi.org/10.1016/j.palaeo.2007.08.017**

Vincent, E., and Berger, W.H., 1985. Carbon dioxide and polar cooling in the Miocene: the Monterey Hypothesis. *In* Sundquist, E.T., and Broecker, W.S. (Eds.), *The Carbon Cycle and Atmospheric CO_2: Natural Variations Archean to Present.* Geophysical Monograph, 32:455–468. **https://doi.org/10.1029/GM032p0455**

Warny, S., Askin, R.A., Hannah, M.J., Mohr, B.A.R., Raine, J.I., Harwood, D.M., Florindo, F., and the SMS Science Team, 2009. Palynomorphs from a sediment core reveal a sudden remarkably warm Antarctica during the middle Miocene. *Geology,* 37(10):955–958. **https://doi.org/10.1130/G30139A.1**

Whitworth, T., III, Orsi, A.H., Kim, S.-J., Nowlin, W.D., Jr., and Locarnini, R.A., 1995. Water masses and mixing near the Antarctic slope front. *In* Jacobs, S.S., and Weiss, R.F. (Eds.), *Antarctic Research Series* (Volume 75): *Ocean, Ice, and Atmosphere: Interactions at the Antarctic Continental Margin:* Washington, DC (American Geophysical Union), 1–27. **http://onlinelibrary.wiley.com/doi/10.1029/AR075p0001/summary**

Wilch, T.I., McIntosh, W.C., and Dunbar, N.W., 1999. Late Quaternary volcanic activity in Marie Byrd Land: potential $^{40}Ar/^{39}Ar$-dated time horizons in West Antarctic ice and marine cores. *Geological Society of America Bulletin,* 111(10):1563–1580. **https://doi.org/10.1130/0016-7606(1999)111<1563:LQVAIM>2.3.CO;2**

Williams, T., and Handwerger, D., 2005. A high-resolution record of early Miocene Antarctic glacial history from ODP Site 1165, Prydz Bay. *Paleoceanography,* 20(2):PA2017. **https://doi.org/10.1029/2004PA001067**

Williams, T., Morin, R.H., Jarrard, R.D., Jackolski, C.L., Henrys, S.A., Niessen, F., Magens, D., Kuhn, G., Monien, D., and Powell, R.D., 2012. Lithostratigraphy from downhole logs in Hole AND-1B, Antarctica. *Geosphere,* 8(1):127–140. **https://doi.org/10.1130/GES00655.1**

Wilson, D.S., and Luyendyk, B.P., 2009. West Antarctic paleotopography estimated at the Eocene–Oligocene climate transition. *Geophysical Research Letters,* 36(16):L16302. **https://doi.org/10.1029/2009GL039297**

Wilson, D.S., Pollard, D., DeConto, R.M., Jamieson, S.S.R., and Luyendyk, B.P., 2013. Initiation of the West Antarctic Ice Sheet and estimates of total Antarctic ice volume in the earliest Oligocene. *Geophysical Research Letters,* 40(16):4305–4309. **https://doi.org/10.1002/grl.50797**

Wilson, G.S., Levy, R.H., Naish, T.R., Powell, R.D., Florindo, F., Ohneiser, C., Sagnotti, L., Winter, D.M., Cody, R., Henrys, S., Ross, J., Krissek, L., Niessen, F., Pompillio, M., Scherer, R., Alloway, B.V., Barrett, P.J., Brachfeld, S., Browne, G., Carter, L., Cowan, E., Crampton, J., DeConto, R.M., Dunbar, G., Dunbar, N., Dunbar, R., von Eynatten, H., Gebhardt, C., Giorgetti, G., Graham, I., Hannah, M., Hansaraj, D., Harwood, D.M., Hinnov, L., Jarrard, R.D., Joseph, L., Kominz, M., Kuhn, G., Kyle, P., Läufer, A., McIntosh, W.C., McKay, R., Maffioli, P., Magens, D., Millan, C., Monien, D., Morin, R., Paulsen, T., Persico, D., Pollard, D., Raine, J.I., Riesselman, C., Sandroni, S., Schmitt, D., Sjunneskog, C., Strong, C.P., Talarico, F., Taviani, M., Villa, G., Vogel, S., Wilch, T., Williams, T., Wilson, T.J., and Wise, S., 2012. Neogene tectonic and climatic evolution of the Western Ross Sea, Antarctica—chronology of events from the AND-1B drill hole. *Global and Planetary Change,* 96–97:189–203. **https://doi.org/10.1016/j.gloplacha.2012.05.019**

Woodruff, F., and Savin, S.M., 1985. $\delta^{13}C$ values of Miocene Pacific benthic foraminifera: correlations with sea level and biological productivity. *Geology,* 13(2):119–122. **https://doi.org/10.1130/0091-7613(1985)13<119:CVOMPB>2.0.CO;2**

Wright, J.D., Miller, K.G., and Fairbanks, R.G., 1991. Evolution of modern deepwater circulation: evidence from the late Miocene Southern Ocean. *Paleoceanography,* 6(2):275–290. **https://doi.org/10.1029/90PA02498**

You, Y., Huber, M., Müller, R.D., Poulsen, C.J., and Ribbe, J., 2009. Simulation of the Middle Miocene Climate Optimum. *Geophysical Research Letters,* 36(4):L04702. **https://doi.org/10.1029/2008GL036571**

Zachos, J., Pagani, M., Sloan, L., Thomas, E., and Billups, K., 2001. Trends, rhythms, and aberrations in global climate 65 Ma to present. *Science,* 292(5517):686–693. **https://doi.org/10.1126/science.1059412**

Zachos, J.C., Flower, B.P., and Paul, H., 1997. Orbitally paced climate oscillations across the Oligocene/Miocene boundary. *Nature,* 388(6642):567–570. **http://dx.doi.org/10.1038/41528**

Table T1. Summary of Ross Sea stratigraphy based on Brancolini et al. (1995).

Sequence	Sequence seismic character	Age	Bottom unconformity
RSS-8	Aggradational topset beds underlying locally backstepping grounding zone wedge	Pleistocene	RSU1 (0.7 Ma?)
RSS-7	Aggradational topset beds	Pliocene	RSU2 (4 Ma?)
RSS-6	Shelf topset beds and prograding trough mouth fan at the shelf edge	late Miocene	RSU3 (12 Ma?)
RSS-5	Alternating subsequences of grounding zone prograding wedges and subhorizontal strata packages	middle Miocene	RSU4 (14–16 Ma?)
RSS-4	Grounding zone prograding wedges and subhorizontal strata packages	early Miocene	RSU4a (18.5 Ma?)
RSS-3	Alternating subsequences of grounding zone prograding wedges and subhorizontal strata packages	early Miocene	RSU5 (21 Ma?)
RSS-2	Alternating subsequences of grounding zone prograding wedges and subhorizontal strata packages	late Oligocene–early Miocene	RSU6 (29 Ma?)
RSS-1 (upper)	Subhorizontal strata filling basement basins	late Eocene–early Oligocene	RSU7
RSS-1 (lower)	Subhorizontal strata filling basement basins	?Late Cretaceous	Basement

Table T2. Summary of Expedition 374 primary and alternate sites. EPSP = Environmental Protection and Safety Panel

Proposed site	Seismic line	Latitude	Longitude	Water depth (m)	Proposed penetration (mbsf)	EPSP approved penetration (mbsf)	Coring plan	Logging plan	Anticipated age at proposed penetration depth (Ma)
Primary sites									
EBOCS-03C	SP300 on Line IO6290-Y2A	76.55380°S	174.75794°W	558	545	545	Hole A: RCB	Hole A: triple combo, FMS-sonic, VSI	mid-Miocene
EBOCS-01D	SP690 on Line PD90-36	75.68392°S	179.67179°W	566	950	950	Hole A: RCB	Hole A: triple combo, FMS-sonic, VSI	mid-Miocene
EBOCS-04B	SP5162 on Line PD90-30	76.17651°S	172.88398°W	480	520	520	Hole A: RCB	Hole A: triple combo, FMS-sonic, VSI	Pliocene
RSCR-02B	SP4050 on Line ATC82B-208	74.50592°S	172.85452°W	2550	1000	1000	Hole A: APC Hole B: APC/XCB/RCB	Hole B: triple combo, FMS-sonic, VSI	mid-Miocene
RSCR-11A	SP1800 on Line IT91A-88B	71.84603°S	175.67904°W	1534	500	500	Hole A: APC Hole B: APC/XCB/RCB	Hole B: triple combo, FMS-sonic, VSI	Pliocene
EBOCS-02B	SP3160 on Line PD90-35	76.08827°S	178.09119°W	658	500	500	Hole A: RCB	Hole A: triple combo, FMS-sonic, VSI	mid-Miocene
Alternate sites									
EBOCS-05A	SP1838 on Line PD90-36	75.54986°S	179.20599°E	525	700	700	Hole A: RCB	Hole A: triple combo, FMS-sonic, VSI	mid-Miocene
EBOCS-06A	SP100 on Line IO6290-X4	75.91448°S	175.34958°W	515	700	700	Hole A: RCB	Hole A: triple combo, FMS-sonic, VSI	mid-Miocene
EBOCS-07C	SP3500 on Line IO6290-Y7	76.19502°S	173.70576°W	540	750	750	Hole A: RCB	Hole A: triple combo, FMS-sonic, VSI	Pliocene
RSCR-01B	SP10430 on Line IT88-01C	75.24660°S	175.00582°W	1400	1000	1000	Hole A: APC Hole B: APC/XCB/RCB	Hole B: triple combo, FMS-sonic, VSI	mid-Miocene
RSCR-03A	SP1660 on Line IT94A-127	75.00100°S	173.92012°W	1824	800	800	Hole A: APC Hole B: APC/XCB/RCB	Hole B: triple combo, FMS-sonic, VSI	mid-Miocene
RSCR-10A	SP5000 on Line TAN0602_08	74.21739°S	173.63372°W	2390	1000	1000	Hole A: APC Hole B: APC/XCB/RCB	Hole B: triple combo, FMS-sonic, VSI	mid-Miocene
RSCR-08C	SP10095 on Line BGR80-008	73.36928°S	178.91774°E	700	1000	1000	Hole A: APC Hole B: APC/XCB/RCB	Hole B: triple combo, FMS-sonic, VSI	mid-Miocene
RSCR-12B	SP6500 on Line IT91A-88	71.85123°S	178.16371°E	1952	620	650	Hole A: APC Hole B: APC/XCB/RCB	Hole B: triple combo, FMS-sonic, VSI	late Miocene?

Table T3. Operations and time estimates for Expedition 374.

Exp-374 West Antarctic Ice Sheet Climate (P751)

Operations Plan Summary

Site No.	Location (Latitude Longitude)	Seafloor Depth (mbrf)	Operations Description	Transit (days)	Drilling/ Coring (days)	Logging (days)
Wellington			Begin Expedition 5.0 port call days			
			Transit ~1581nmi tolce breaker rendezvous@ 10.5	6.3		
			Transit ~566nmi toEBOCS-03C@ 10.5	2.3		
EBOCS-03C	76° 33.2277' S	569	Hole A - RCB to 545 mbsf and log w/ triple combo, FMS sonic and VSI	0	2.8	1.3
EPSP	174° 45.4762' W					
to 545 mbsf						
			Sub-Total Days On-Site: 4.1			
			Transit ~88nmi toEBOCS-01D@ 10.5	0.3		
EBOCS-01D	75° 41.0353' S	577	Hole A - RCB to 950 mbsf and log w/ triple combo, FMS sonic and VSI	0	5.2	1.8
EPSP	179° 40.3074' W					
to 950 mbsf						
			Sub-Total Days On-Site: 6.9			
			Transit ~103nmi toEBOCS-04B@ 10.5	0.4		
EBOCS-04B	76° 10.5907' S	491	Hole A - RCB to 520 mbsf and log w/ triple combo, FMS sonic and VSI	0	2.5	1.3
EPSP	172° 53.0390' W					
to 520 mbsf						
			Sub-Total Days On-Site: 3.8			
			Transit ~100nmi toRSCR-02B@ 10.5	0.4		
RSCR-02B	74° 30.3551' S	2561	Hole A - APC to 250 mbsf	0	1.9	0.0
EPSP	172° 51.2711' W		Hole B - APC/XCB to 350 mbsf	0	2.3	0.0
to 1000 mbsf			Hole C - RCB to 1000 mbsf and log w/ triple combo, FMS sonic and VSI	0	6.8	2.0
			Sub-Total Days On-Site: 13.0			
			Transit ~167nmi toRSCR-11A@ 10.5	0.7		
RSCR-11A	71° 50.7616' S	1545	Hole A - APC to 250 mbsf	0	1.5	0.0
EPSP	175° 40.7424' W		Hole B - APC to 250 mbsf	0	1.2	0.0
to 500 mbsf			Hole C - APC/XCB to 500 mbsf and log w/ triple combo, FMS sonic and VSI	0	2.8	1.2
			Sub-Total Days On-Site: 6.7			
			Transit ~258nmi toEBOCS-02B@ 10.5	1.0		
EBOCS-02B	76° 5.2964' S	669	Hole A - RCB to 500 mbsf and log w/ triple combo, FMS sonic and VSI	0	2.5	1.3
EPSP	178° 5.5140' W					
to 500 mbsf						
			Sub-Total Days On-Site: 3.8			
			Transit ~523nmi tolce breaker rendezvous@ 10.5	2.2		
			Transit ~1581nmi toWellington@ 10.5	6.3		
Wellington			End Expedition	19.8	29.5	8.7

Port Call:	5.0	Total Operating Days:	58.0
Sub-Total On-Site:	38.2	Total Expedition:	63.0

Table T4. Operations plan for Expedition 374 alternate sites.

Exp-374 West Antarctic Ice Sheet Climate (P751)

Alternate Sites

Site No.	Location (Latitude Longitude)	Seafloor Depth (mbrf)	Operations Description	Drilling Coring (days)	LWD/MWD Log (days)
EBOCS-05A	75° 32.9913' S	531	Hole A - RCB to 700 mbsf and log w/ triple combo, FMS sonic and VSI	3.3	1.5
EPSP	179° 12.3592' E				
to 700 mbsf					
			Sub-Total Days On-Site: 4.8		
EBOCS-06A	75° 54.8689' S	511	Hole A - RCB to 420 mbsf and log w/ triple combo, FMS sonic and VSI	2.0	1.2
EPSP	175° 20.9749' W				
to 700 mbsf					
			Sub-Total Days On-Site: 3.2		
EBOCS-07C	76° 11.7013' S	535	Hole A - RCB to 750 mbsf and log w/ triple combo, FMS sonic and VSI	3.5	1.5
EPSP	173° 42.3458' W				
to 750 mbsf					
			Sub-Total Days On-Site: 5.0		
RSCR-01B	75° 14.7959' S	1411	Hole A - APC to 250 mbsf	1.5	0.0
EPSP	175° 0.3494' W		Hole B - APC/XCB to 350 mbsf	1.9	0.0
to 1000 mbsf			Hole C - RCB to 1000 mbsf and log w/ triple combo, FMS sonic and VSI	5.7	1.9
			Sub-Total Days On-Site: 10.9		
RSCR-03A	75° 0.0599' S	1835	Hole A - APC to 250 mbsf	1.7	0.0
EPSP	173° 55.2070' W		Hole B - APC/XCB to 350 mbsf	2.1	0.0
to 800 mbsf			Hole C - RCB to 800 mbsf and log w/ triple combo, FMS sonic and VSI	4.4	1.7
			Sub-Total Days On-Site: 9.9		
RSCR-08C	73° 22.1567' S	711	Hole A - APC to 250 mbsf	1.2	0.0
EPSP	178° 55.0646' E		Hole B - APC/XCB to 350 mbsf	1.5	0.0
to 1000 mbsf			Hole C - RCB to 1000 mbsf and log w/ triple combo, FMS sonic and VSI	4.9	1.8
			Sub-Total Days On-Site: 9.4		
RSCR-10A	74° 13.0433' S	2401	Hole A - APC to 250 mbsf	1.8	0.0
EPSP	173° 38.0233' W		Hole B - APC/XCB to 350 mbsf	2.3	0.0
to 1000 mbsf			Hole C - RCB to 1000 mbsf and log w/ triple combo, FMS sonic and VSI	6.7	1.9
			Sub-Total Days On-Site: 12.8		
RSCR-12B	71° 51.0735' S	1963	Hole A - APC to 250 mbsf	1.7	0.0
EPSP	178° 9.8226' E		Hole B - APC to 250 mbsf	1.3	0.0
to 650 mbsf			Hole C - APC/XCB to 620 mbsf and log w/ triple combo, FMS sonic and VSI	3.8	1.3
			Sub-Total Days On-Site: 8.1		

Figure F1. Data reconstructions. A. Compilation of atmospheric CO_2 proxies throughout the Cenozoic (left). Proxy methods (see legend) are from Masson-Delmotte et al. (2013). "Best and worst case" representative concentration pathways (RCPs) for historic and future atmospheric CO_2 emissions (right) are from Meinshausen et al. (2011). B. Composite deep ocean benthic $\delta^{18}O$ record for the last 65 My, which represents a combined signal of global ice volume and deep ocean temperature after approximately 35 Ma (Zachos et al., 2001). C. Long-term trend in deep-sea temperature through the Cenozoic based on removal of the ice volume component of the benthic $\delta^{18}O$ record using sequence stratigraphic records (black line with gray uncertainty band) and Mg/Ca estimates of deep-sea temperatures (Cramer et al., 2009) and scaled $\delta^{18}O$ for the past 10 My (Miller et al., 2011). D. Reconstruction of sea level lowstands (i.e., black lines) with minimum uncertainty ranges (gray shading) and smoothed trend (black dotted line) using sequence stratigraphy for the New Jersey margin. Sea levels >70 m imply a significant tectonic component to this record, particularly prior to the Oligocene (Kominz et al., 2008).

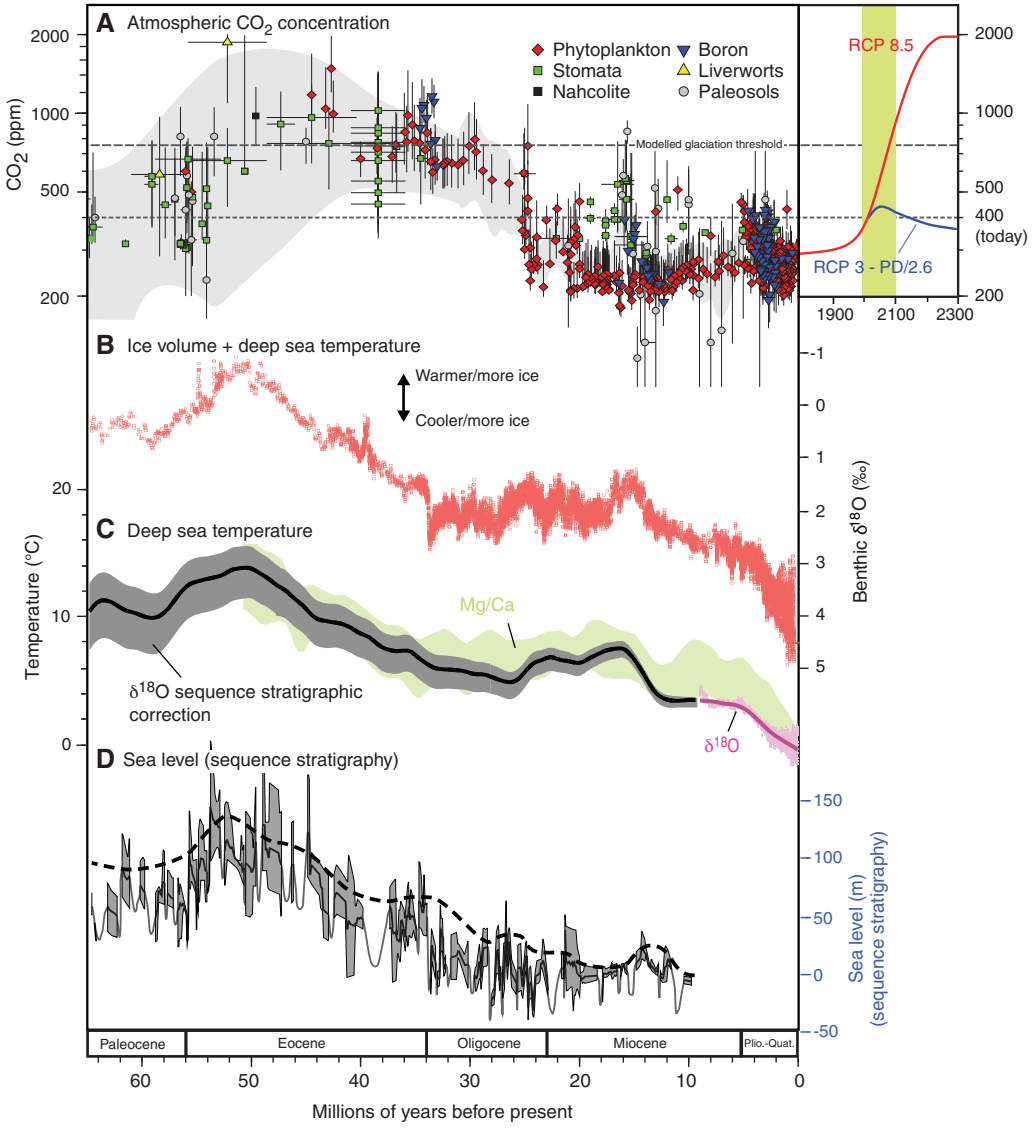

Figure F2. Location maps. A. Antarctica with basic glaciology and previous/proposed DSDP/ODP/Integrated Ocean Drilling Program/IODP drill sites. B. Ross Sea bathymetry with locations of proposed Expedition 374 sites (including alternates) and existing seismic network. EB = Eastern Basin, CB = Central Basin, VLB = Victoria Land Basin, IB = Iselin Bank.

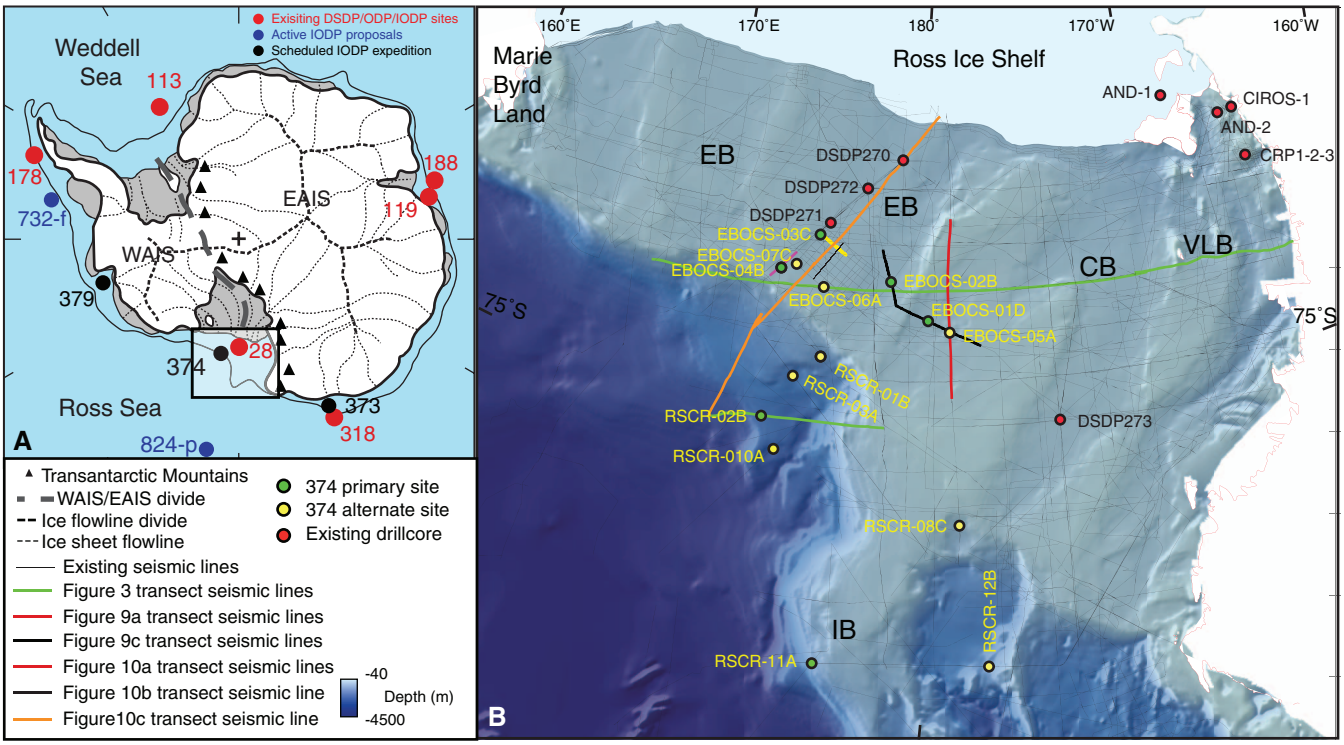

Figure F3. Ross Sea seismic stratigraphy and previous drilling (see Figure **F1** for transect lines). Expedition 374 sites form a continental shelf-to-rise transect designed to tie into inner shelf sites and to trace the Neogene and Quaternary evolution of the WAIS and the forcings and feedbacks influencing past variability.

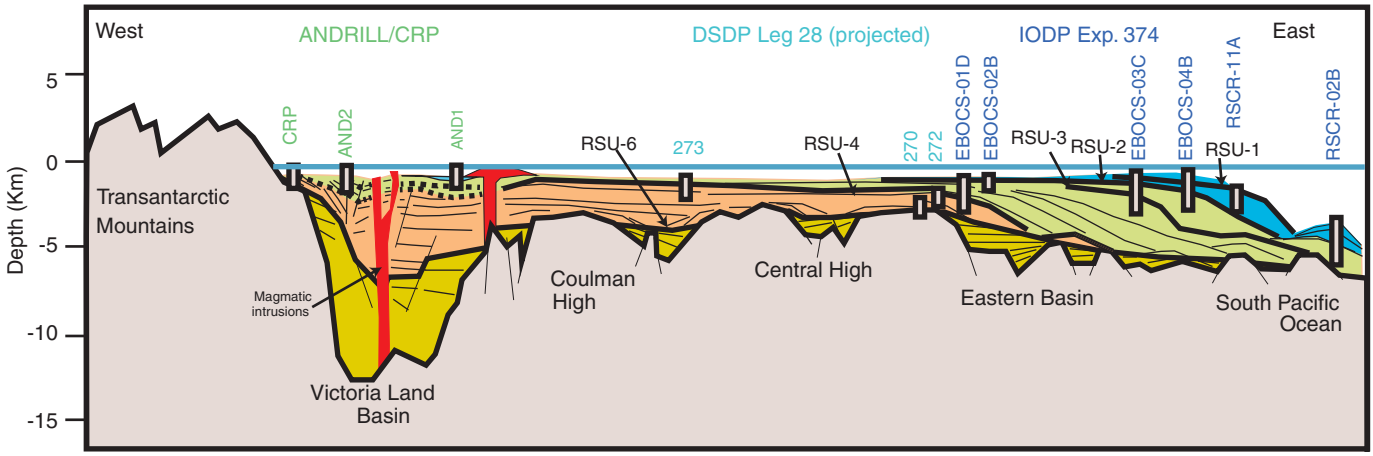

Figure F4. Expedition 374 sites are located in the most sensitive sector of the Antarctic for assessing ice sheet responses to (A) sea level and (B) ocean heat flux. C–F. A more terrestrial West Antarctica in the Oligocene could support a larger ice sheet than present, despite a warmer climate (Wilson et al., 2013). Thus, the timing of Ross Sea overdeepening has important implications for sea level budgets and for understanding mass balance controls. G. The integration of sedimentologic data with modeling was key to the success of ANDRILL (blue circle). Despite discontinuous sedimentation, targeting time intervals with short duration magnetic reversals enabled orbital-scale WAIS reconstructions. Models indicate that grounded ice sheets occur at Expedition 374 sites (EBOCS-01 to 04; black circles) during periods of maximum Antarctic ice volume. These ice-proximal sites will enable the assessment of the Antarctic contributions to sea level lowstands, building significantly on the record of ANDRILL. Not all modeled glacial maxima are characterized by advance of ice to the continental shelf edge.

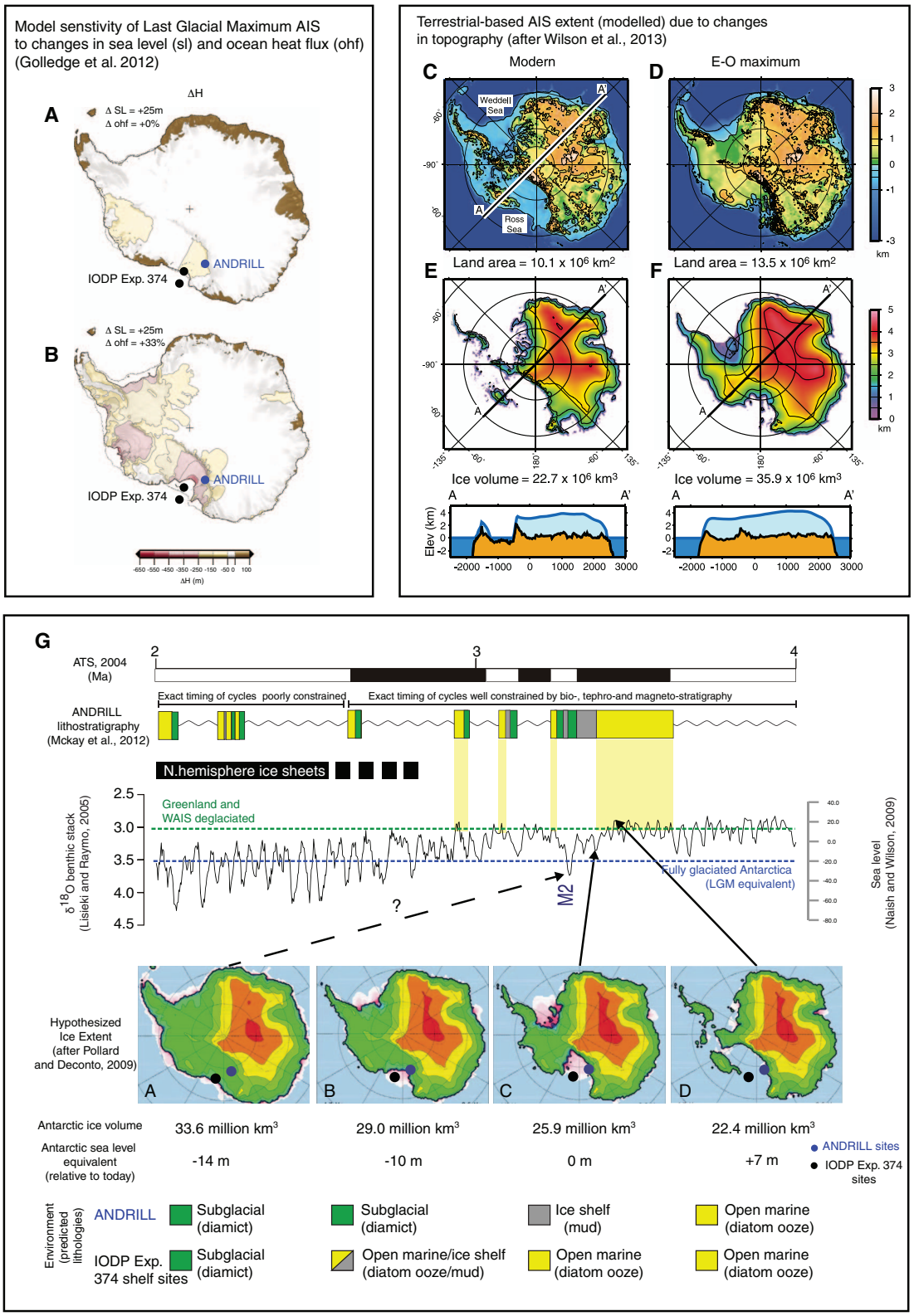

Figure F5. Neogene Ross Sea continental shelf lithofacies interpretations (after McKay et al., 2009; Fielding et al., 2011). GSE = glacial surface of erosion (sharp contacts associated with subglacial deformation features). MST = mean summer temperature. A. Late Pleistocene diamictite overlying deformed mudstone (MST) (AND-1B; 82.7–82.85 mbsf). B. Pliocene diamictite overlying deformed diatomite (AND-1B; 211.3–211.45 mbsf) and thin interval of stratified gravels, sands, and muds overlying diamictite indicative of glacial retreat in sediment-starved polar regime (AND-1B; 224.9–225.05 mbsf). C. Rhythmically laminated glaciomarine mudstone indicative of subglacial meltwater discharge (AND-1B; 1033.3–1033.45 mbsf), stratified coarse sandstones deposited by meltwater discharge in a subglacial fan system (AND-1B; 1062.75–1062.9 mbsf), and carbonate (bivalve fossils) in glaciomarine deposits (AND-2A; 430.52–430.7 mbsf).

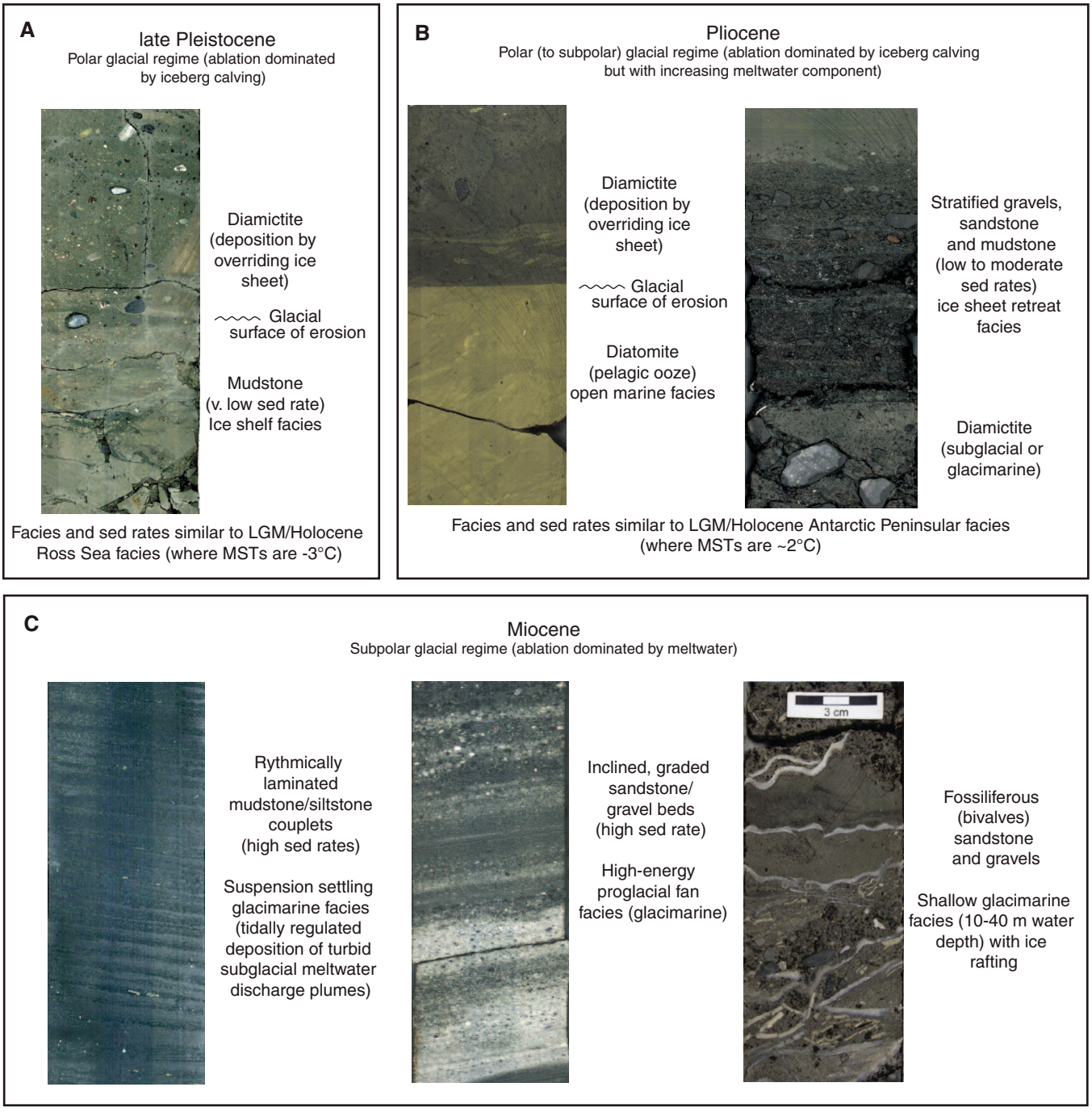

Figure F6. Chronostratigraphic summary of Ross Sea drilling. Seismic stratigraphy is constrained by drilling in the Victoria Land Basin (SR-VLB), but not in the Central and Eastern Basins (RSU). Expedition 374 sites will reduce uncertainties associated with RSU4 to RSU2 and assess the spatial coherency of these erosional features. Far-field climate ($\delta^{18}O$), CO_2, carbon cycle ($\delta^{13}C$), Equatorial Pacific carbonate compensation depth (CCD), and sea level records discussed in the text are indicated (modified from ANDRILL Coulman High Drilling NSF Proposal).

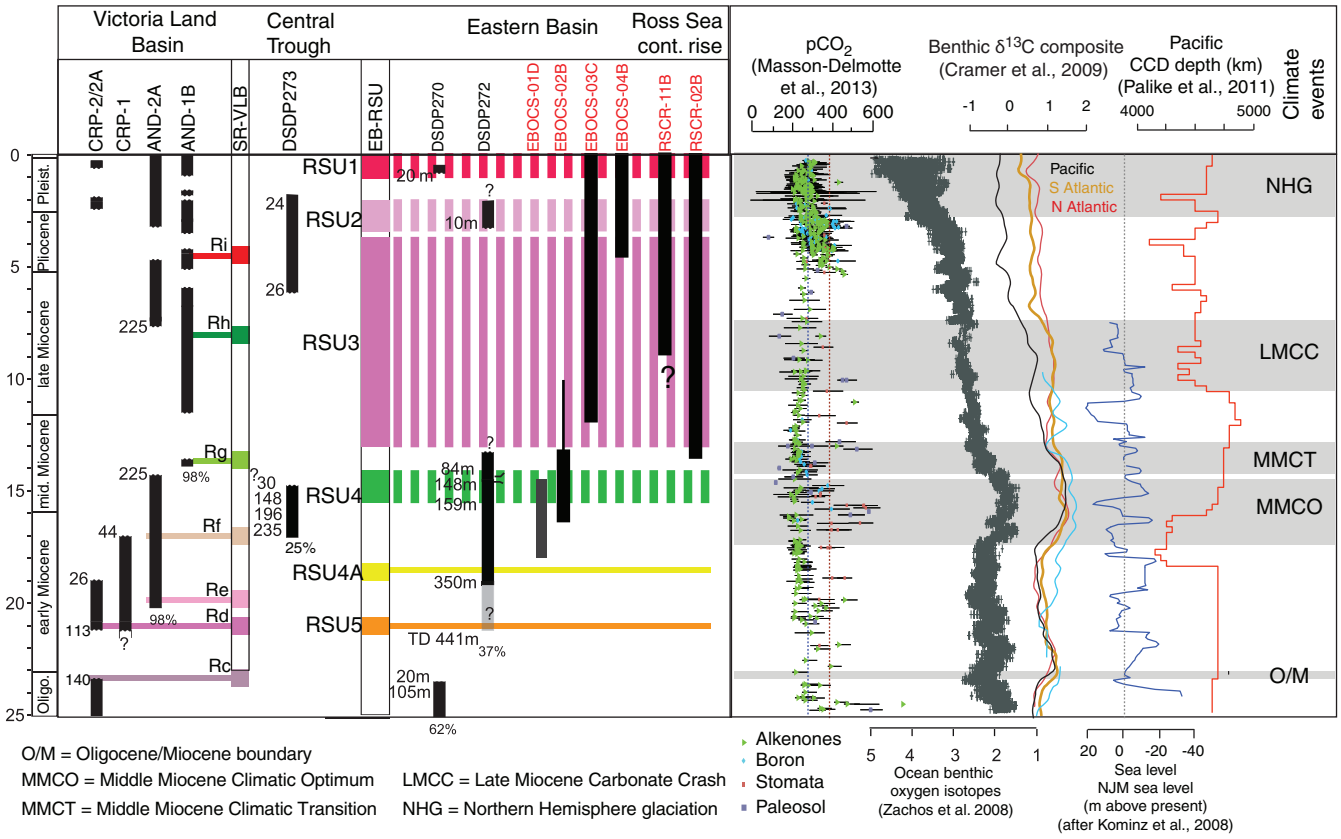

Figure F7. Ross Sea physical oceanography highlighting the role the ASC in influencing regional water masses. A. Observational conditions over the past 50 y. B. Hypothesized changes related to the invigoration of the ASC. C. Cross-section of observation conditions shown in A. D. Cross-section of C. Note the increase in Antarctic Surface Water in the Ross Sea, resulting in (1) a greater dynamical barrier for shelf MCDW incursions and (2) decreased production of High-Salinity Shelf Water (SW) influencing deep waters (e.g., Antarctic Deep Water [ADW] vs. Antarctic Bottom Water [AABW]). Figure modified from Smith et al. (2012).

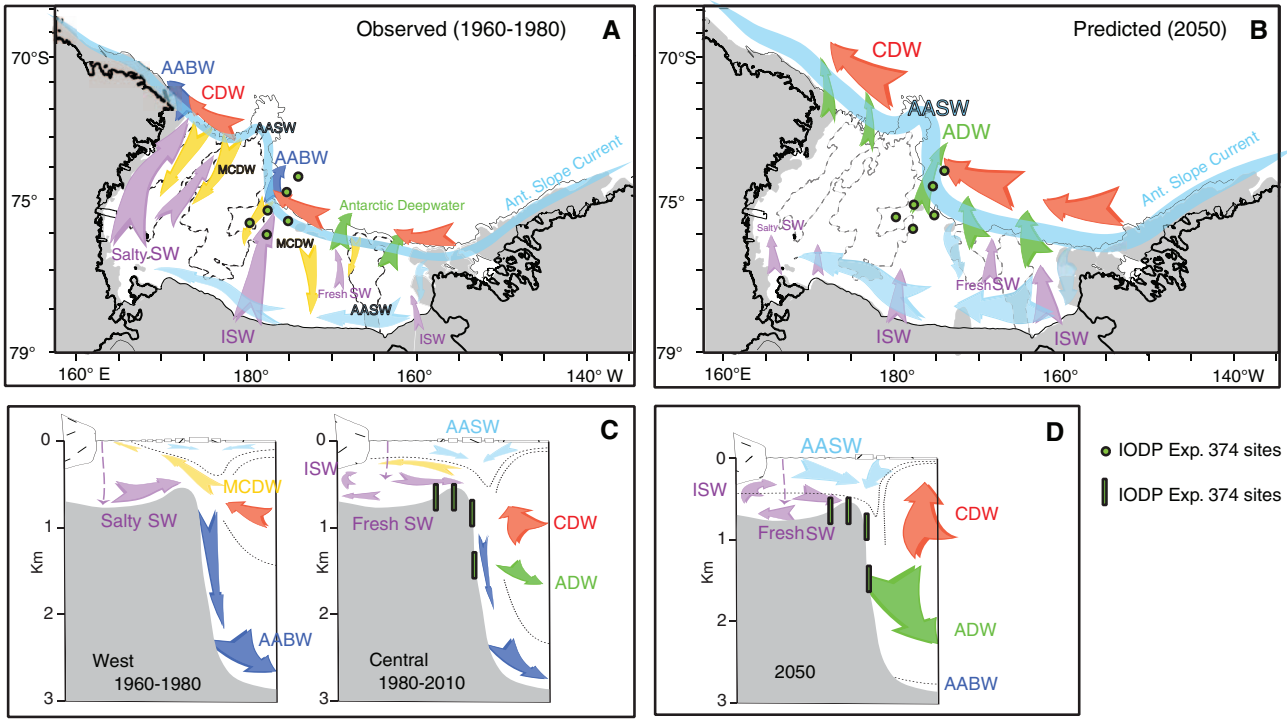

Figure F8. Depth maps for selected regional seismic ANTOSTRAT unconformities, with interpretations of ice sheet history (after Brancolini et al., 1995). RSU4, RSU3 and RSU2 maps have now been extended into the continental slope and rise area (not shown) as part of the IPY Rossmap project.

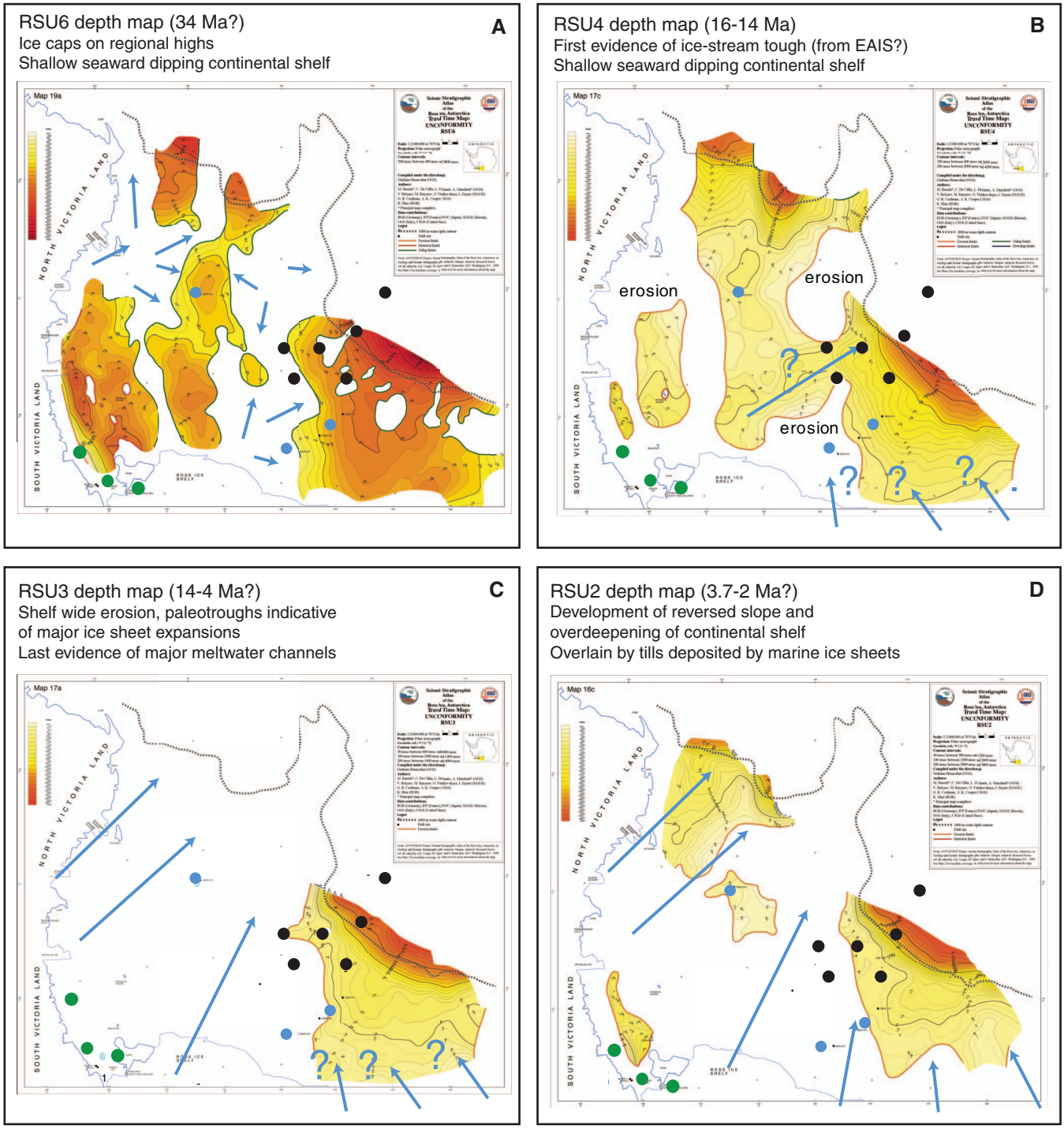

Figure F9. A. Sites EBOCS-01D, 05A (alternate), and 02B. B. Line drawings of seismic Lines BGR80-80 and 80-04, highlighting the glacial trough associated with RSU4. C. Seismic Profiles PD90-35 and 36. Site EBOCS-01D will target glacial and glaciomarine sediments above and below RSU4 (green line). Site EBOCS-05A (alternate) will recover a younger section below RSU4 (inferred to be deposited during the MMCO). Site EBOCS-02B will recover a higher resolution record of subglacial tills and glaciomarine meltwater outwash sediments above RSU4 (late Miocene?). Seismic line locations are shown in Figure **F2**.

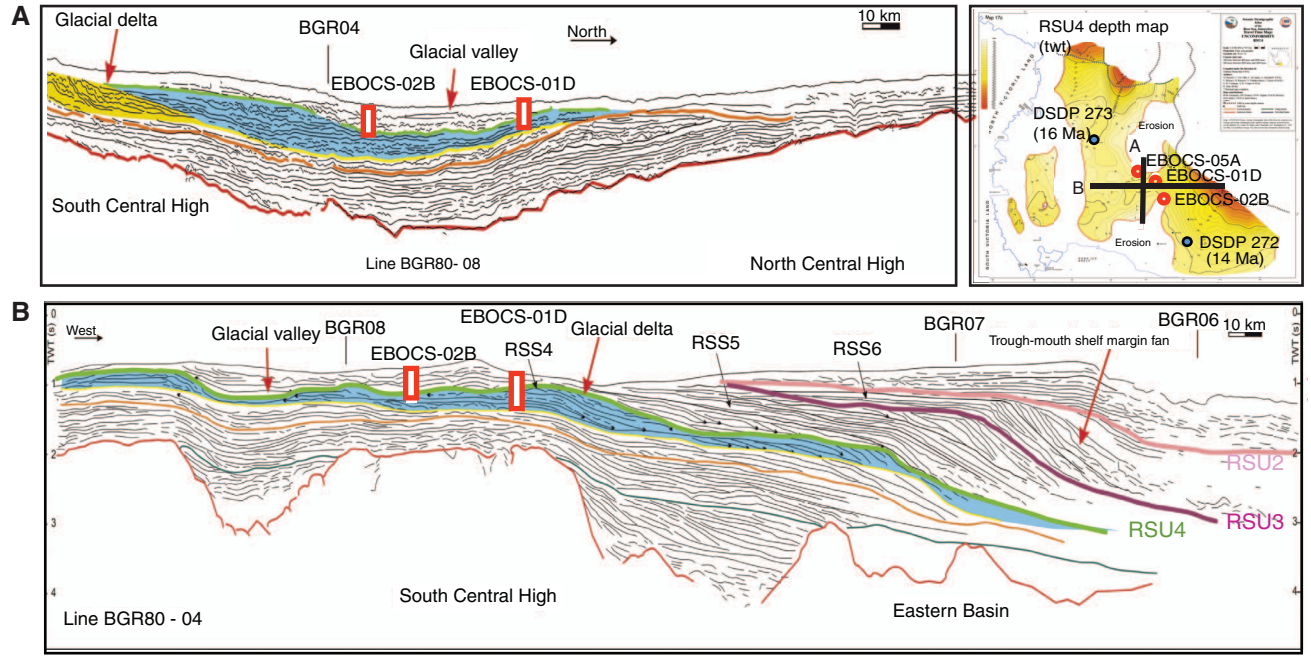

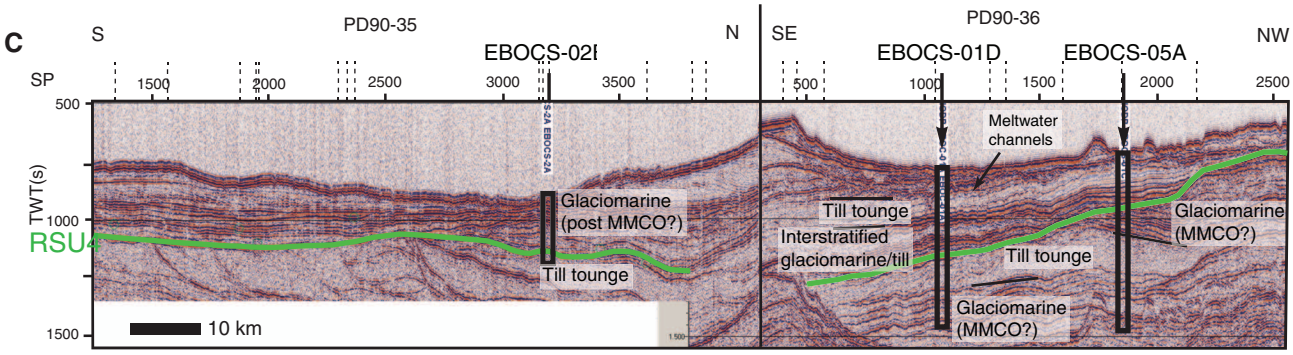

Figure F10. Stratigraphic linkages and targets for Sites EBOCS-03C (RSU3, RSU2, and RSU1) and 04B (RSU2 and RSU1; blue line). These reflectors may be traced from the shelf to continental slope/rise Sites RSCR-01B (alternate, shown) and 02B (not shown). On the continental slope, the onlapping reflectors above RSU3 (magenta) at alternate Site RSCR-01B (part A) are interpreted as the fine-grained distal component of a trough mouth fan, with reworking by along-slope currents, overlying a levee system (below RSU3). RSCR-02B (not shown) consists of levee deposits above and below RSU3 and is a more continuous Neogene to Quaternary record (see **Site summaries** for details). Seismic line locations are shown in Figure **F2**.

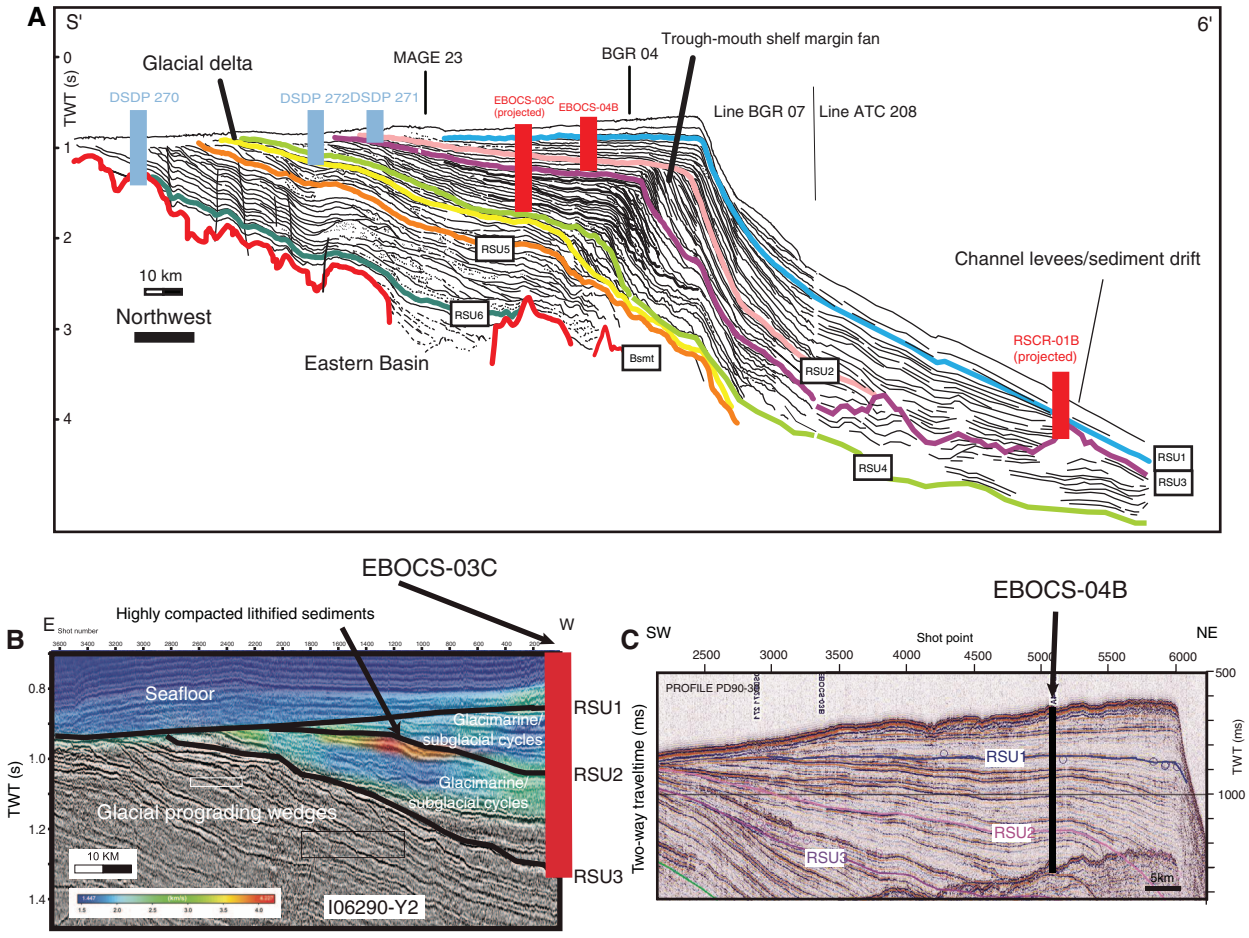

Figure F11. (Top) Interpreted seismic Profile ATC82B-208 across Site RSCR-02B showing major unconformities and water masses influencing the sites. (Middle) Regional 3-D bathymetry and generalized oceanography of the Ross Sea with location of primary (large yellow circles) and alternate (small yellow circles) sites on the continental slope and rise, showing the competing influence of downslope and along-slope currents at the sites. (Bottom) Interpreted seismic Profile IT91-A-88B across Site RSCR-11A showing the major unconformity. This site is interpreted to be a sediment drift deposited by Antarctic Slope Current (ASC) on the continental slope. ISW = Ice Shelf Water; HSSW = High-Salinity Shelf Water; AABW = Antarctic Bottom Water; LS-RSBW = Low Salinity Ross Sea Bottom Water; HS-RSBW = High Salinity Ross Sea Bottom Water. AASW = Antarctic Surface Water; MCDW = Modified Circumpolar Deep Water. CDW = Circumpolar Deep Water; RIS = Ross Ice Shelf.

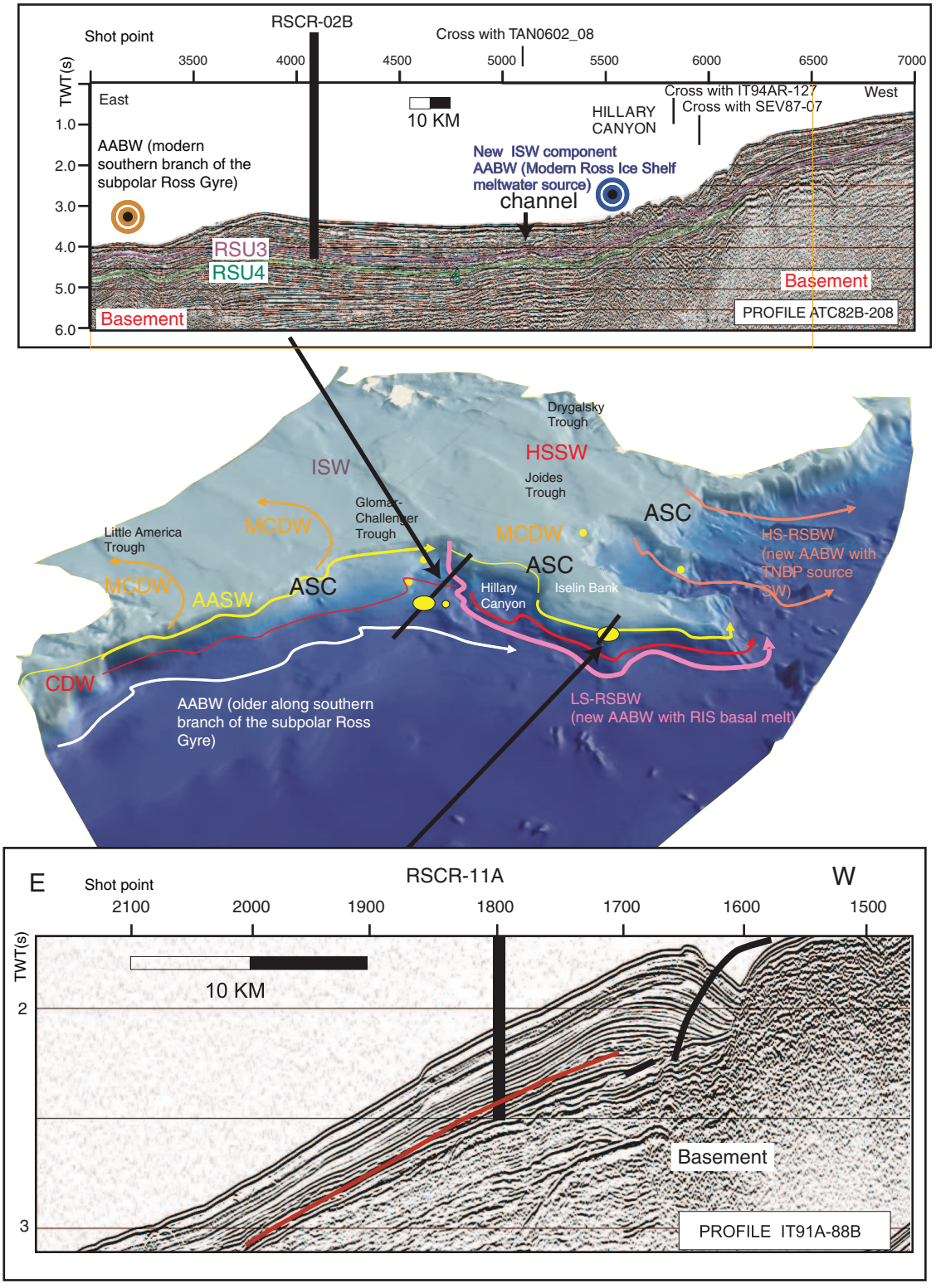

Site summaries

Site EBOCS-01D

Priority:	Primary
Position:	75.68392°S, 179.67179°W
Water depth (m):	566
Target drilling depth (mbsf):	950
Approved maximum penetration (mbsf):	950
Survey coverage (track map; seismic profile):	Bathymetric sketch and site track map (Figure **AF1**) Deep-penetration seismic reflection: • Primary line: SP690 on Line PD90-36 (Figure **AF2**)
Objective(s):	• Establish timing of first marine-based ice streams into Ross Sea • Recover a mid- to upper Miocene climate, oceanic, and ice sheet record from glaciomarine and subglacial till above RSU4 • Recover a record from 75°S of the Middle Miocene Climatic Optimum below RSU4
Drilling program:	Hole A: RCB to 950 mbsf with nonmagnetic core barrels
Downhole measurements program:	Hole A: • Triple combo • FMS-sonic • VSI
Nature of rock anticipated:	Glaciomarine and subglacial diamicts and mudstones, with possible open marine mudstone and biogenic ooze

Site EBOCS-02B

Priority:	Primary
Position:	76.08827°S, 178.09119°W
Water depth (m):	658
Target drilling depth (mbsf):	500
Approved maximum penetration (mbsf):	500
Survey coverage (track map; seismic profile):	Bathymetric sketch and site track map (Figure **AF3**) Deep-penetration seismic reflection: • Primary line: SP3160 on Line PD90-35 (Figure **AF4**) • Crossing line: SP1063 on analog Line NBP94-09 (Figure **AF5**)
Objective(s):	• Establish timing of first marine-based ice streams into Ross Sea (RSU4) • Determine if glacial advance associated with RSU4 was from localized ice caps or shelf-wide ice sheet advance • Recover a mid- to upper Miocene climate, oceanic, and ice sheet record from glaciomarine and subglacial till above RSU4
Drilling program:	Hole A: RCB to 500 mbsf with nonmagnetic core barrels
Downhole measurements program:	Hole A: • Triple combo • FMS-sonic • VSI
Nature of rock anticipated:	Glaciomarine and subglacial diamicts and mudstones, with possible open marine mudstone and biogenic ooze

Site EBOCS-03C

Priority:	Primary
Position:	76.55380°S, 174.75794°W
Water depth (m):	558
Target drilling depth (mbsf):	545
Approved maximum penetration (mbsf):	545
Survey coverage (track map; seismic profile):	Bathymetric sketch and site track map (Figure **AF6**) Deep-penetration seismic reflection: • Primary line: SP300 on Line IO6290-Y2A (Figure **AF7**)
Objective(s):	• Constrain age of first shelf-wide advance of WAIS (RSU3) • Recover a post-RSU4 paleoclimate, glacimarine, and ice sheet stratigraphic record that spans the mid-Miocene climate transition to present • Constrain age of overdeepening event associated with RSU2 and assess response of ice sheet variability
Drilling program:	Hole A: RCB to 545 mbsf with nonmagnetic core barrels
Downhole measurements program:	Hole A: • Triple combo • FMS-sonic • VSI
Nature of rock anticipated:	Glaciomarine and subglacial diamicts and mudstones, with possible open marine mudstone and biogenic ooze

Site EBOCS-04B

Priority:	Primary
Position:	76.17651°S, 172.88398°W
Water depth (m):	480
Target drilling depth (mbsf):	520
Approved maximum penetration (mbsf):	520
Survey coverage (track map; seismic profile):	Bathymetric sketch and site track map (Figure **AF8**) Deep-penetration seismic reflection: • Primary line: SP5162 on Line PD90-30 (Figure **AF9**) • Crossing line: SP190 on Line NBP9601-T16 (Figure **AF10**)
Objective(s):	• Recover a post-RSU2 paleoclimate, glacimarine, and ice sheet stratigraphic record that spans the Pliocene (late Miocene?) to present • Constrain age of overdeepening event associated with RSU2 and assess response of ice sheet variability
Drilling program:	Hole A: RCB to 520 mbsf with nonmagnetic core barrels
Downhole measurements program:	Hole A: • Triple combo • FMS-sonic • VSI
Nature of rock anticipated:	Glaciomarine and subglacial diamicts alternating with glaciomarine mudstones and possible biogenic ooze

Site RSCR-02B

Priority:	Primary
Position:	74.50592°S, 172.85452°W
Water depth (m):	2550
Target drilling depth (mbsf):	1000
Approved maximum penetration (mbsf):	1000
Survey coverage (track map; seismic profile):	Bathymetric sketch and site track map (Figure **AF11**) Deep-penetration seismic reflection: • Primary line: SP4050 on Line ATC82B-208 (Figure **AF12**)
Objective(s):	• Obtain a near-continuous post-RSU3 (mid-Miocene to Pleistocene?) and pre-RSU3 (mid-Miocene to Pliocene) sediment sequence to provide a high-resolution chronology and an ice-distal record of glacial/interglacial cycles • Recover a high-resolution record for correlation to inner and outer shelf records and mid- to high-latitude deep-sea records of glacial and environmental change • Reconstruct Antarctic Slope Current vigor and Ross Sea Bottom Water production
Drilling program:	Hole A: APC to 250 mbsf with nonmagnetic core barrels, orientation (Icefield tool), and APCT-3 Hole B: APC/XCB to 350 mbsf with nonmagnetic core barrels and orientation (APC only) Hole C: RCB to 1000 mbsf with nonmagnetic core barrels
Downhole measurements program:	Hole C: • Triple combo • FMS-sonic • VSI
Nature of rock anticipated:	Turbiditic/contouritic mud alternating with hemipelagic biogenic mud

Site RSCR-11A

Priority:	Primary
Position:	71.84603°S, 175.67904°W
Water depth (m):	1534
Target drilling depth (mbsf):	500
Approved maximum penetration (mbsf):	500
Survey coverage (track map; seismic profile):	Bathymetric sketch and site track map (Figure **AF13**) Deep-penetration seismic reflection: • Primary line: SP1800 on Line IT91A-88B (Figure **AF14**) • Crossing line: SP5173 on Line TAN0602-10 (Figure **AF15**)
Objective(s):	• Obtain a near-continuous Pliocene to present sediment sequence to provide a high-resolution chronology and an ice-distal record of glacial/interglacial cycles • Recover a high-resolution record for correlation to inner and outer shelf records and mid- to high-latitude deep-sea records of glacial and environmental change • Reconstruct Antarctic Slope Current vigor and Ross Sea Bottom Water production
Drilling program:	Hole A: APC to 250 mbsf with nonmagnetic core barrels, orientation (Icefield tool), and APCT-3 Hole B: APC to 250 mbsf with nonmagnetic core barrels and orientation Hole C: APC/XCB to 500 mbsf with nonmagnetic core barrels and orientation (APC only)
Downhole measurements program:	Hole C: • Triple combo • FMS-sonic • VSI
Nature of rock anticipated:	Drift sediments

Site EBOCS-05A

Priority:	Alternate
Position:	75.54986°S, 179.20599°E
Water depth (m):	525
Target drilling depth (mbsf):	700
Approved maximum penetration (mbsf):	700
Survey coverage (track map; seismic profile):	Bathymetric sketch and site track map (Figure **AF16**) Deep-penetration seismic reflection: • Primary line: SP1838 on Line PD90-36 (Figure **AF17**) • Crossing line: SP1724 on line BGR80-08 (Figure **AF18**)
Objective(s):	• Establish timing of first marine-based ice streams into Ross Sea • Determine if glacial advance associated with RSU4 was from local ice caps or shelf-wide ice sheet advance • Recover a mid- to upper Miocene climate, oceanic, and ice sheet record from glaciomarine and subglacial till above RSU4 • Recover a record from 75°S of the Middle Miocene Climatic Optimum below RSU4
Drilling program:	Hole A: RCB to 700 mbsf with nonmagnetic core barrels
Downhole measurements program:	Hole A: • Triple combo • FMS-sonic • VSI
Nature of rock anticipated:	Glaciomarine and subglacial diamicts and mudstones, with possible lithified open marine mudstone and biogenic ooze

Site EBOCS-06A

Priority:	Alternate
Position:	75.91448°S, 175.34958°W
Water depth (m):	515
Target drilling depth (mbsf):	700
Approved maximum penetration (mbsf):	700
Survey coverage (track map; seismic profile):	Bathymetric sketch and site track map (Figure **AF19**) Deep-penetration seismic reflection: • Primary line: SP1315 on line IO6290-Y7 (Figure **AF20**) • Crossing line: SP100 on line IO6290-X4 (Figure **AF21**)
Objective(s):	• Constrain age of first shelf-wide advance of WAIS (RSU3) • Recover a post-RSU4 paleoclimate, glacimarine, and ice sheet stratigraphic record that spans the mid-Miocene climate transition to present • Constrain age of overdeepening event associated with RSU2 and assess response of ice sheet variability
Drilling program:	Hole A: RCB to 700 mbsf with nonmagnetic core barrels
Downhole measurements program:	Hole A: • Triple combo • FMS-sonic • VSI
Nature of rock anticipated:	Glaciomarine and subglacial diamicts and mudstones, with possible lithified open marine mudstone and biogenic ooze

Site EBOCS-07C

Priority:	Alternate
Position:	76.19502°S, 173.70576°W
Water depth (m):	540
Target drilling depth (mbsf):	750
Approved maximum penetration (mbsf):	750
Survey coverage (track map; seismic profile):	Bathymetric sketch and site track map (Figure **AF22**) Deep-penetration seismic reflection: • Primary line: SP3500 on Line IO6290-Y7B (Figure **AF23**)
Objective(s):	• Recover a post-RSU3 paleoclimate, glacimarine, and ice sheet stratigraphic record that spans the Pliocene (late Miocene?) to present • Constrain age of overdeepening event associated with RSU2 and assess response of ice sheet variability
Drilling program:	Hole A: RCB to 750 mbsf with nonmagnetic core barrels
Downhole measurements program:	Hole A: • Triple combo • FMS-sonic • VSI
Nature of rock anticipated:	Lithified glaciomarine and subglacial diamicts and mudstones, with possible lithified open marine mudstone and biogenic ooze

Site RSCR-01B

Priority:	Alternate
Position:	75.24660°S, 175.00582°W
Water depth (m):	1400
Target drilling depth (mbsf):	1000
Approved maximum penetration (mbsf):	1000
Survey coverage (track map; seismic profile):	Bathymetric sketch and site track map (Figure **AF24**) Deep-penetration seismic reflection: • Primary line: SP10430 on Line IT88-01C (Figure **AF25**)
Objective(s):	• Obtain a near-continuous post-RSU2 (mid-Miocene to Pleistocene?) and pre-RSU3 (mid-Miocene to Pliocene) sediment sequence to provide a high-resolution chronology and an ice-distal record of glacial/interglacial cycles • Recover a high-resolution record for correlation to inner and outer shelf records and mid- to high-latitude deep-sea records of glacial and environmental change • Reconstruct Antarctic Slope Current vigor and Ross Sea Bottom Water production
Drilling program:	Hole A: APC to 250 mbsf with nonmagnetic core barrels, orientation (Icefield tool), and APCT-3 Hole B: APC/XCB to 350 mbsf with nonmagnetic core barrels and orientation (APC only) Hole C: RCB to 1000 mbsf with nonmagnetic core barrels
Downhole measurements program:	Hole C: • Triple combo • FMS-sonic • VSI
Nature of rock anticipated:	Fine-grained turbidites alternating with hemipelagic biogenic mud

Site RSCR-03A

Priority:	Alternate
Position:	75.00100°S, 173.92012°W
Water depth (m):	1824
Target drilling depth (mbsf):	800
Approved maximum penetration (mbsf):	800
Survey coverage (track map; seismic profile):	Bathymetric sketch and site track map (Figure **AF26**) Deep-penetration seismic reflection: • Primary line: SP1660 on Line IT94A-127 (Figure **AF27**)
Objective(s):	• Obtain a near-continuous pre-RSU3 (mid-Miocene to Pliocene) sediment sequence to provide a high-resolution chronology and an ice-distal record of glacial/interglacial cycles • Recover a high-resolution record for correlation to inner and outer shelf records and mid- to high-latitude deep-sea records of glacial and environmental change • Reconstruct Antarctic Slope Current vigor and Ross Sea Bottom Water production
Drilling program:	Hole A: APC to 250 mbsf with nonmagnetic core barrels, orientation (Icefield tool), and APCT-3 Hole B: APC/XCB to 350 mbsf with nonmagnetic core barrels and orientation (APC only) Hole C: RCB to 800 mbsf with nonmagnetic core barrels
Downhole measurements program:	Hole C: • Triple combo • FMS-sonic • VSI
Nature of rock anticipated:	Fine-grained turbidites alternating with hemipelagic biogenic mud

Site RSCR-10A

Priority:	Alternate
Position:	74.21739°S, 173.63372°W
Water depth (m):	2390
Target drilling depth (mbsf):	1000
Approved maximum penetration (mbsf):	1000
Survey coverage (track map; seismic profile):	Bathymetric sketch and site track map (Figure **AF11**) Deep-penetration seismic reflection: • Primary line: SP5000 on Line TAN0602-08 (Figure **AF28**)
Objective(s):	• Obtain a near-continuous post-RSU3 (mid-Miocene to Pleistocene?) and pre-RSU3 (mid-Miocene to Pliocene) sediment sequence to provide a high-resolution chronology and an ice-distal record of glacial/interglacial cycles • Recover a high-resolution record for correlation to inner and outer shelf records and mid- to high-latitude deep-sea records of glacial and environmental change • Reconstruct Antarctic Slope Current vigor and Ross Sea Bottom Water production
Drilling program:	Hole A: APC to 250 mbsf with nonmagnetic core barrels, orientation (Icefield tool), and APCT-3 Hole B: APC/XCB to 350 mbsf with nonmagnetic core barrels and orientation (APC only) Hole C: RCB to 1000 mbsf with nonmagnetic core barrels
Downhole measurements program:	Hole C: • Triple combo • FMS-sonic • VSI
Nature of rock anticipated:	Diatom-bearing mud with dispersed clasts

Site RSCR-08C

Priority:	Alternate
Position:	73.36928°S, 178.91774°E
Water depth (m):	700
Target drilling depth (mbsf):	1000
Approved maximum penetration (mbsf):	1000
Survey coverage (track map; seismic profile):	Bathymetric sketch and site track map (Figure **AF29**) Deep-penetration seismic reflection: • Primary line: SP10095 on Line BGR80-008A (Figure **AF30**) • Crossing line: SP3491 on Line KSL14-02 (Figure **AF31**)
Objective(s):	• Obtain a near-continuous post-RSU3 (mid-Miocene to Pleistocene?) and pre-RSU3 (mid-Miocene to Pliocene) sediment sequence to provide a high-resolution chronology and an ice-distal record of glacial/interglacial cycles • Recover a high-resolution record for correlation to inner and outer shelf records and mid- to high-latitude deep-sea records of glacial and environmental change • Reconstruct Antarctic Slope Current vigor and Ross Sea Bottom Water production
Drilling program:	Hole A: APC to 250 mbsf with nonmagnetic core barrels, orientation (Icefield tool), and APCT-3 Hole B: APC/XCB to 350 mbsf with nonmagnetic core barrels and orientation (APC only) Hole C: RCB to 1000 mbsf with nonmagnetic core barrels
Downhole measurements program:	Hole C: • Triple combo • FMS-sonic • VSI
Nature of rock anticipated:	Sediment drift (mud?) alternating with hemipelagic biogenic mud

Site RSCR-12B

Priority:	Alternate
Position:	71.85123°S, 178.16371°E
Water depth (m):	1952
Target drilling depth (mbsf):	620
Approved maximum penetration (mbsf):	650
Survey coverage (track map; seismic profile):	Bathymetric sketch and site track map (Figure **AF32**) Deep-penetration seismic reflection: • Primary line: SP6500 on Line IT91A-88 (Figure **AF33**) • "Crossing line: SP8724 on line KSL14-04 (Figure **AF34**)
Objective(s):	• Obtain a near-continuous Pliocene/late Miocene? to present sediment sequence to provide a high-resolution chronology and an ice-distal record of glacial/interglacial cycles • Recover a high-resolution record for correlation to inner and outer shelf records and mid- to high-latitude deep-sea records of glacial and environmental change • Reconstruct Antarctic Slope Current vigor and Ross Sea Bottom Water production
Drilling program:	Hole A: APC to 250 mbsf with nonmagnetic core barrels, orientation (Icefield tool), and APCT-3 Hole B: APC to 250 mbsf with nonmagnetic core barrels and orientation Hole C: APC/XCB to 620 mbsf with nonmagnetic core barrels and orientation (APC only)
Downhole measurements program:	Hole C: • Triple combo • FMS-sonic • VSI
Nature of rock anticipated:	Mid-slope sediment drift forming on a basement terrace associated with along slope current

Figure AF1. Contoured bathymetric maps showing location of proposed primary Site EBOCS-01D on seismic reflection Profile PD90-36 (Figure **AF2**). A. Bathymetry from Davey (2004). Contour interval = 25 m. B. Swath bathymetry collected during seismic survey cruises.

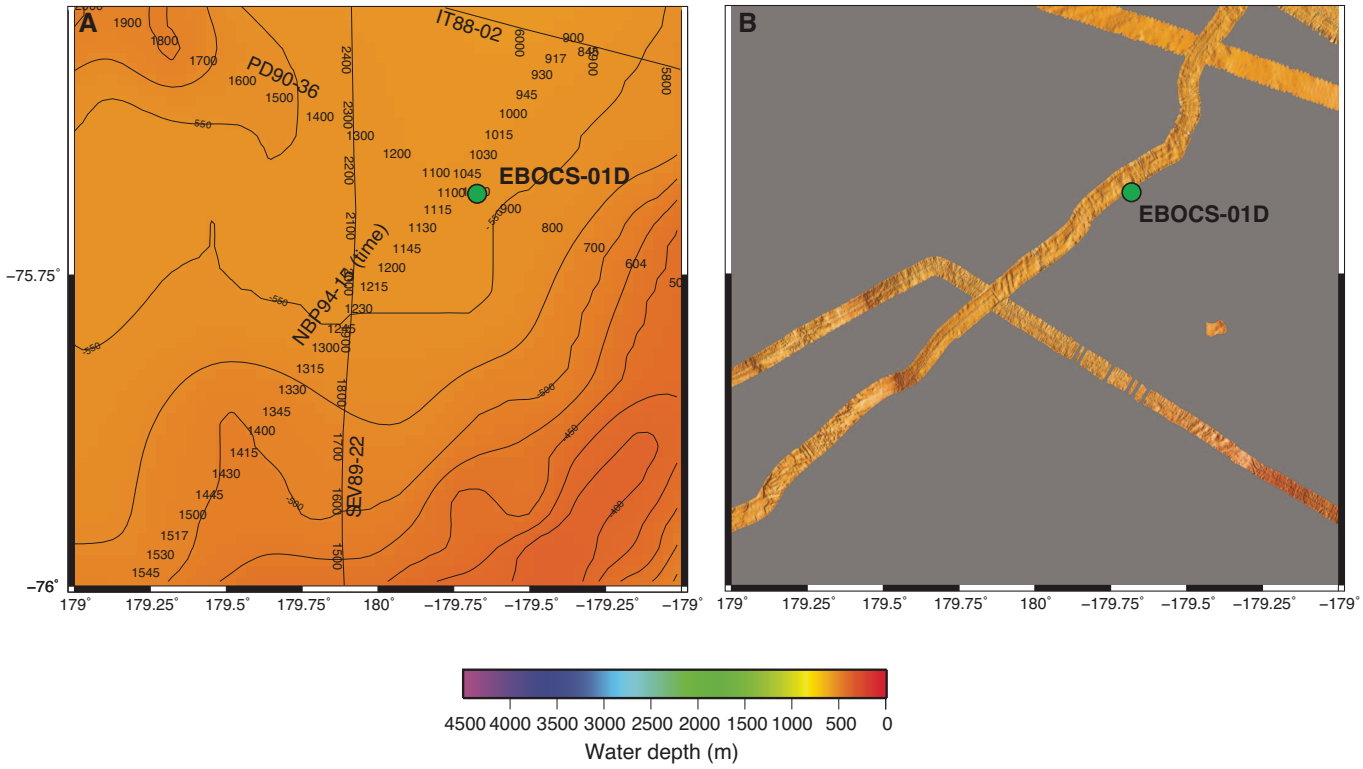

Figure AF2. Seismic reflection profile Line PD90-36 with location of proposed primary Site EBOCS-01D (75.68392°S, 179.67179°W; SP 690; water depth = 566 m; target depth = 950 mbsf; approved maximum penetration 950 mbsf). SP = shotpoint.

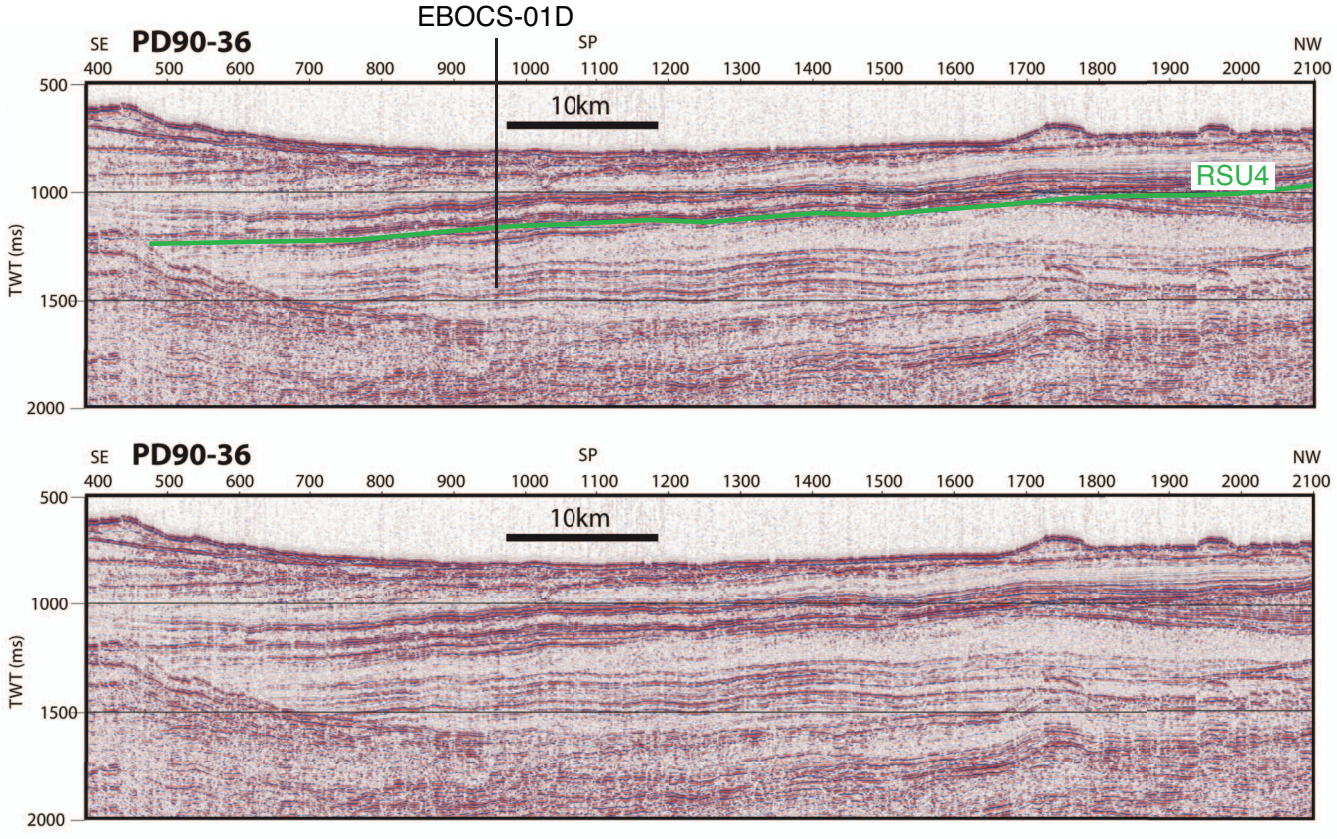

Figure AF3. Contoured bathymetric maps showing location of proposed primary Site EBOCS-02B on seismic reflection Profiles PD90-35 (Figure **AF4**) and NBP94-09 (Figure **AF5**). A. Bathymetry from Davey (2004). Contour interval = 25 m. B. Swath bathymetry collected during seismic survey cruises.

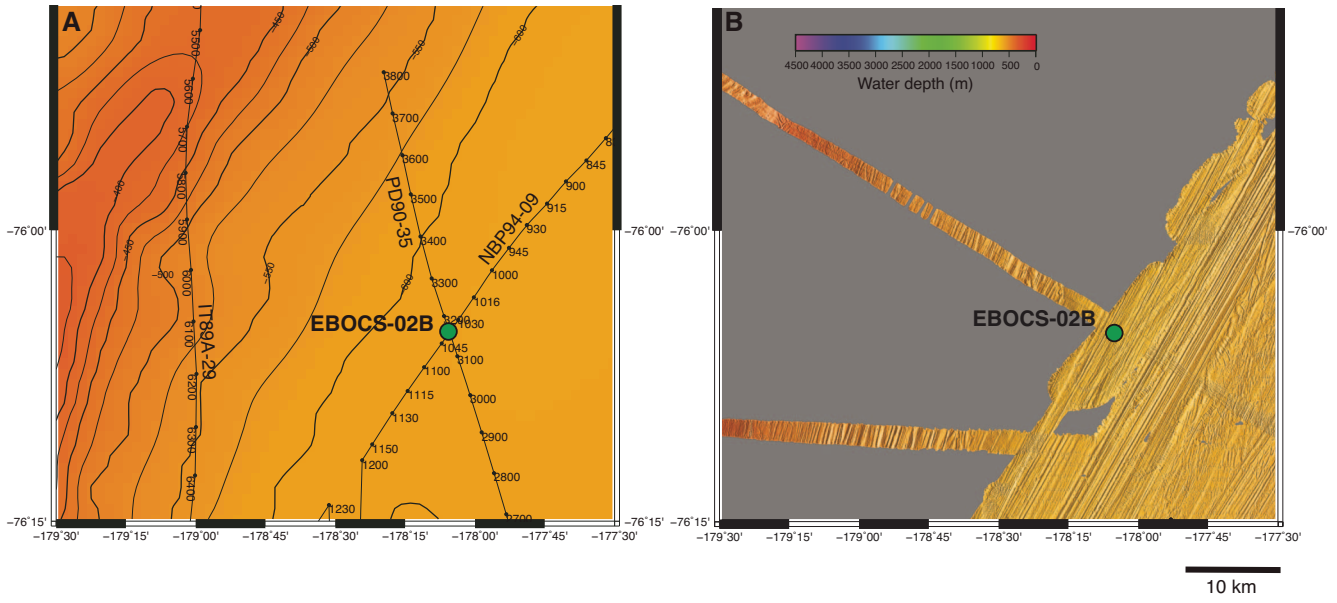

Figure AF4. Seismic reflection profile Line PD90-35 with location of proposed primary Site EBOCS-02B (76.08827°S, 178.09119°W; SP 3160; water depth = 658 m; target depth = 500 mbsf; approved maximum penetration = 500 mbsf).

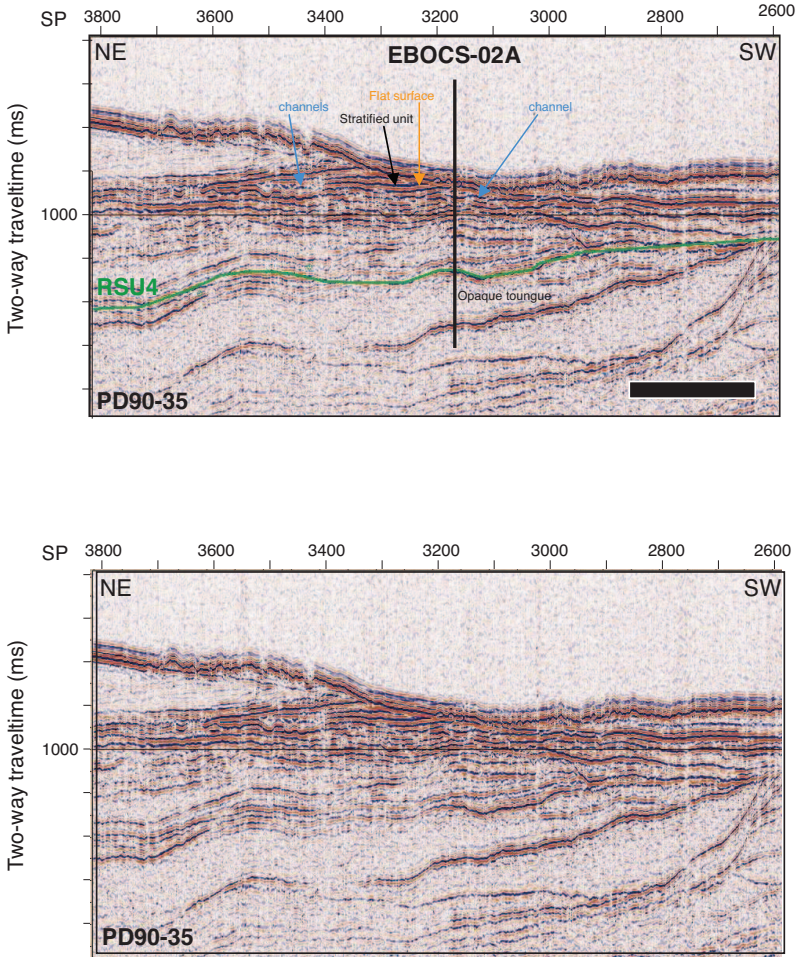

Figure AF5. Analog Line NBP94-09 with location of proposed primary Site EBOCS-02B (76.08827°S, 178.09119°W; SP 1063; water depth = 658 m; target depth = 500 mbsf; approved maximum penetration = 500 mbsf).

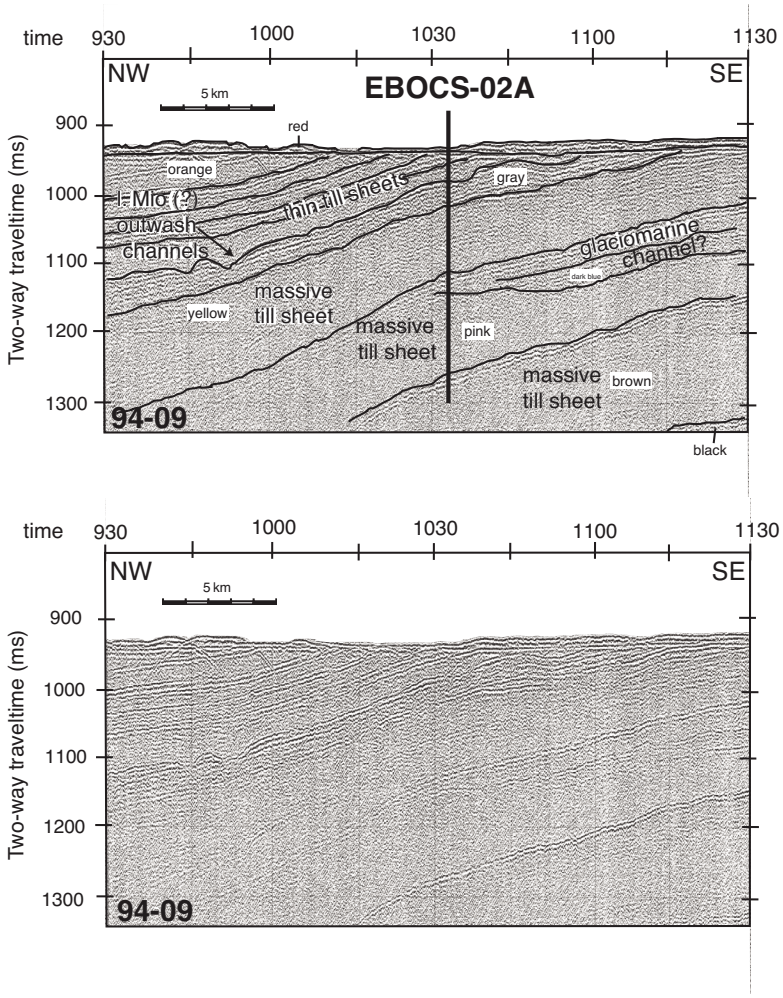

Figure AF6. Contoured bathymetric maps showing location of proposed primary Site EBOCS-03C on seismic reflection Profile IO6290-Y2 (Figure **AF7**). A. Bathymetry from Davey (2004). Contour interval = 25 m. B. Swath bathymetry collected during seismic survey cruises.

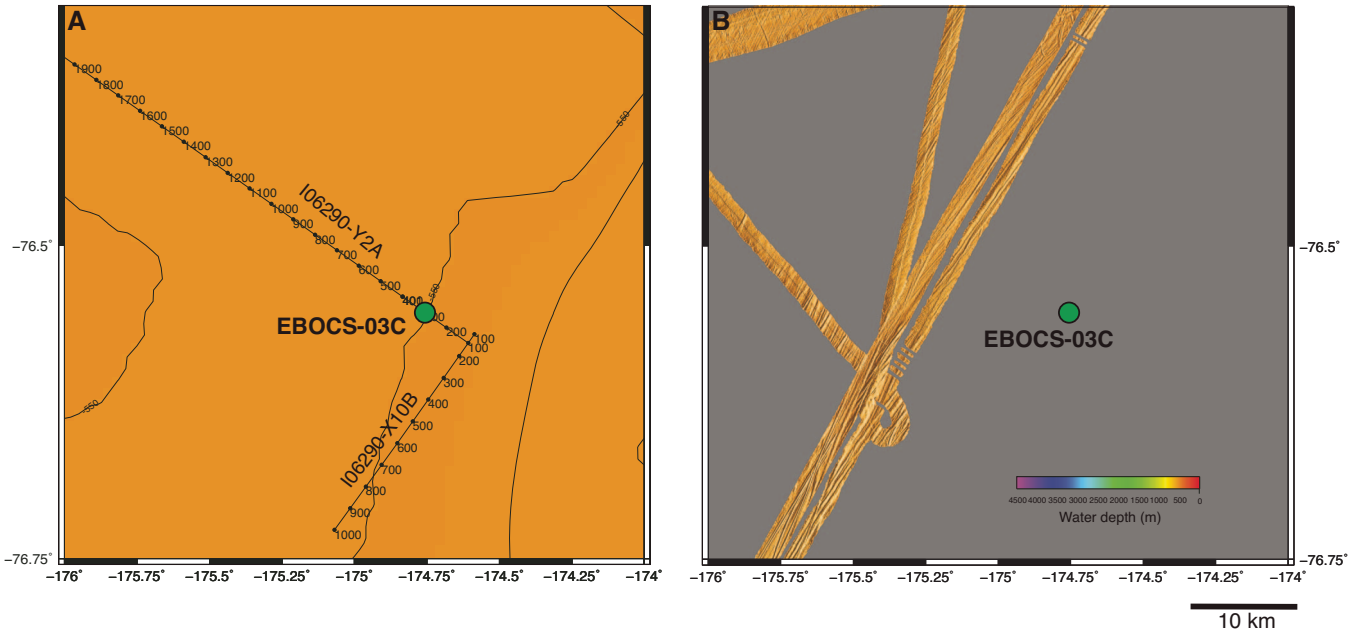

Figure AF7. Seismic reflection profile Line I06290-Y2 with location of proposed primary Site EBOCS-03C (76.55380°S, 174.75794°W; SP 300; water depth = 558 m; target depth = 545 mbsf; approved maximum penetration = 545 mbsf).

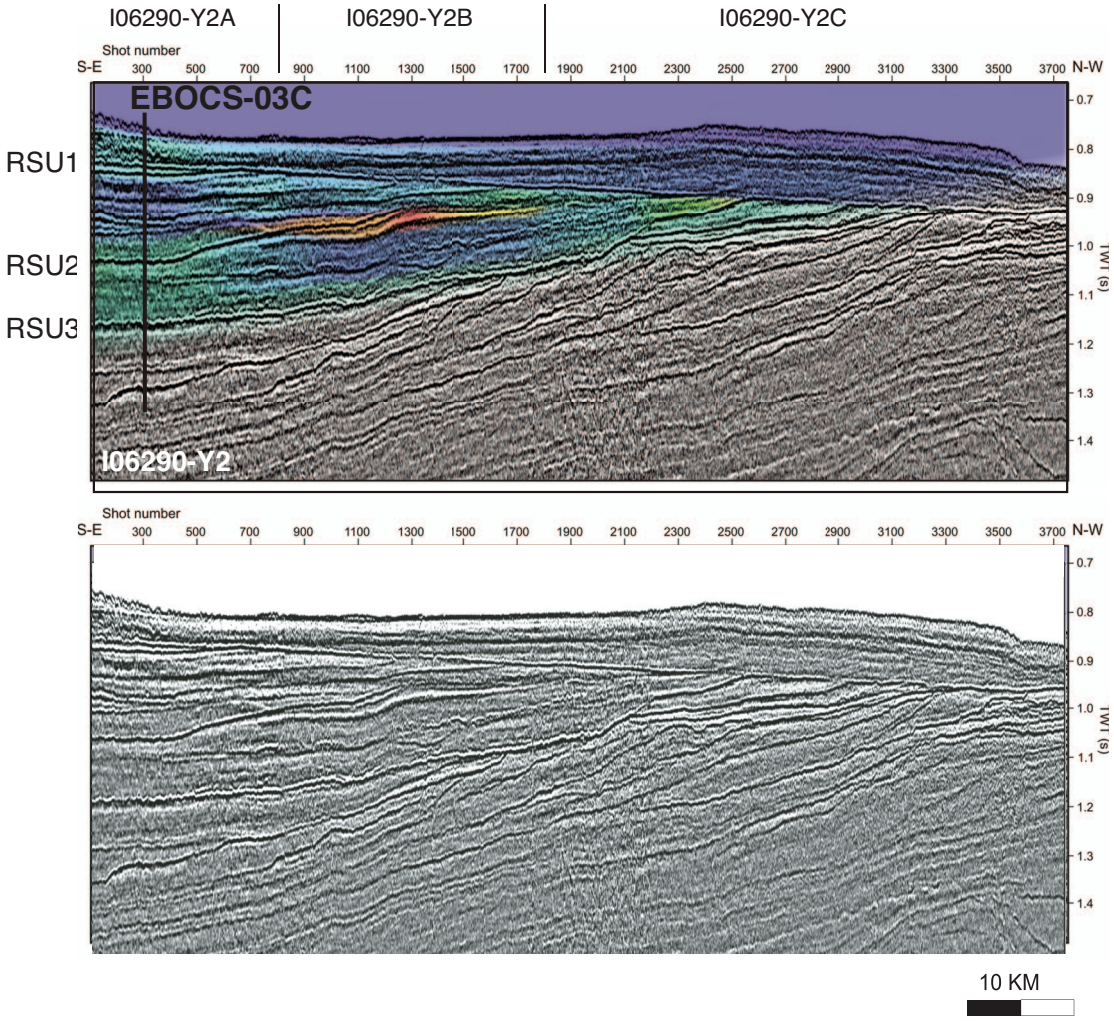

Figure AF8. Contoured bathymetric maps showing location of proposed primary Site EBOCS-04B on seismic reflection Profiles PD90-30 (Figure **AF9**) and NBP9601-T16 (Figure **A10**). A. Bathymetry from Davey (2004). Contour interval = 25 m. B. Swath bathymetry collected during seismic survey cruises.

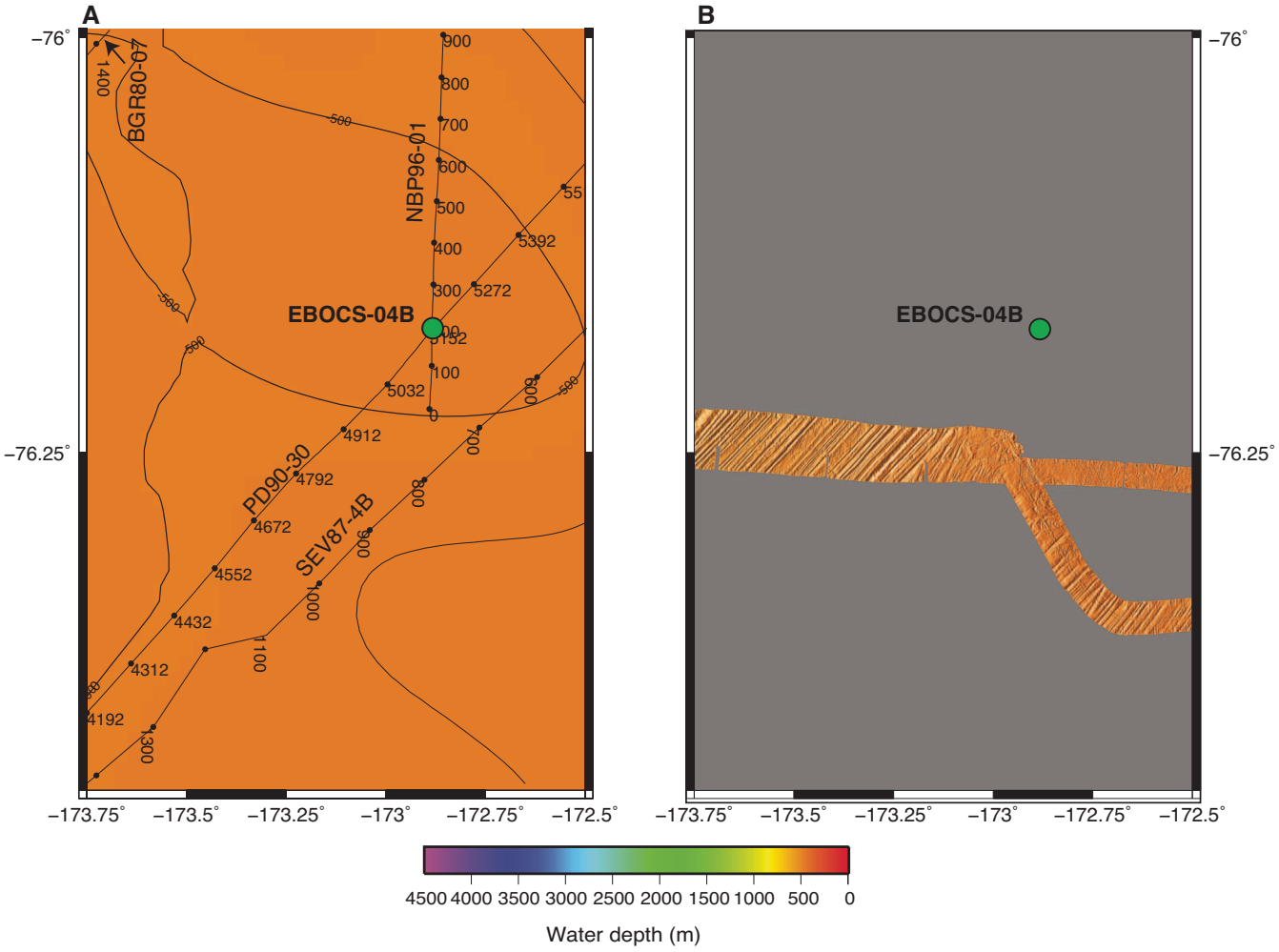

Figure AF9. Seismic reflection profile Line PD90-30 with location of proposed primary Site EBOCS-04B (76.17651°S, 172.88398°W; SP 5162; water depth = 480 m; target depth = 520 mbsf; approved maximum penetration = 520 mbsf).

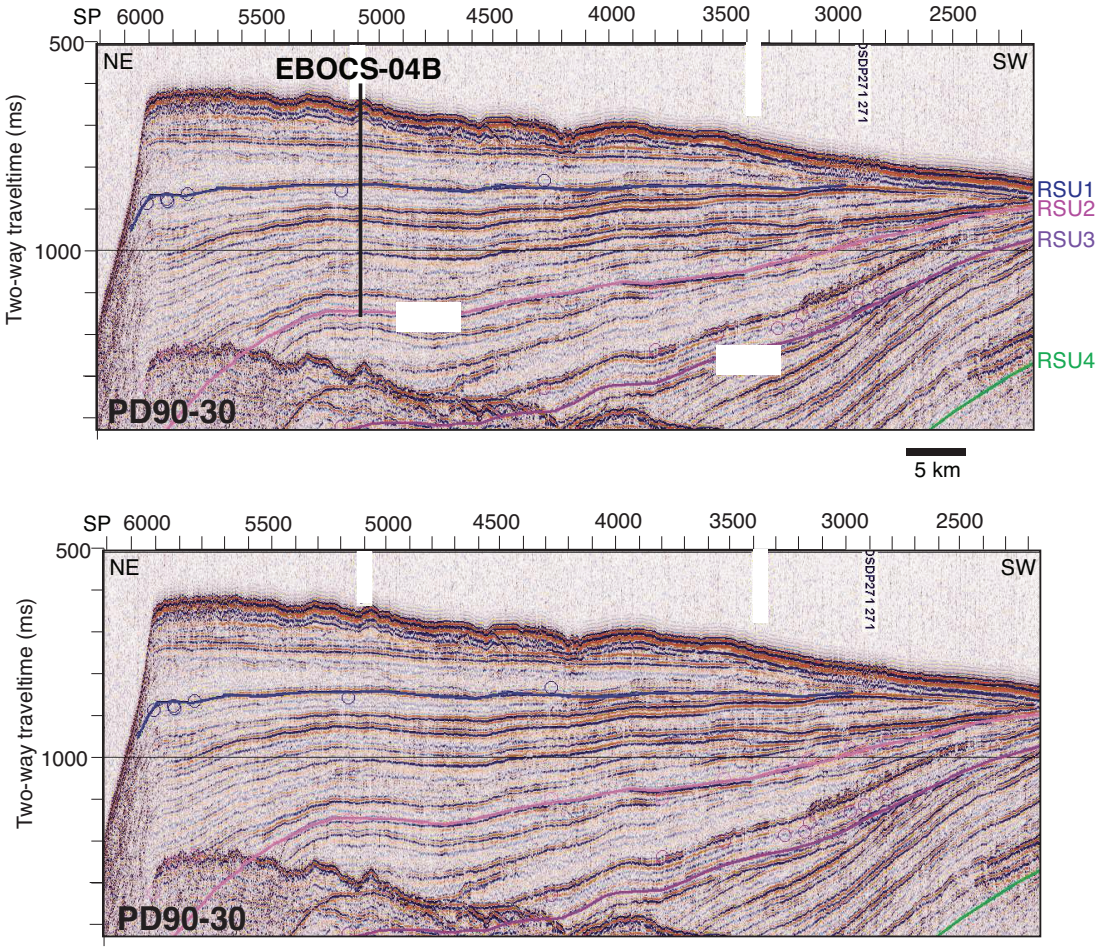

Figure AF10. Seismic reflection profile Line NBP9601-T16 with location of proposed primary Site EBOCS-04B (76.17651°S, 172.88398°W; SP 190; water depth = 480 m; target depth = 520 mbsf; approved maximum penetration = 520 mbsf).

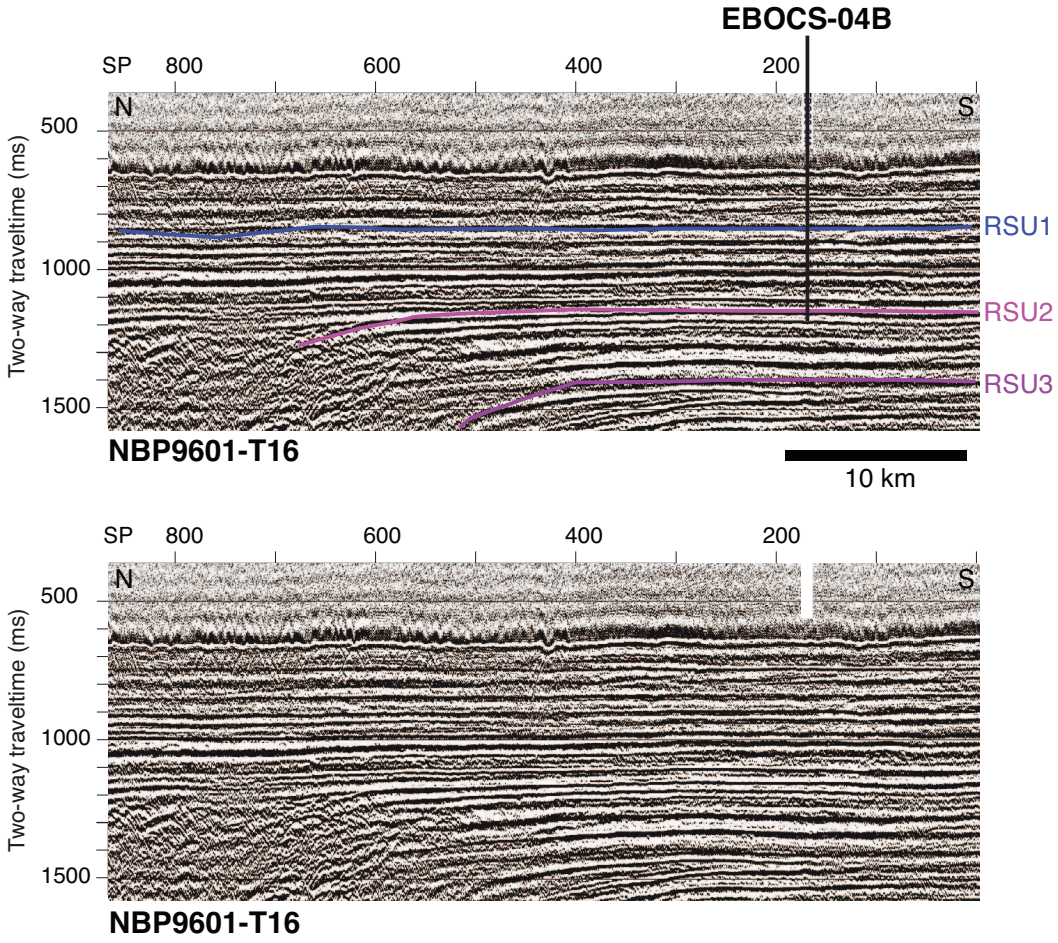

Figure AF11. Contoured bathymetric maps showing location of proposed primary Site RSCR-02B on seismic reflection Profile ATC82B-208 (Figure **AF12**) and proposed alternate Site RSCR-10A on seismic reflection Profile TAN0602-08 (Figure **AF28**). A. Bathymetry from Davey (2004). Contour interval = 25 m. B. Swath bathymetry collected during seismic survey cruises.

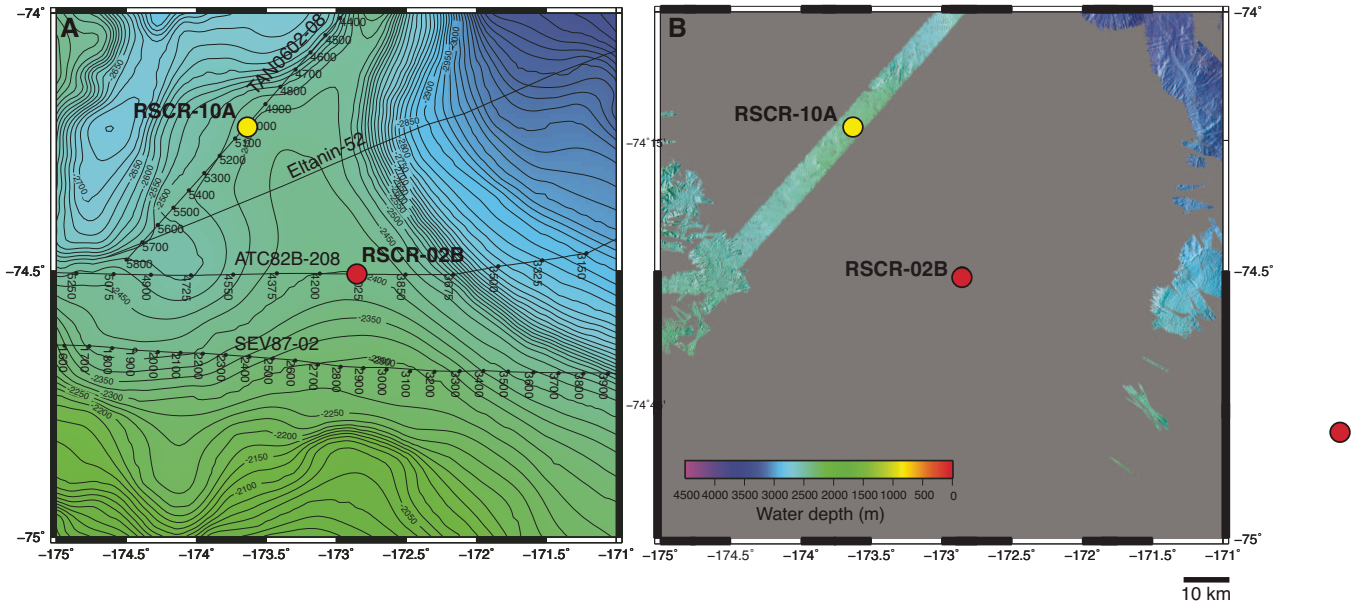

Figure AF12. Seismic reflection profile Line ATC82B-208 with location of proposed primary Site RSCR-02B (74.50592°S, 172.85452°W; SP 4050; water depth 2550 m; target depth = 1000 mbsf; approved maximum depth = 1000 mbsf). Top panel shows full line. Bottom panels show interpreted (left) and uninterpreted (right) close-up of the box in the top panel.

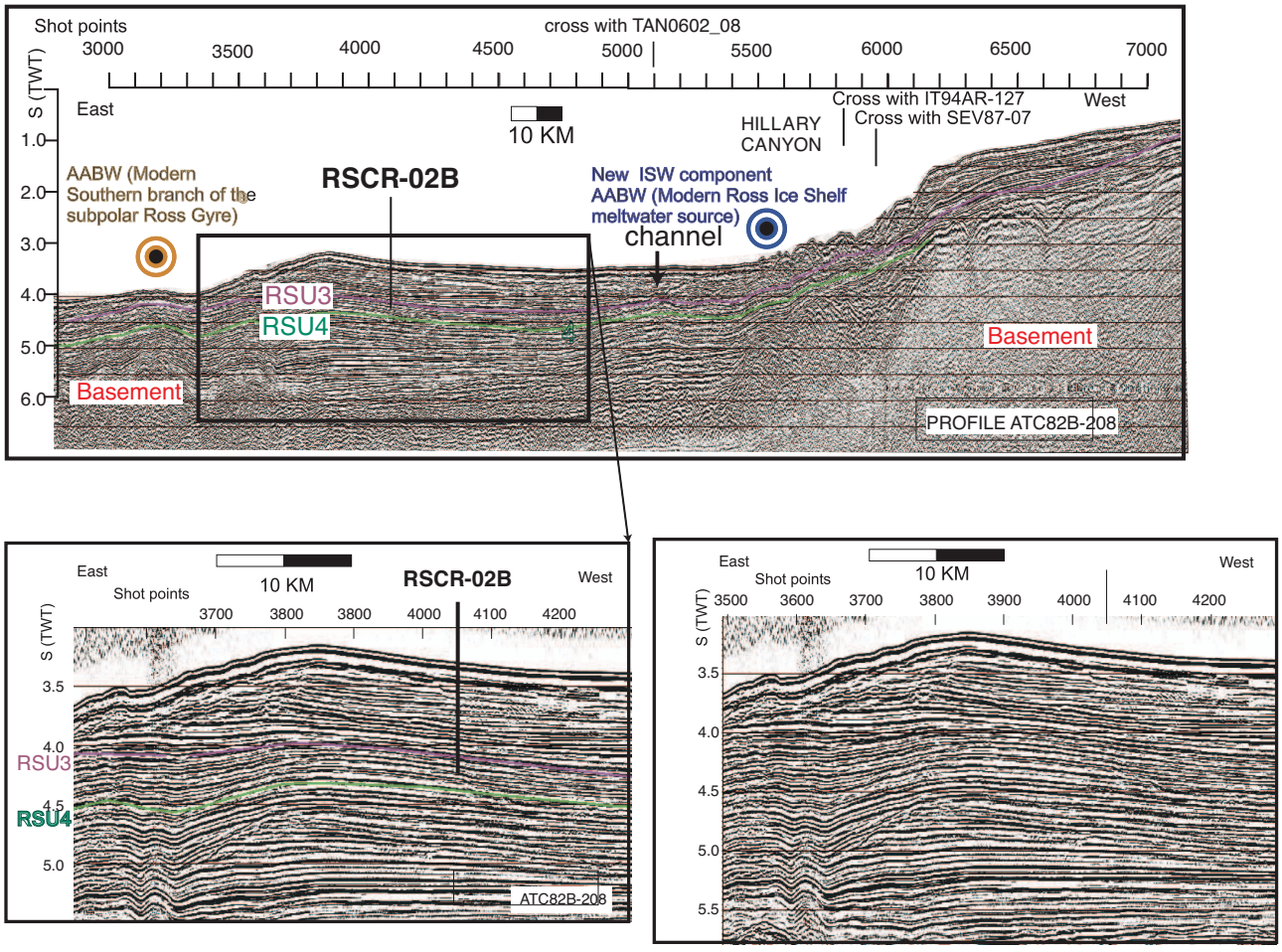

Figure AF13. Contoured bathymetric maps showing location of proposed primary Site RSCR-11A on seismic reflection Profiles IT91A-88B (Figure **AF14**) and TAN0602-10 (Figure **AF15**). A. Bathymetry from Davey (2004). Contour interval = 25 m. B. Swath bathymetry collected during seismic survey cruises.

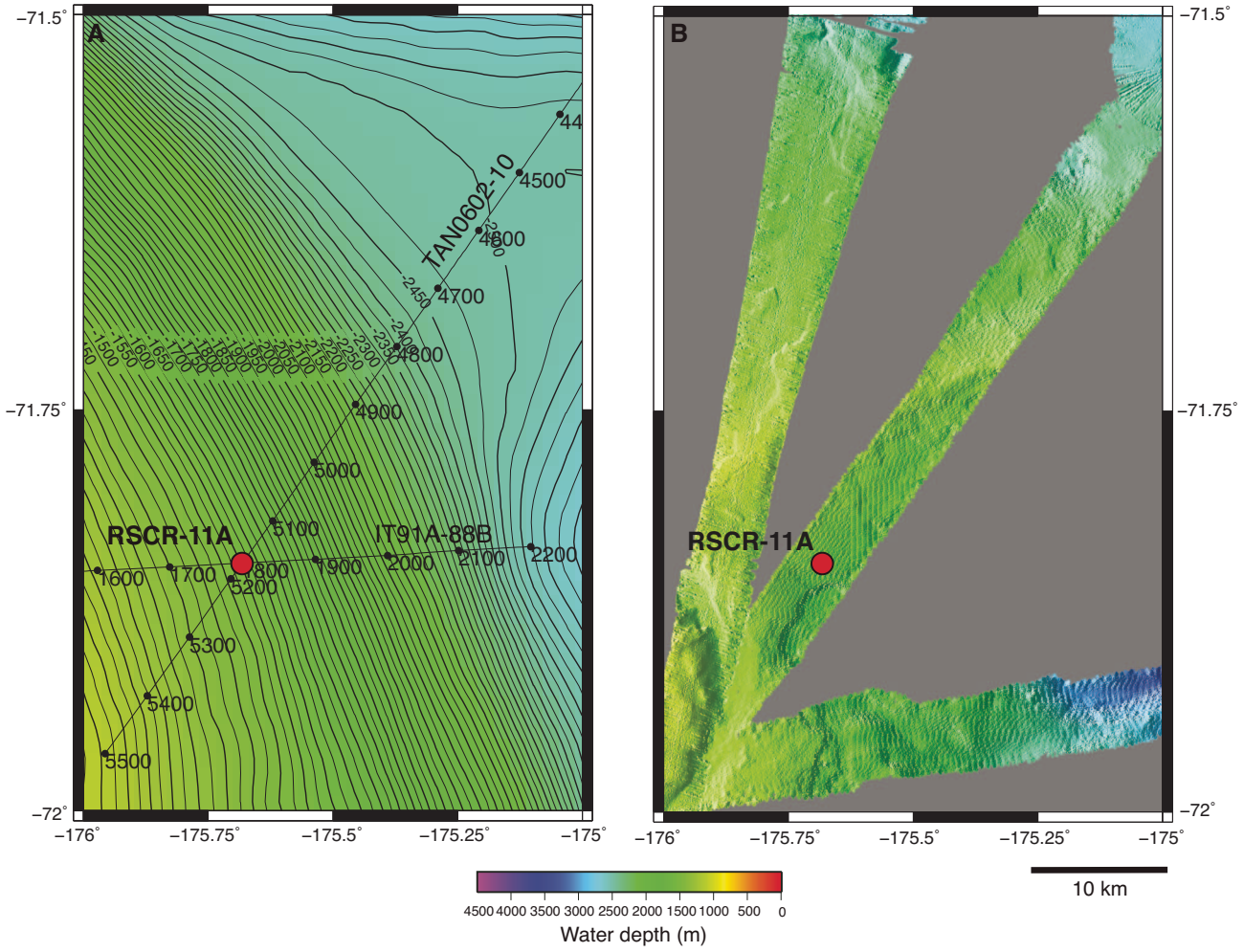

Figure AF14. Seismic reflection profile Line IT91A-88B with location of proposed primary Site RSCR-11A (71.84603°S, 175.67904°W; SP 1800; water depth = 1534 m; target depth = 500 mbsf; approved maximum penetration = 500 mbsf).

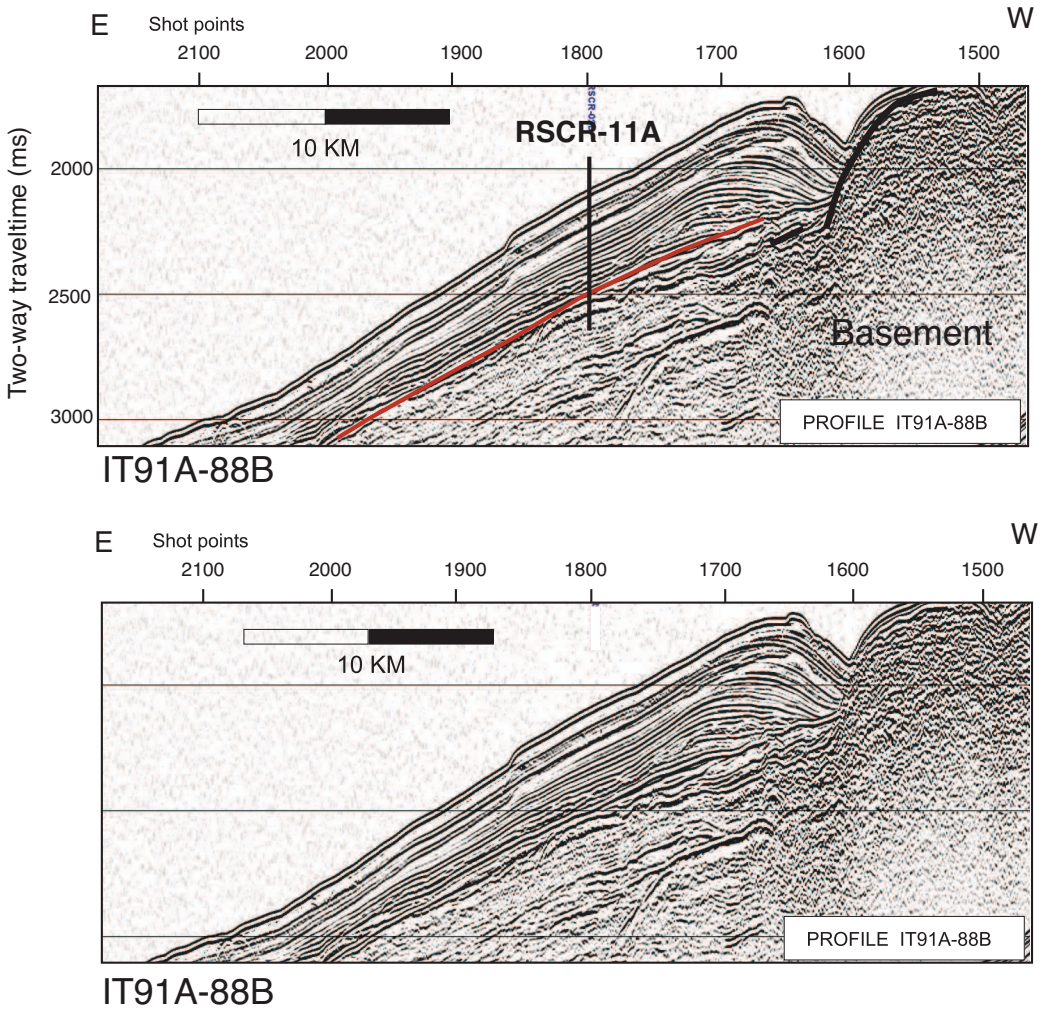

Figure AF15. Seismic reflection profile Line TAN0602-10 with location of proposed primary Site RSCR-11A (71.84603°S, 175.67904°W; SP 5173; water depth = 1534 m; target depth = 500 mbsf; approved maximum penetration = 500 mbsf).

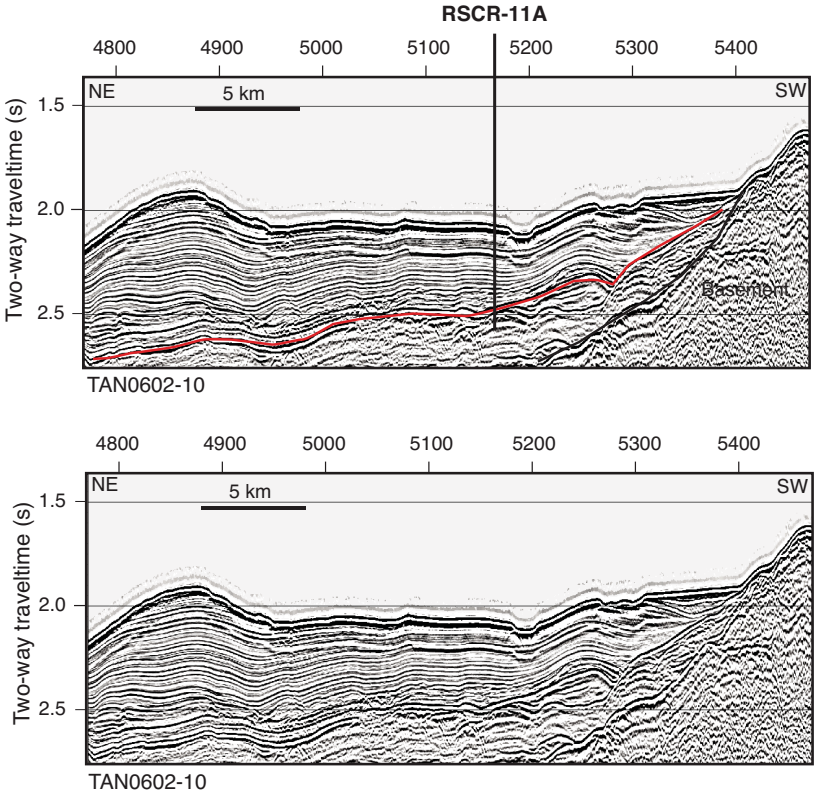

Figure AF16. Contoured bathymetric maps showing location of proposed alternate Site EBOCS-05A on seismic reflection Profiles PD90-36 (Figure **AF17**) and BGR80-08 (Figure **AF18**). A. Bathymetry from Davey (2004). Contour interval = 25 m. B. Swath bathymetry collected during seismic survey cruises.

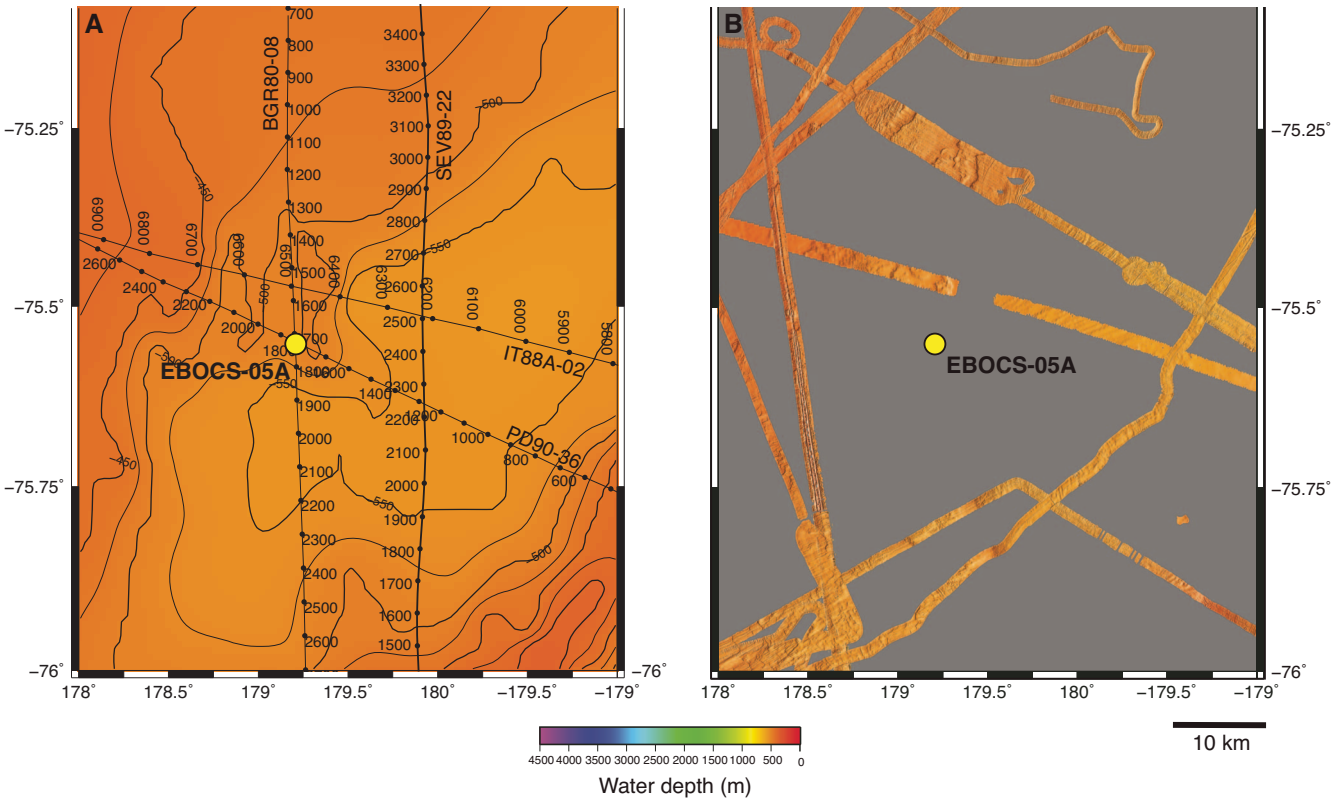

Figure AF17. Seismic reflection profile Line PD90-36 with location of proposed alternate Site EBOCS-05A (75.54986°S, 179.20599°E; SP 1838; water depth = 525 m; target penetration depth = 700 mbsf; approved maximum penetration = 700 mbsf).

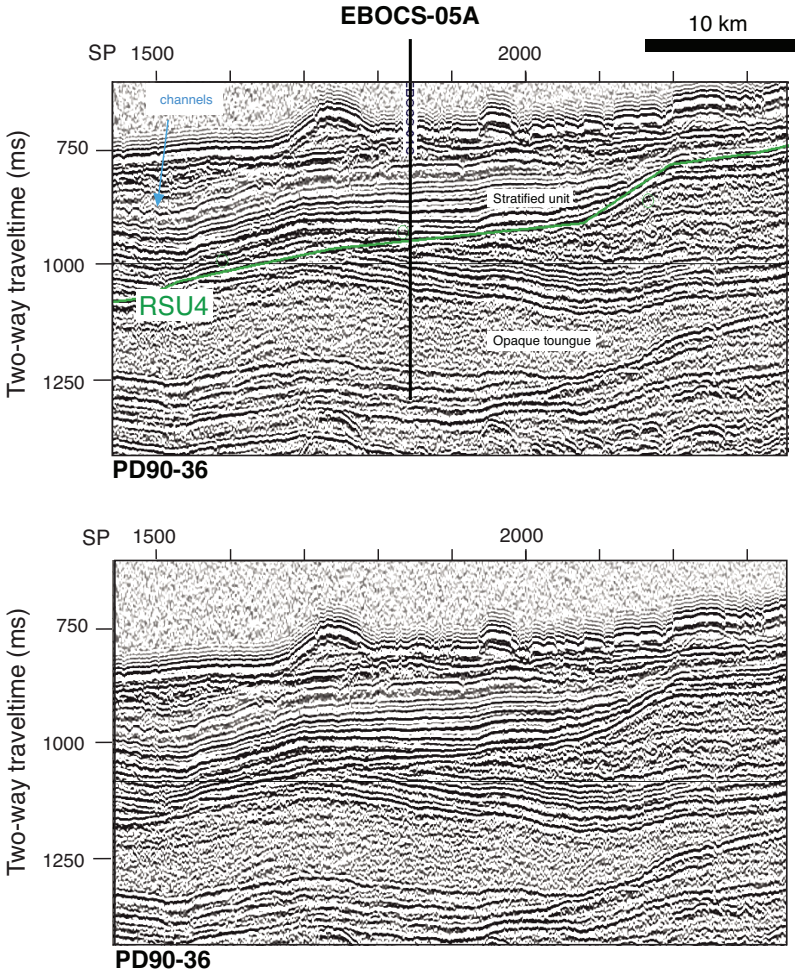

Figure AF18. Seismic reflection profile Line BGR-80-08 with location of proposed alternate Site EBOCS-05A (75.54986°S, 179.20599°E; SP 1724; water depth = 525 m; target penetration depth = 700 mbsf; approved maximum penetration = 700 mbsf).

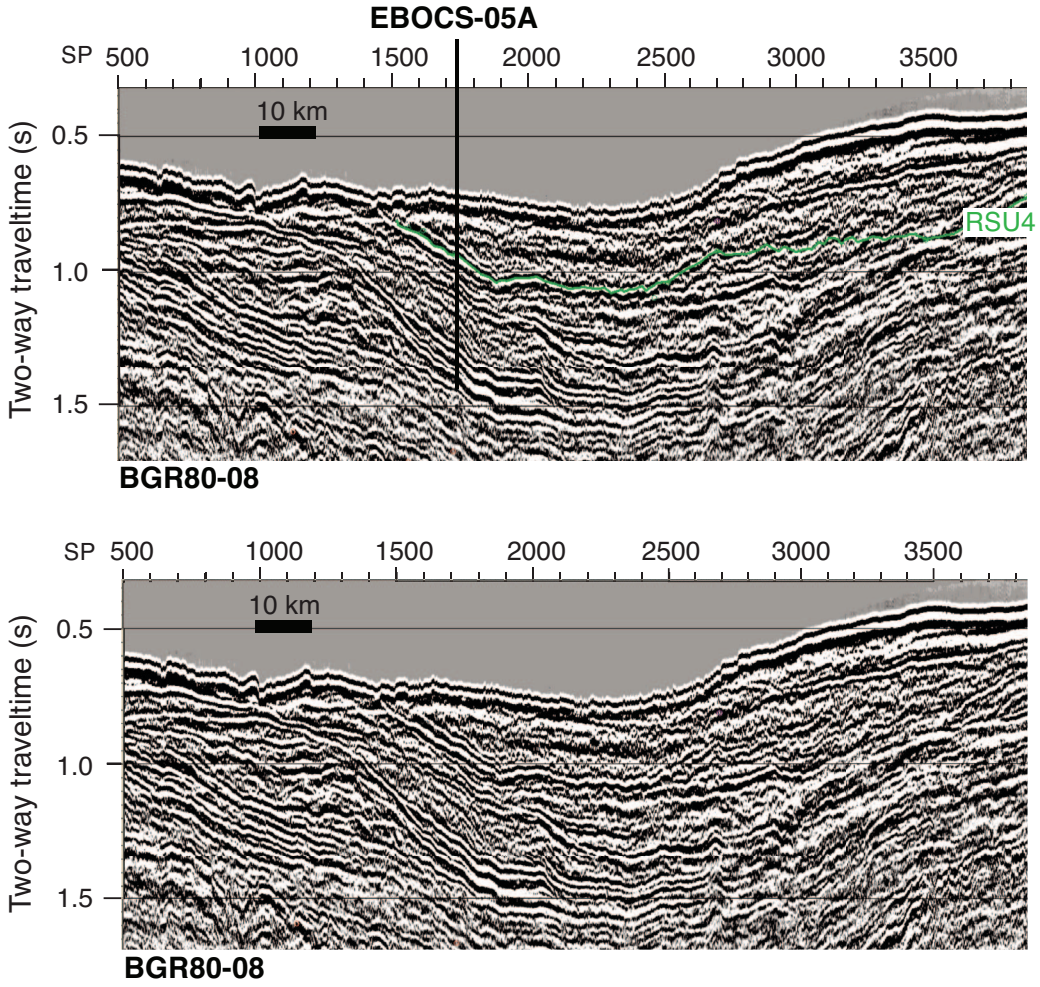

Figure AF19. Contoured bathymetric maps showing location of proposed alternate Site EBOCS-06A on seismic reflection Profiles IO6290-Y7 (Figure **AF20**) and IO6290-X4 (Figure **AF21**). A. Bathymetry from Davey (2004). Contour interval = 25 m. B. Swath bathymetry collected during seismic survey cruises.

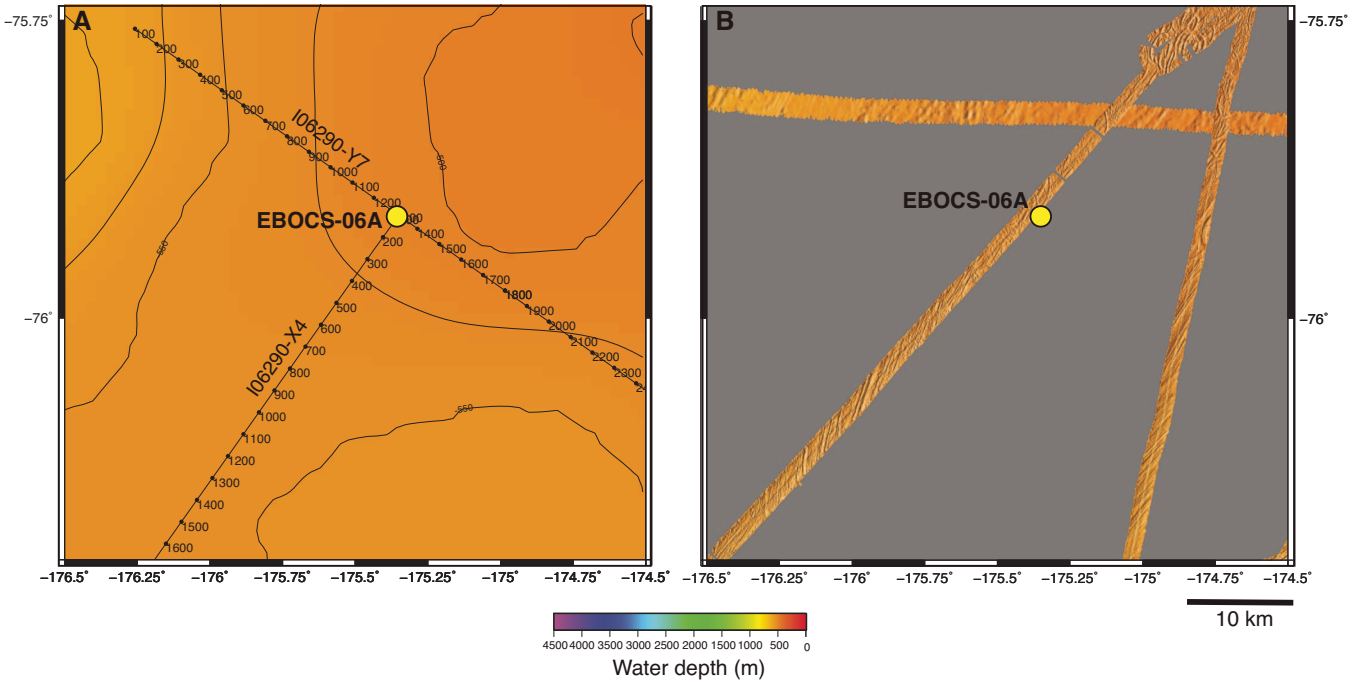

Figure AF20. Seismic reflection profile Line IO6290-Y7 with location of proposed alternate Site EBOCS-06A (75.91448°S, 175.34958°W; SP 1315; water depth = 515 m; target penetration depth = 700 mbsf; approved maximum penetration = 700 mbsf).

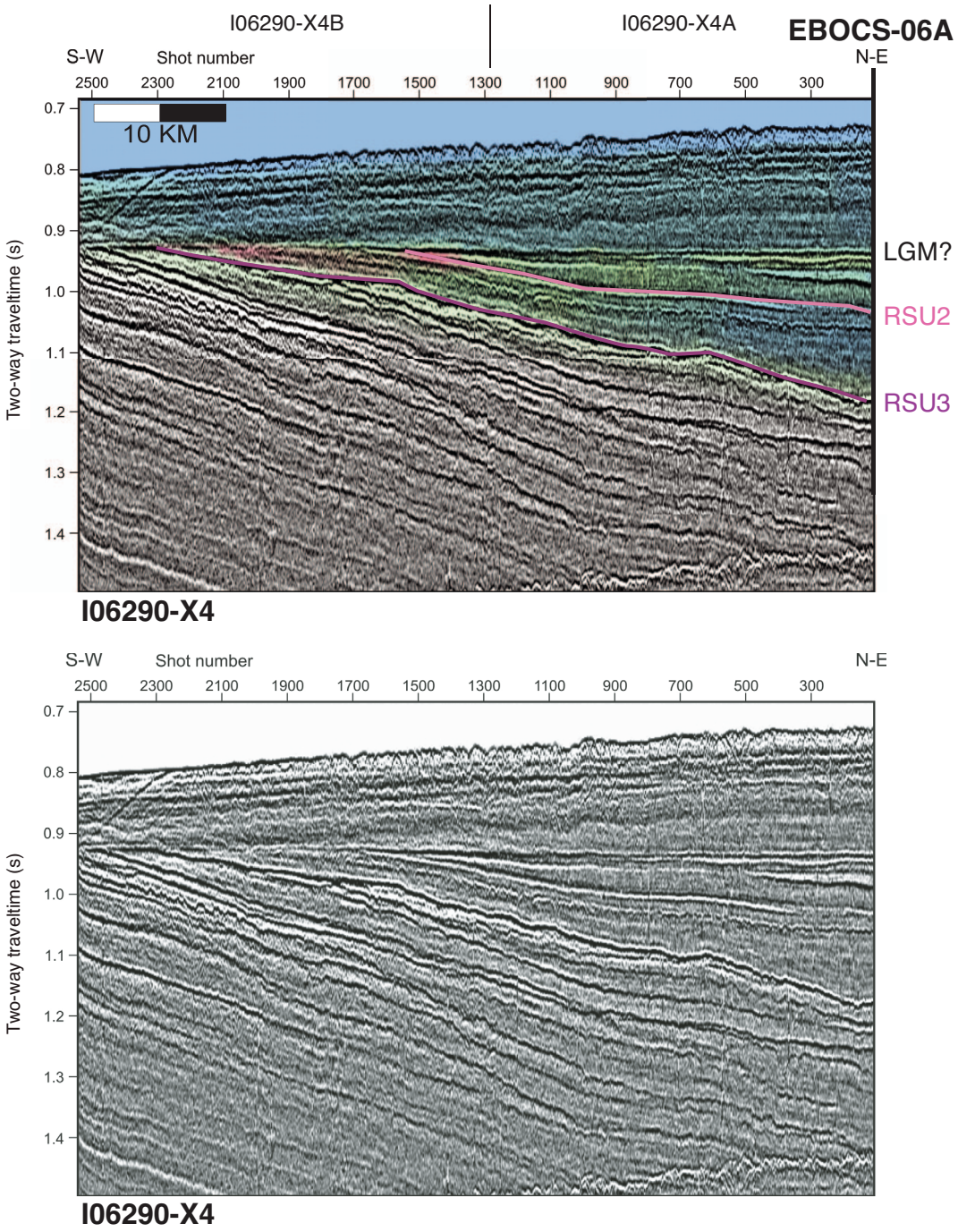

Figure AF21. Seismic reflection profile Line IO6290-X4 with location of proposed alternate Site EBOCS-06A (75.91448°S, 175.34958°W; SP 100; water depth = 515 m; target penetration depth = 700 mbsf; approved maximum penetration = 700 mbsf).

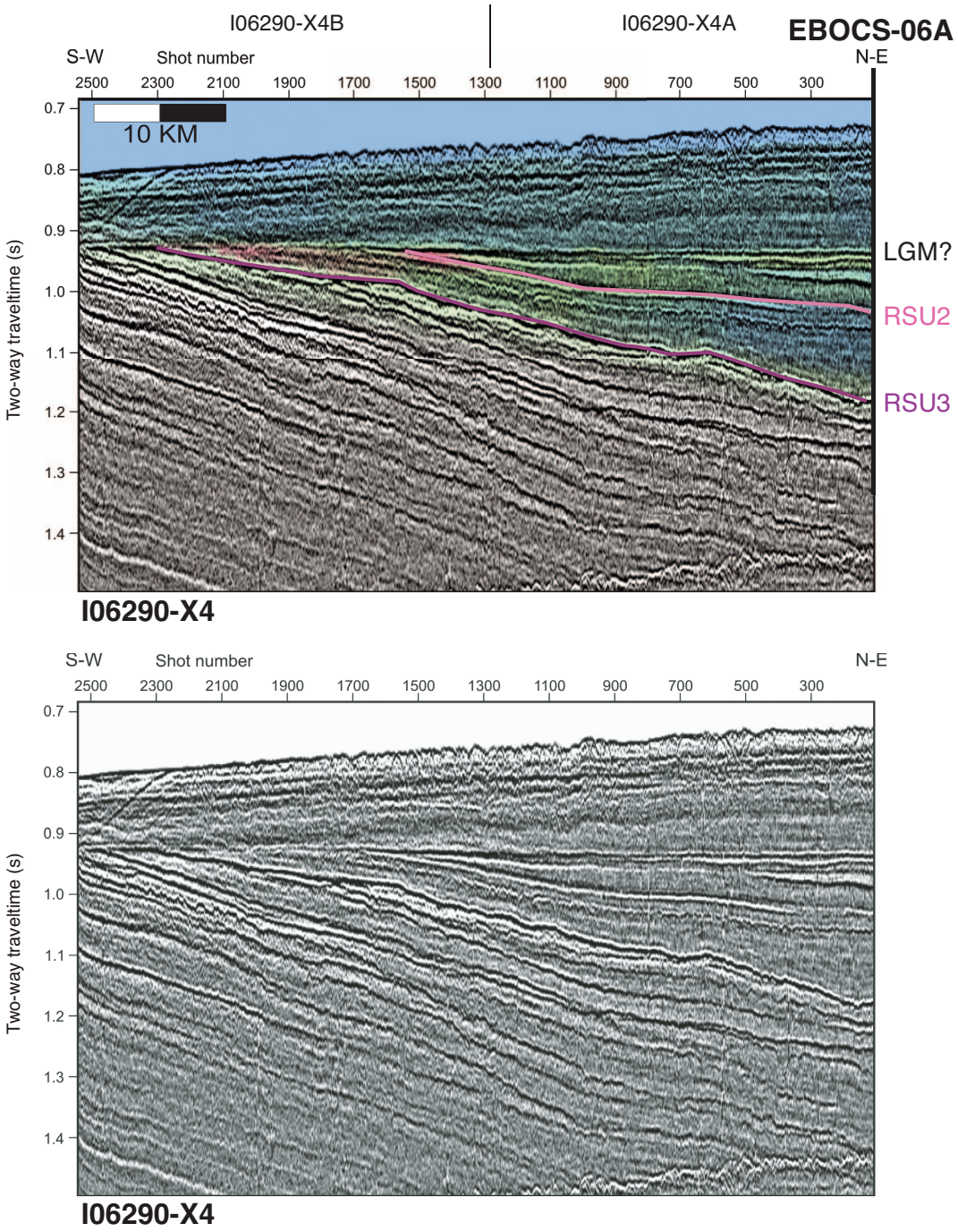

Figure AF22. Contoured bathymetric maps showing location of proposed alternate Site EBOCS-07C on seismic reflection Profile IO6290-Y7B (Figure **AF23**). A. Bathymetry from Davey (2004). Contour interval = 25 m. B. Swath bathymetry collected during seismic survey cruises.

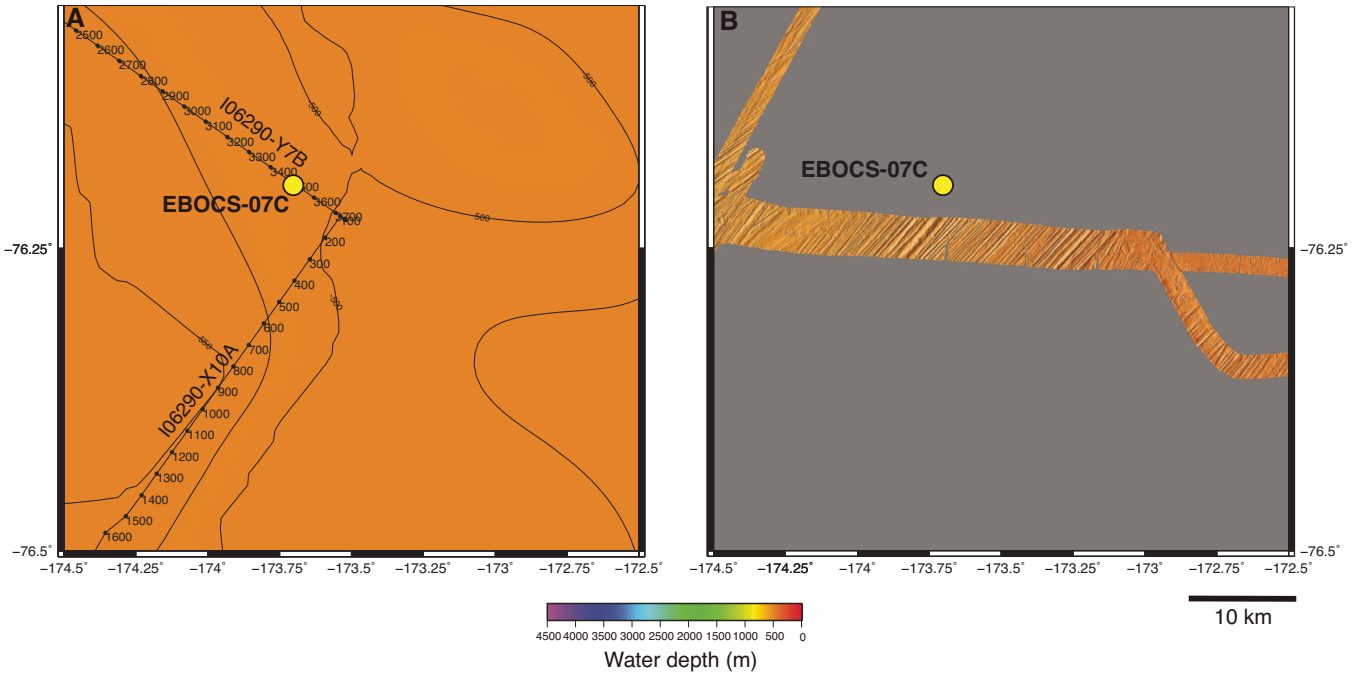

Figure AF23. Seismic reflection profile Line IO6290-Y7 with location of proposed alternate Site EBOCS-07C (76.19502°S, 173.70576°W; SP 3500; water depth = 540 m; target penetration depth = 750 mbsf; approved maximum penetration depth = 750 mbsf).

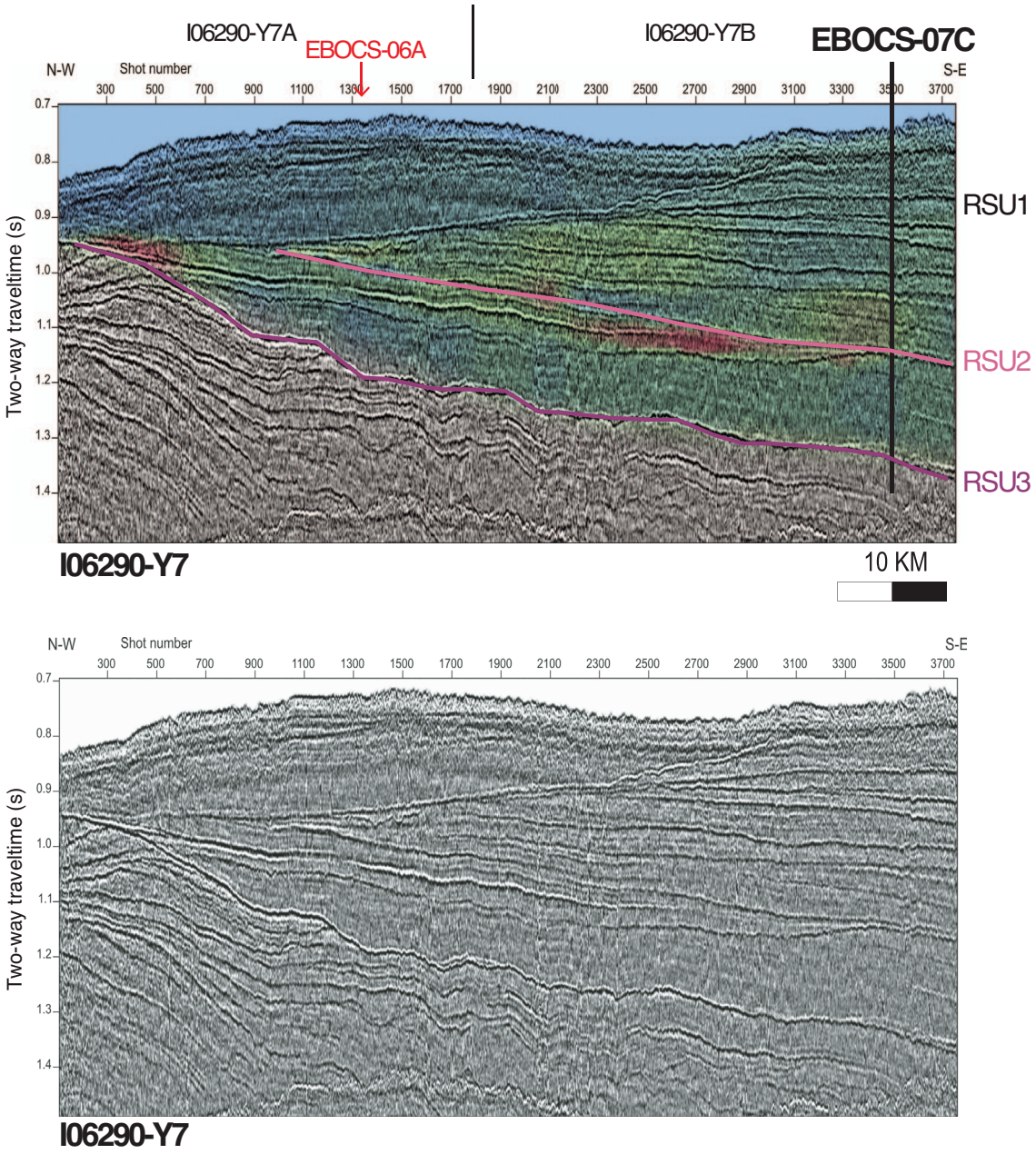

Figure AF24. Contoured bathymetric maps showing location of proposed alternate Site RSCR-01B on seismic reflection Profile IT88-01C (Figure **AF25**). A. Bathymetry from Davey (2004). Contour interval = 25 m. B. Swath bathymetry collected during seismic survey cruises.

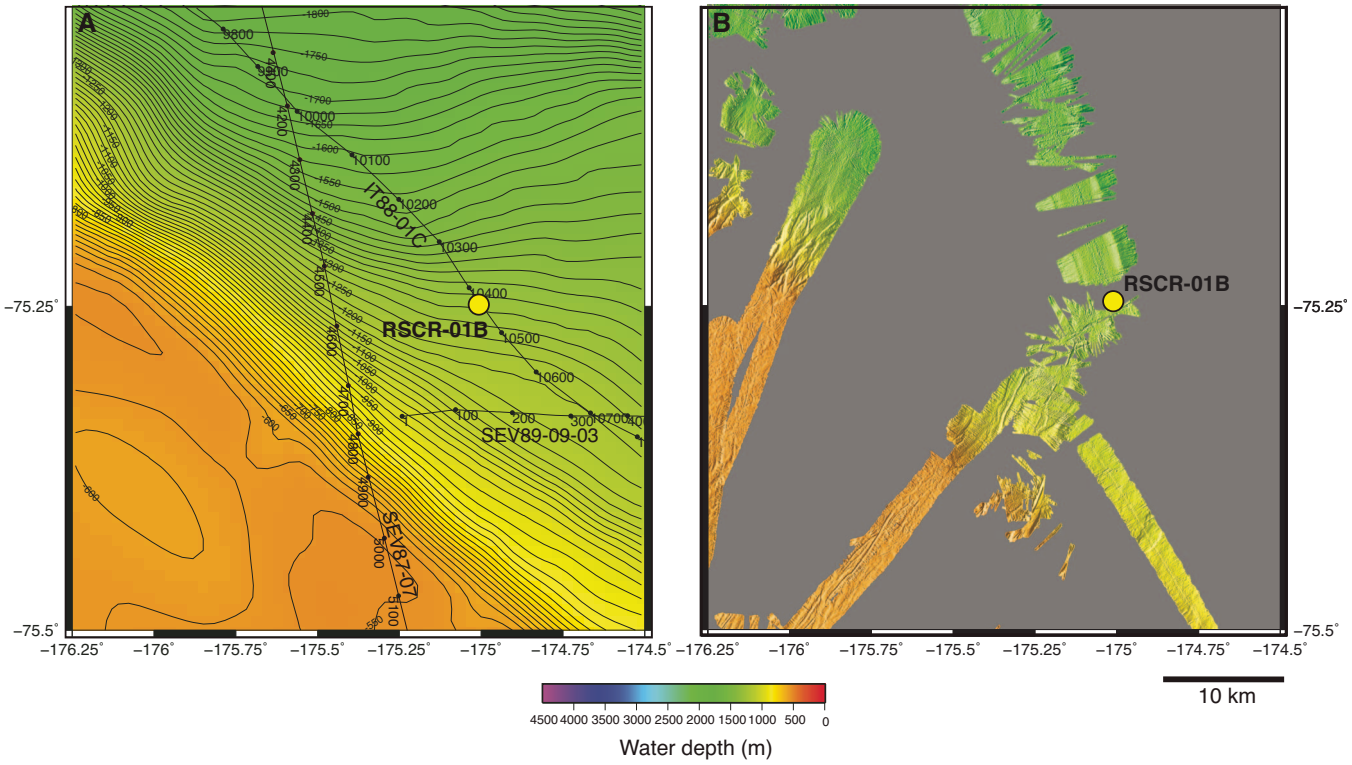

Figure AF25. Seismic reflection profile Line IT88-01C with location of proposed alternate Site RSCR-01B (75.24660°S, 175.00582°W; SP 10430; water depth = 1400 m; target penetration depth = 1000 mbsf; approved maximum penetration = 1000 mbsf).

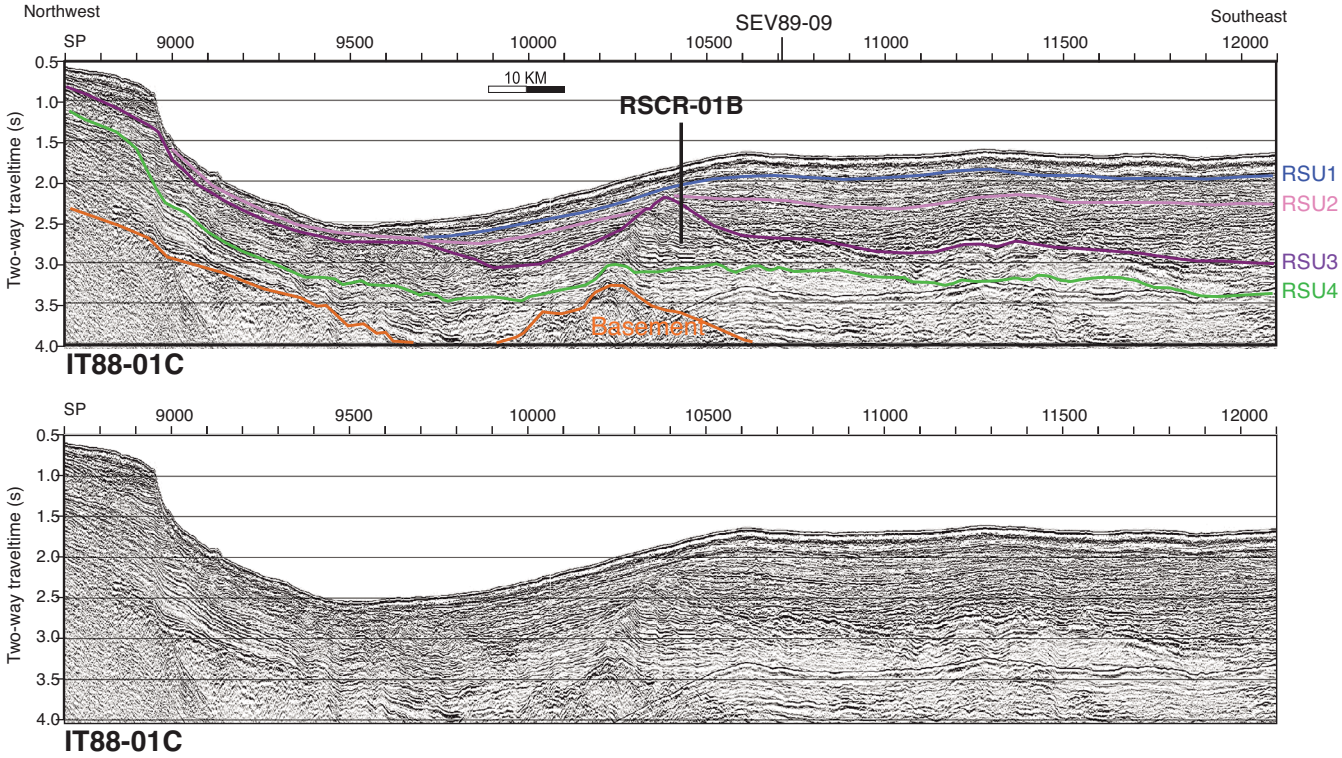

Figure AF26. Contoured bathymetric maps showing location of proposed alternate Site RSCR-03A on seismic reflection Profile IT94A-127 (Figure **AF27**). A. Bathymetry from Davey (2004). Contour interval = 25 m. B. Swath bathymetry collected during seismic survey cruises.

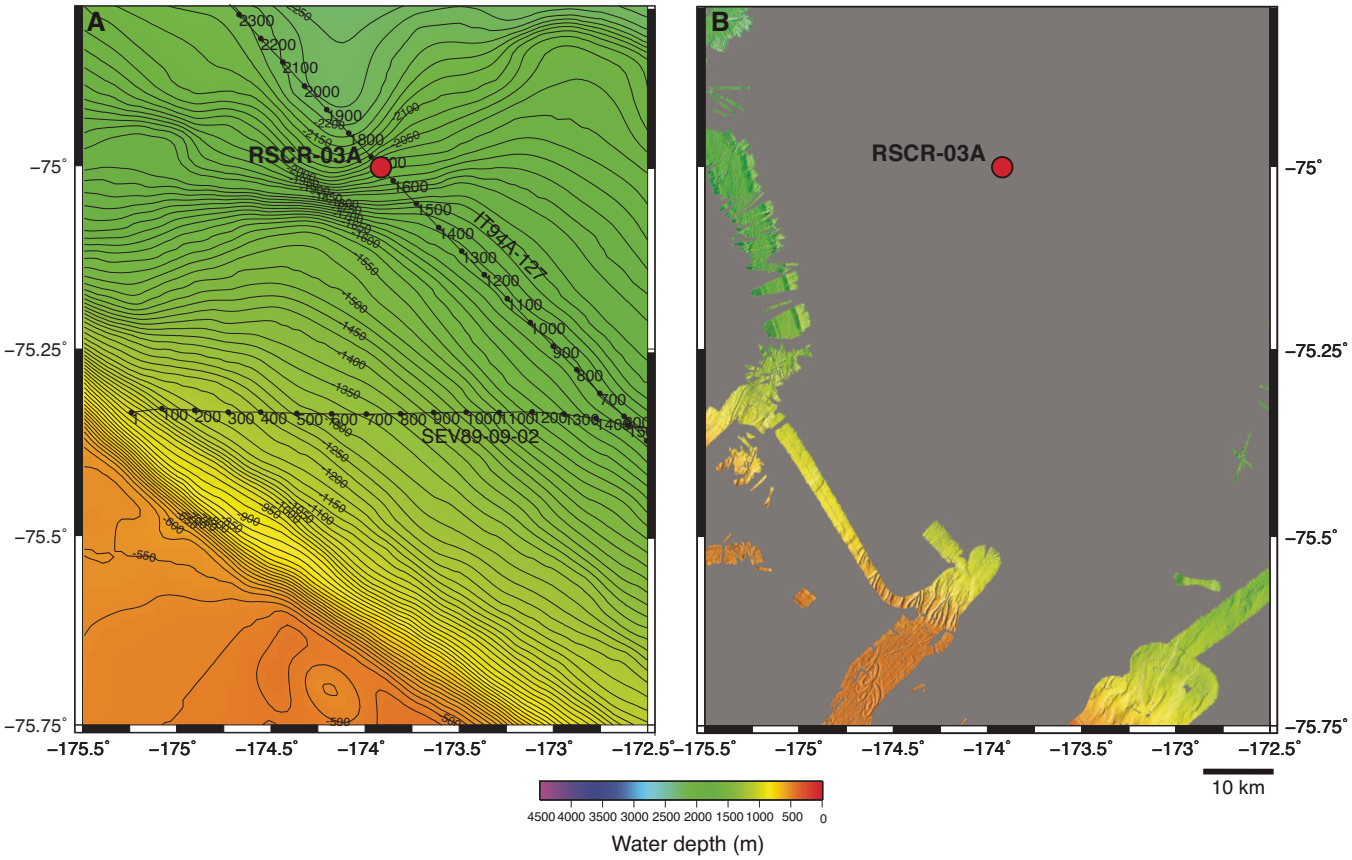

Figure AF27. Seismic reflection profile Line IT94A-127 with location of proposed alternate Site RSCR-03A (75.00100°S, 173.92012°W; SP 1660; water depth = 1824 m; target penetration depth = 800 mbsf; approved maximum depth = 800 mbsf).

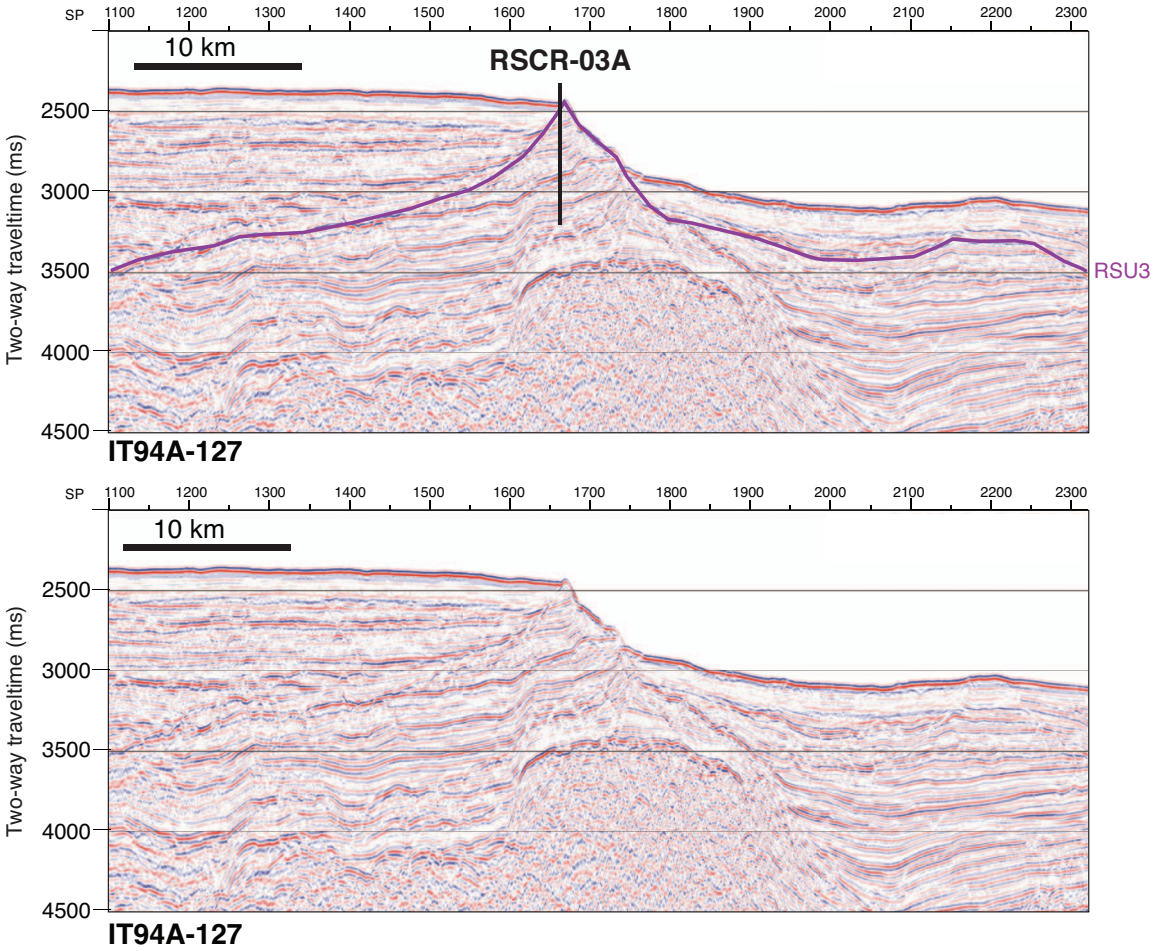

Figure AF28. Seismic reflection profile Line TAN0602-08 with location of proposed alternate Site RSCR-10A (74.21739°S, 173.63372°W; SP 5000; water depth = 2390 m; target penetration depth = 1000 mbsf; approved maximum penetration = 1000 mbsf).

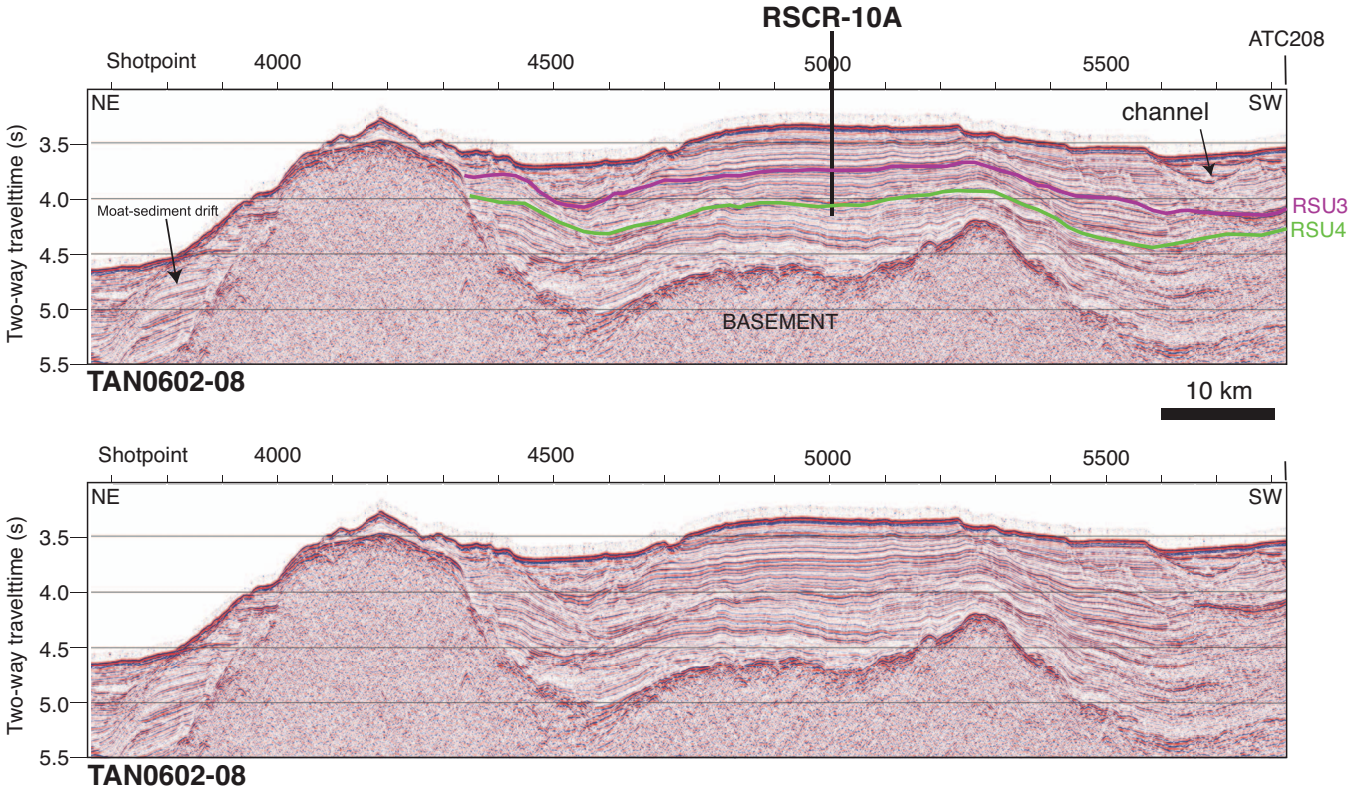

Figure AF29. Contoured bathymetric maps showing location of proposed alternate Site RSCR-08C on seismic reflection Profiles BGR80-008A (Figure **AF30**) and KSL14-02 (Figure **AF31**). A. Bathymetry from Davey (2004). Contour interval = 25 m. B. Swath bathymetry collected during seismic survey cruises.

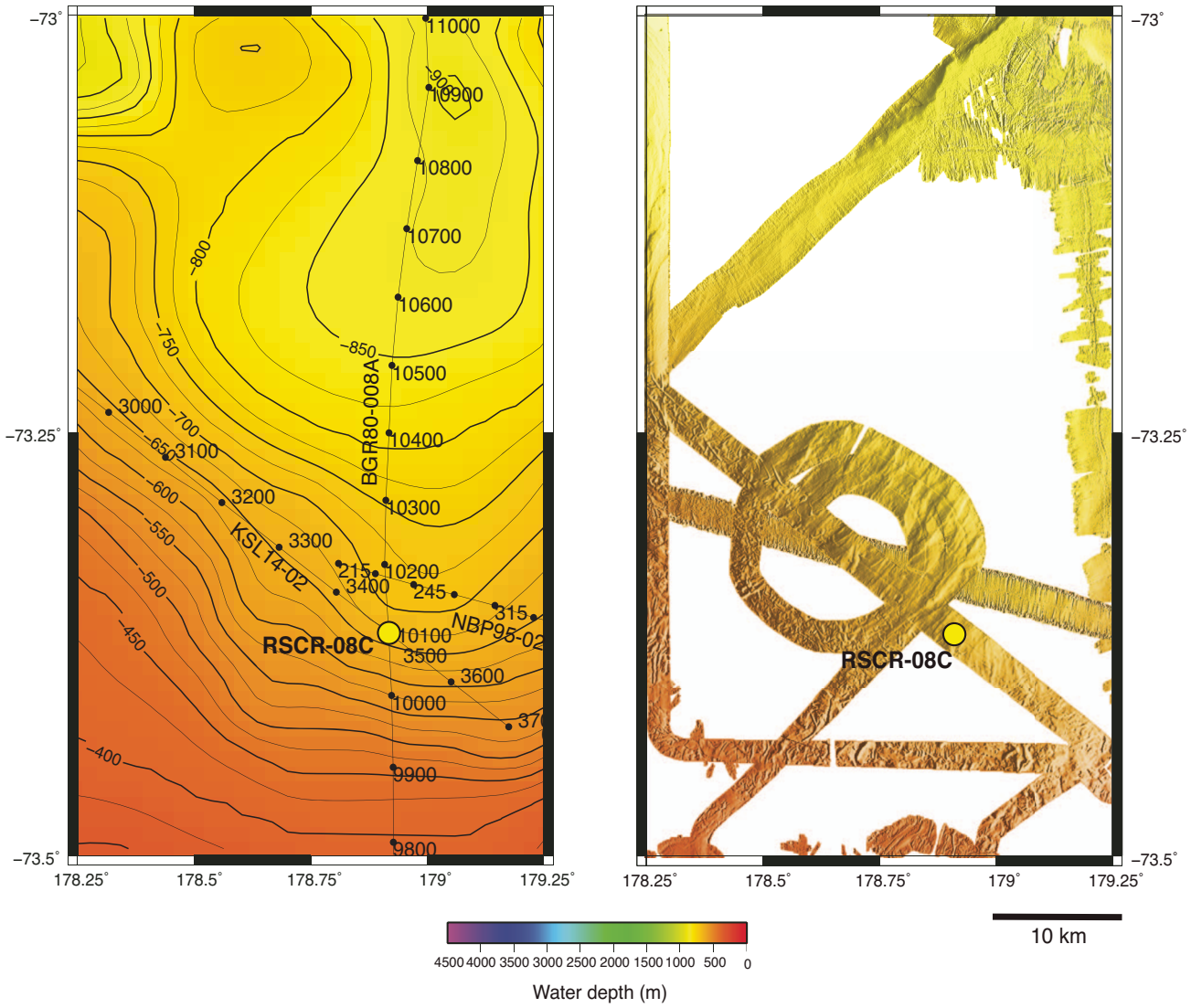

Figure AF30. Seismic reflection profile Line BGR80-008A with location of proposed alternate Site RSCR-08C (73.36928°S, 178.91774°E; SP 10095; water depth = 700 m; target penetration depth = 1000 mbsf; approved maximum penetration = 1000 mbsf).

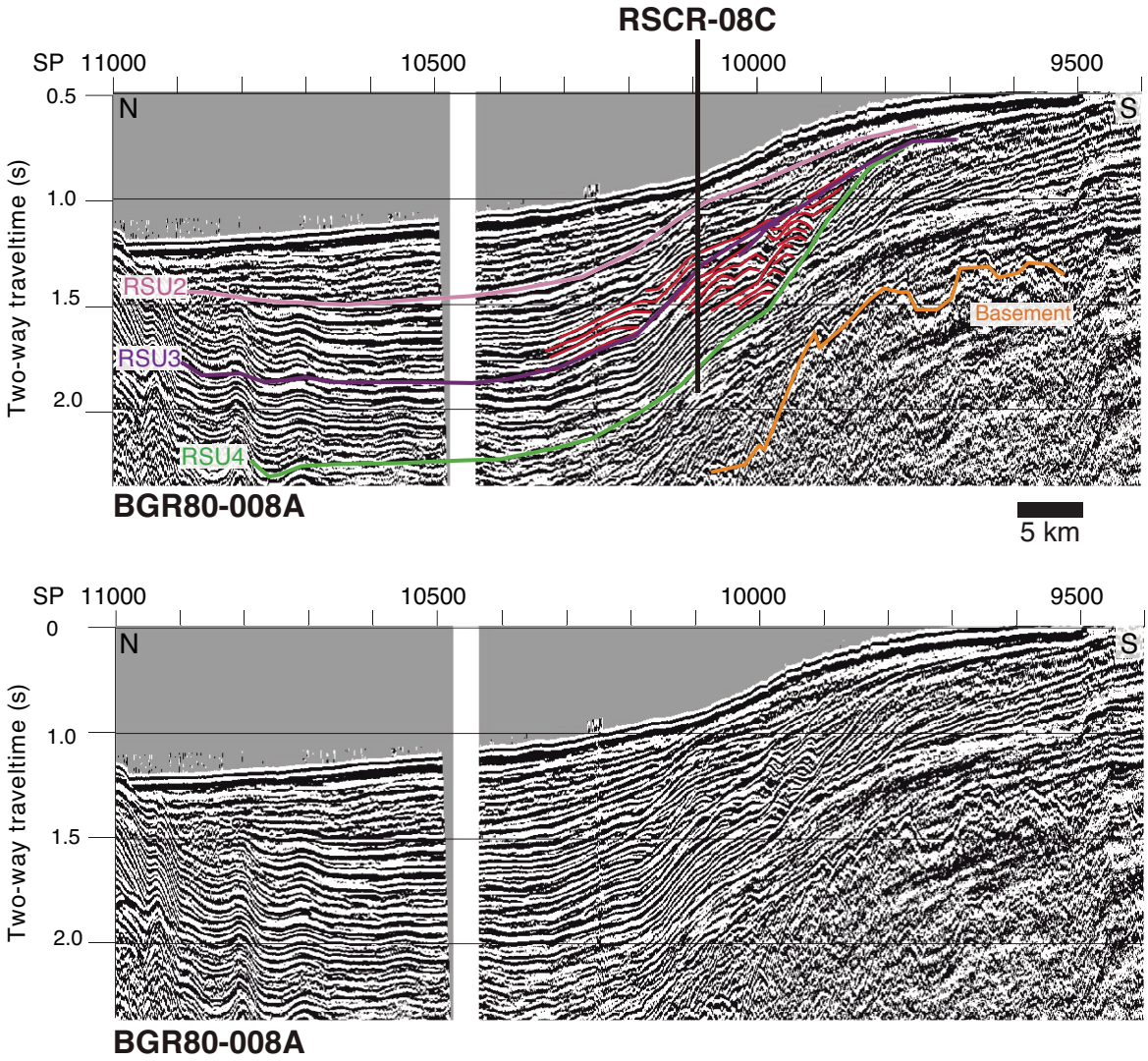

Figure AF31. Seismic reflection profile Line KSL14-02 with location of proposed alternate Site RSCR-08C (73.36928°S, 178.91774°E; SP 3491; water depth = 700 m; target penetration depth = 1000 mbsf; approved maximum penetration = 1000 mbsf).

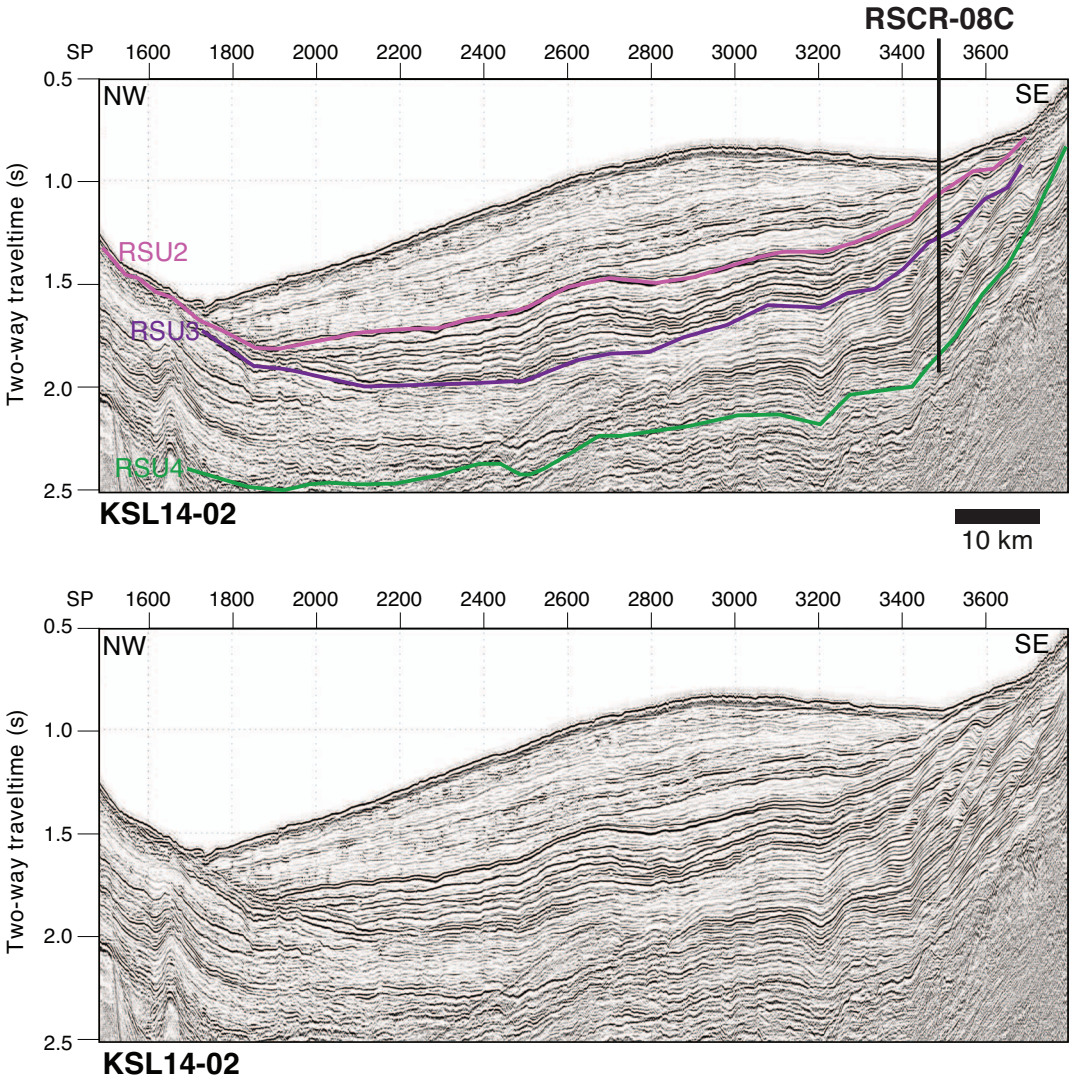

Figure AF32. Contoured bathymetric maps showing location of proposed alternate Site RSCR-12B on seismic reflection profiles IT91A-88 (Figure **AF33**) and KSL14-04 (Figure **AF34**). A. Bathymetry from Davey (2004). Contour interval = 25 m. B. Swath bathymetry collected during seismic survey cruises.

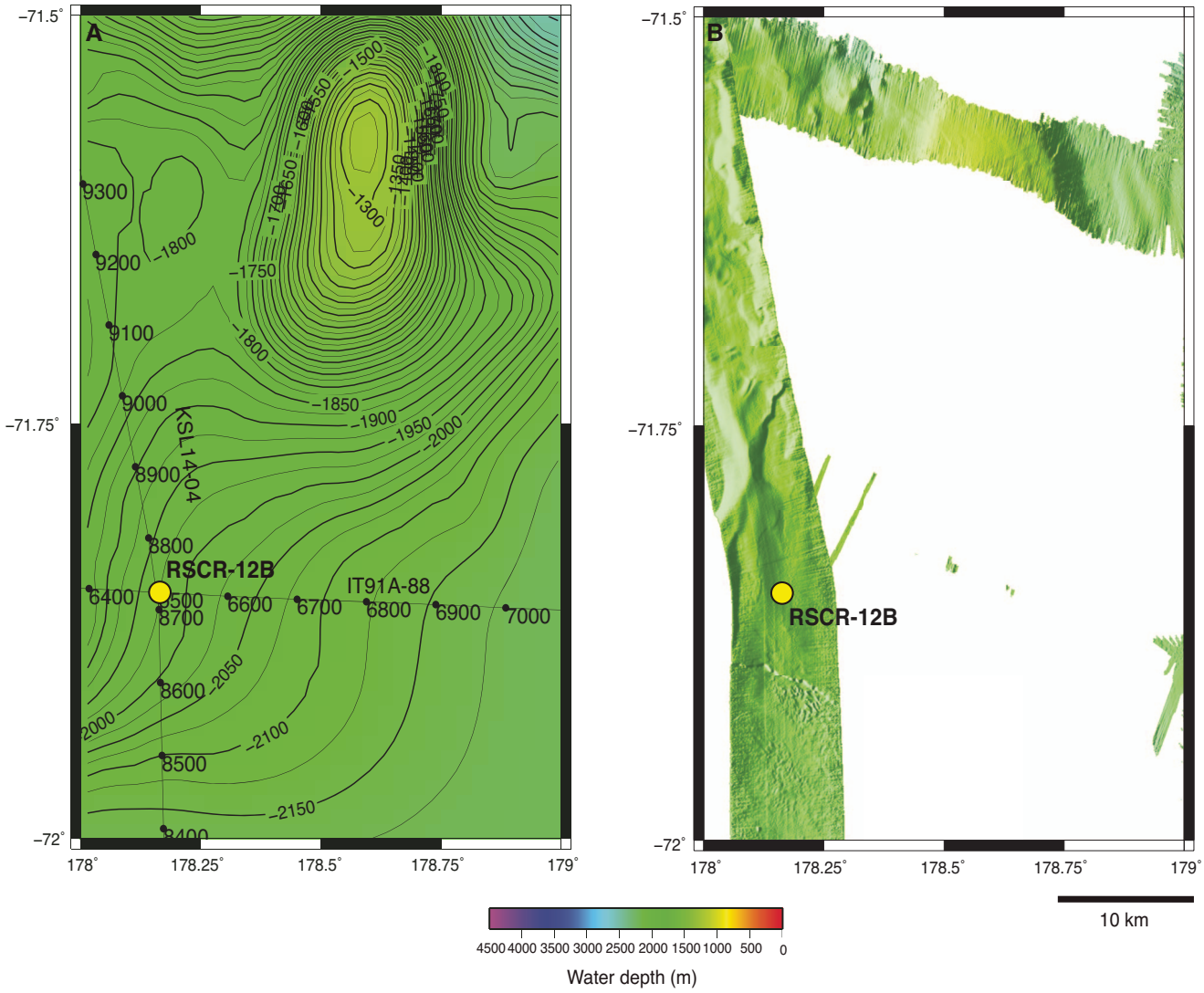

Figure AF33. Seismic reflection profile Line IT91A-88 with location of proposed alternate Site RSCR-12B (71.85123°S, 178.16371°E; SP 6500; water depth = 1952 m; target penetration depth = 620 mbsf; approved maximum penetration = 650 mbsf).

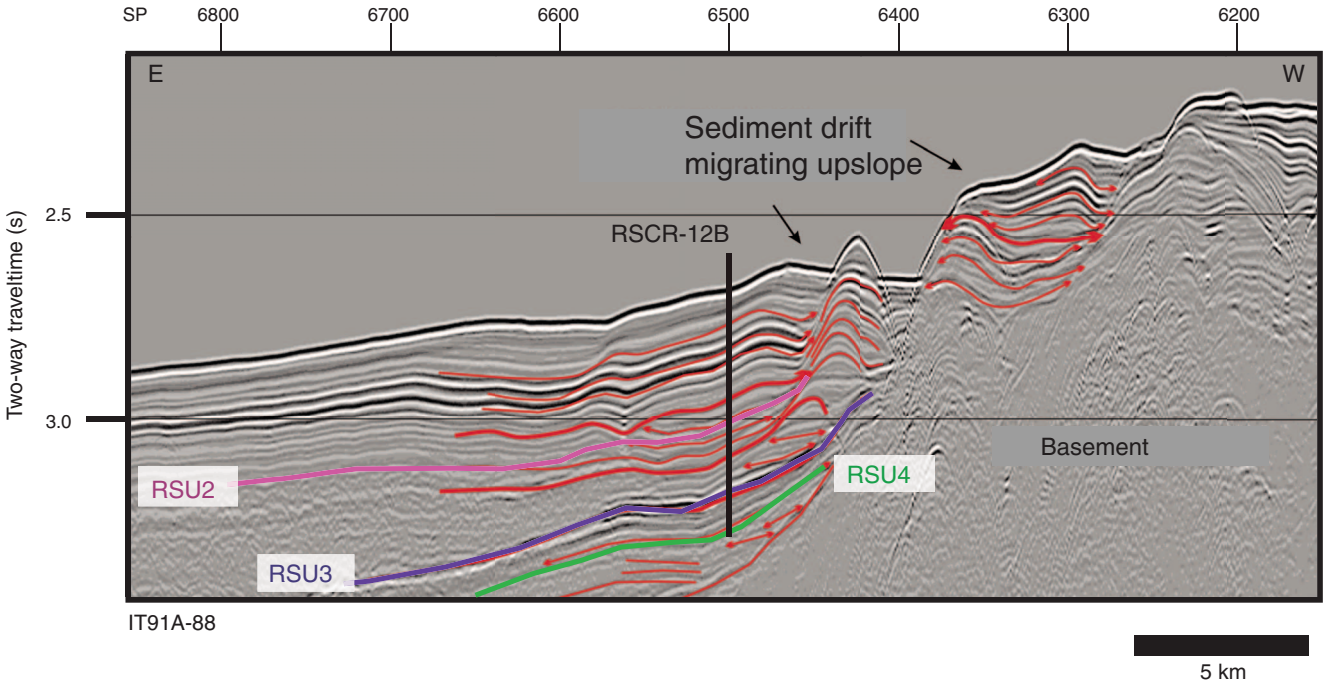

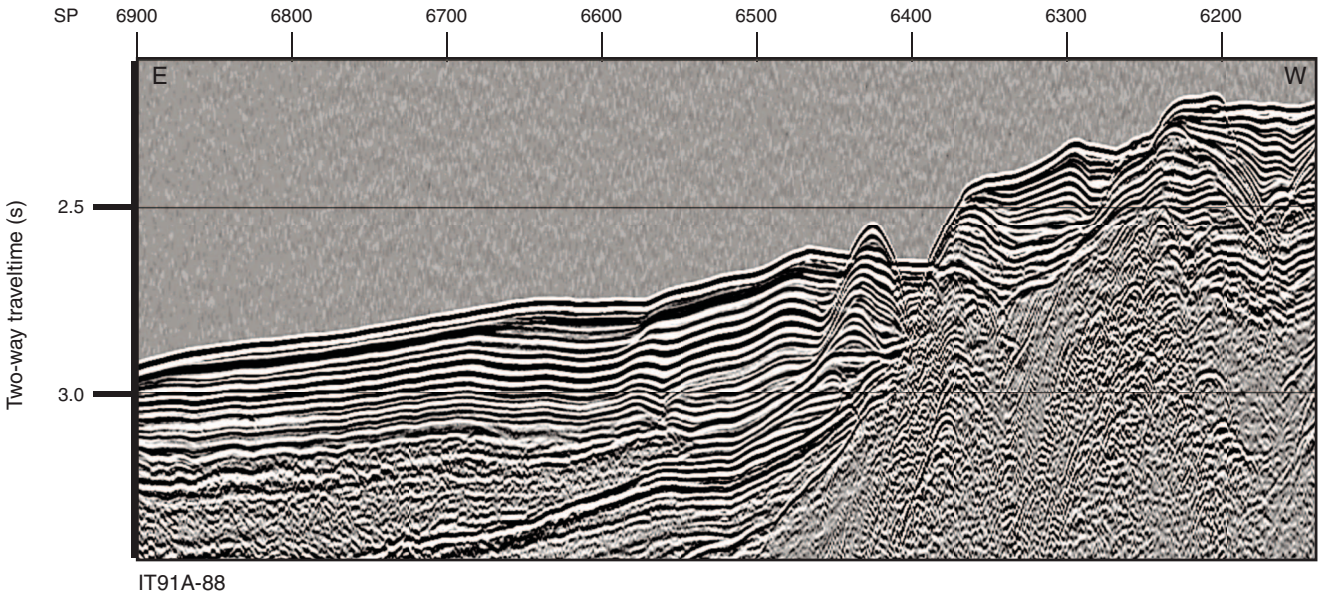

Figure AF34. Seismic reflection profile Line KSL14-04 with location of proposed alternate Site RSCR-12B (71.85123°S, 178.16371°E; SP 8724; water depth = 1952 m; target penetration depth = 620 mbsf; approved maximum penetration = 650 mbsf).